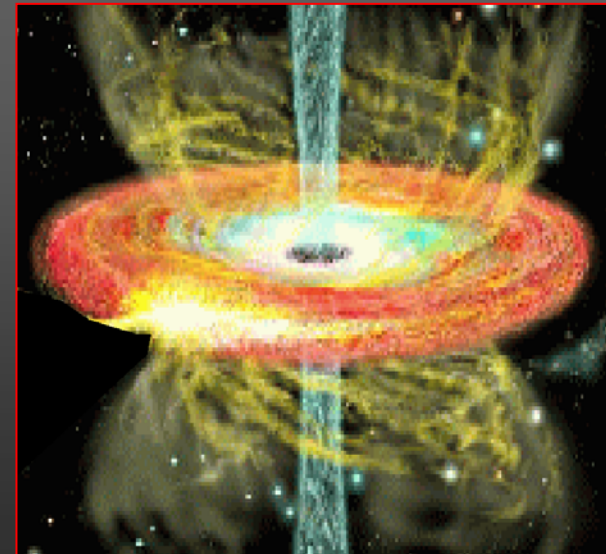
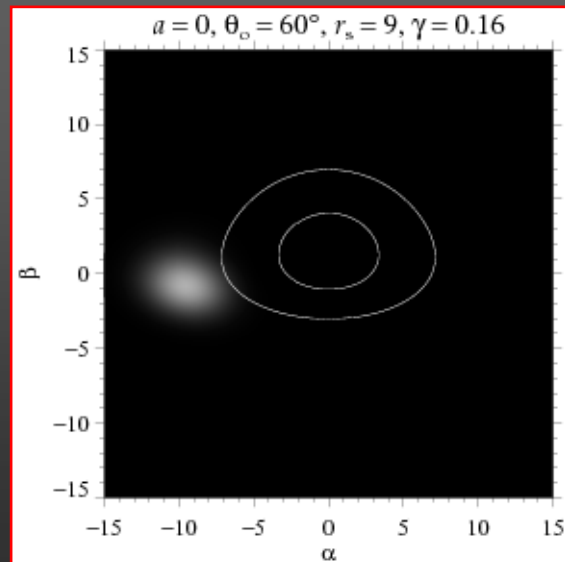
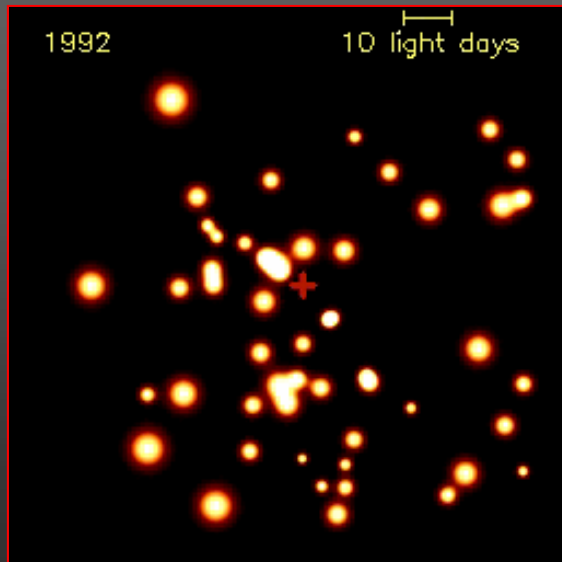


SgrA* at the Center of the Milky Way

Observing the X- and γ -ray Sky
Astrophysical Spring School, April 2006

Andreas Eckart

I. Physikalisches Institut der Universität zu Köln



•I.Part

Imaging: direct, speckle, adaptive optics

Astrometry: relative positions, radio-link

Spectroscopy: stellar populations

Proper motions, radial velocities

Kinematics of the central stellar cluster

Derivation of the enclosed mass

Enclosed mass and structure of the central mass

distribution: compact mass and stellar cusp

Stellar orbits: orbital elements,

•II.Part

Accretion of matter onto SgrA*

Radio, X-ray variability

NIR/X-ray correlations

Adiabatic expansion

NIR polarization

Disk and jet models

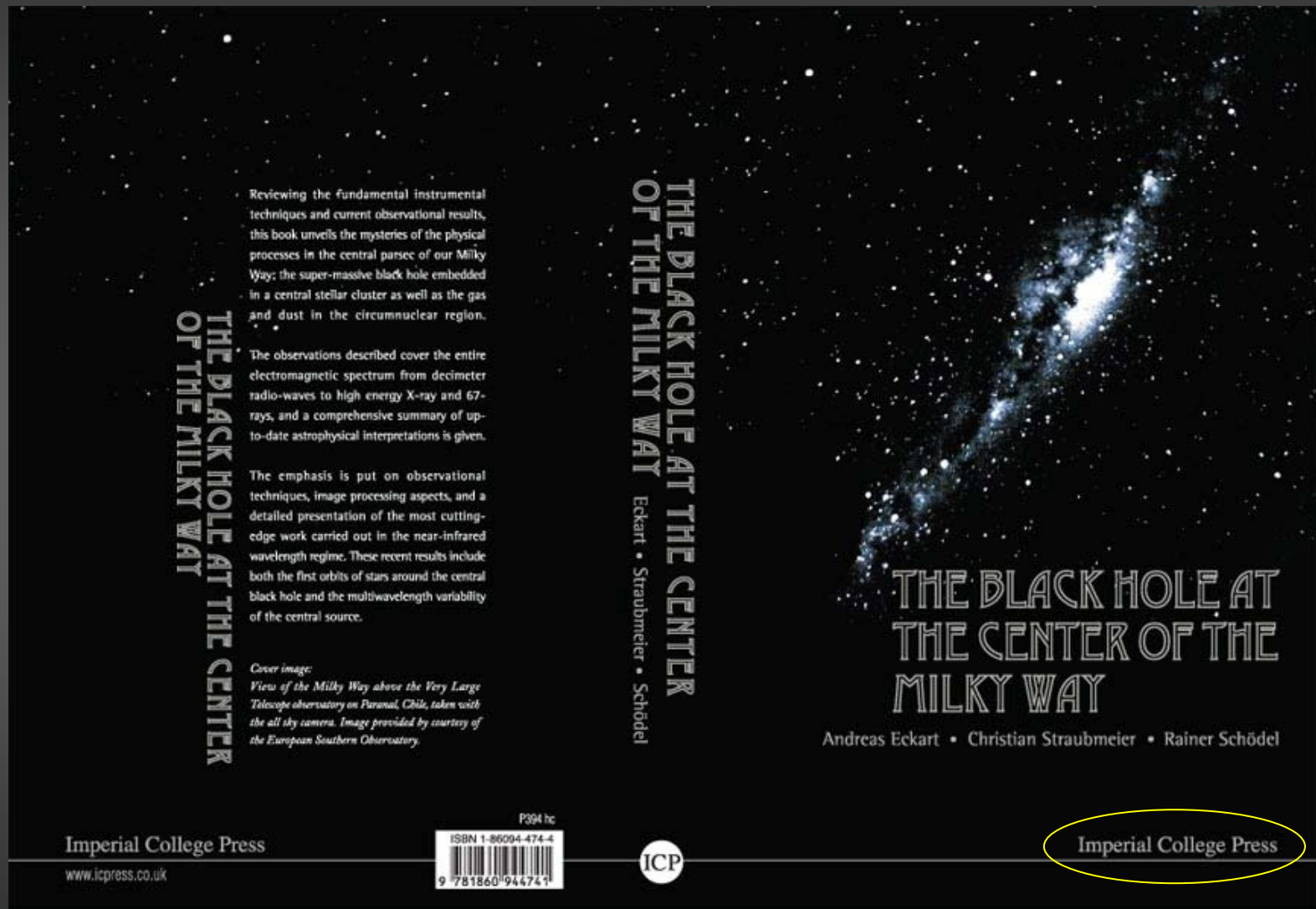
Alternative models for SgrA*

Intermediate Mass BHs

MBHs in external galaxies

Future Experiments

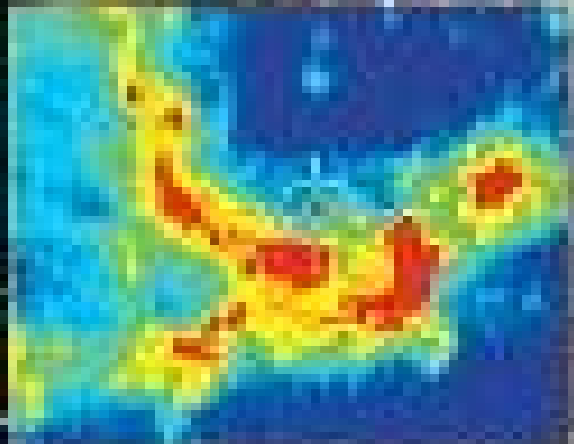
Book on the Galactic Center



Eckart, Schödel, Straubmeier 2005; Imperial College Press; ISBN 1-86094-567-8

Book on the Galactic Center

the black hole at the center of our galaxy

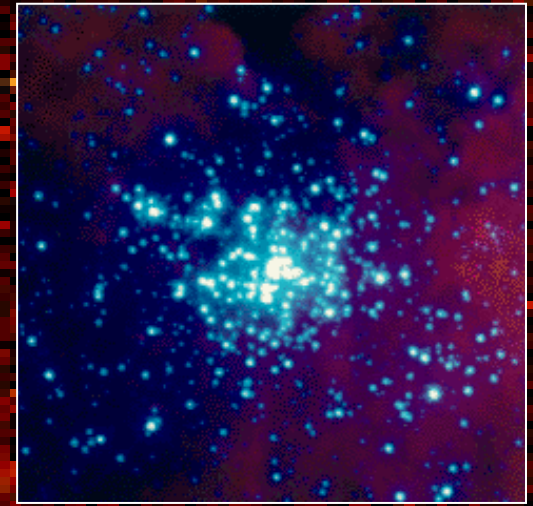


fulvio melia

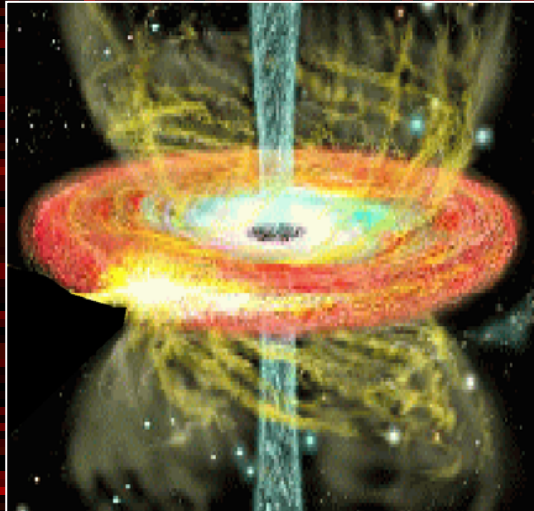
Melia 2004;
Princeton University Press 2003,
ISBN 069 109 5051

Active Galactic Nuclei: Stars or Black Holes?

How can one explain the
large energy release of
Active Galactic Nuclei?



$$E < 0.005 \text{ } Mc^2$$



mass distribution

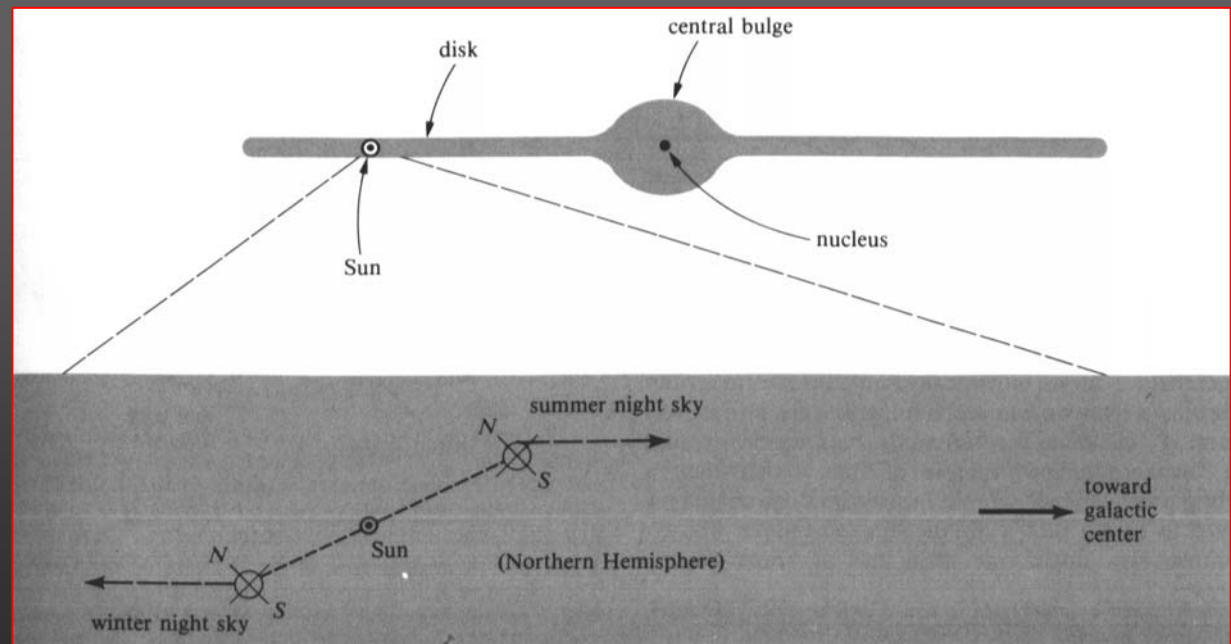
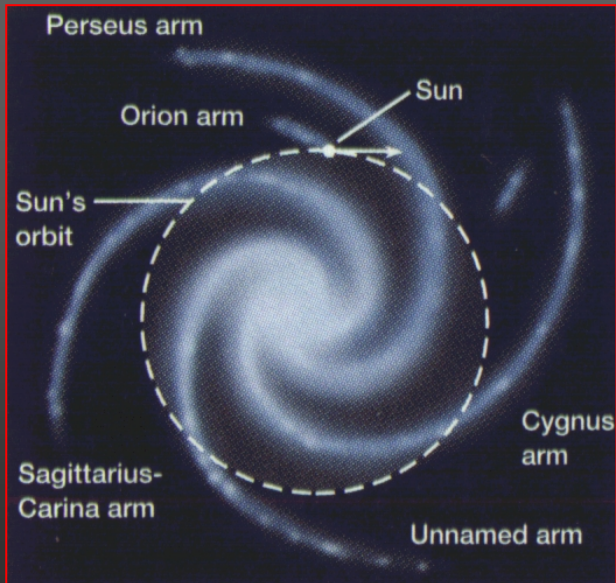
$E < 0.1 \text{ } Mc^2$
variable X-ray and γ -ray
emission
relativistische radio jets



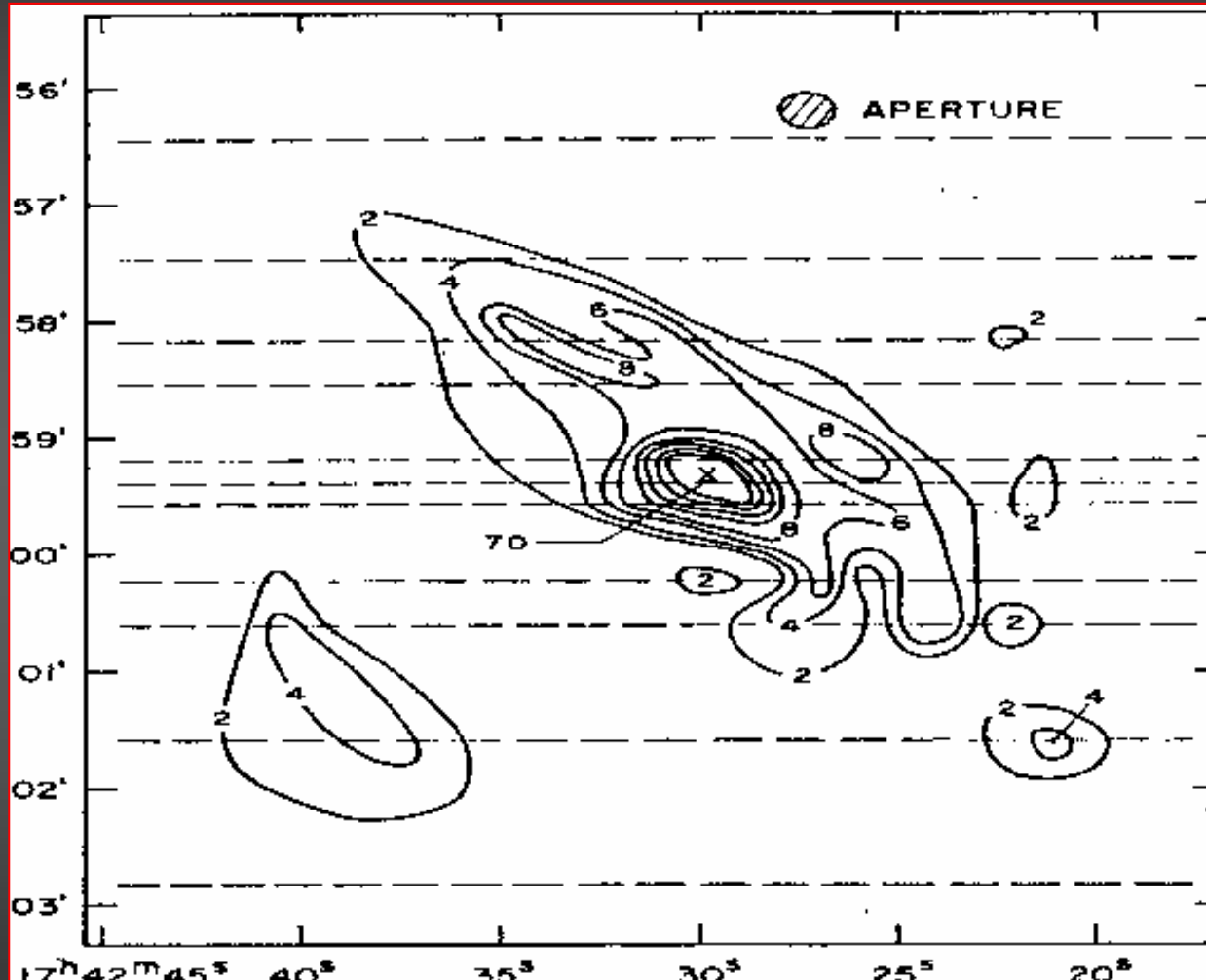
HST WFPC 2

Towards the Center of the Milky Way

closest galactic nucleus
8 kpc distance
 $A_V=30$ $A_K=3$
NIR observations required!

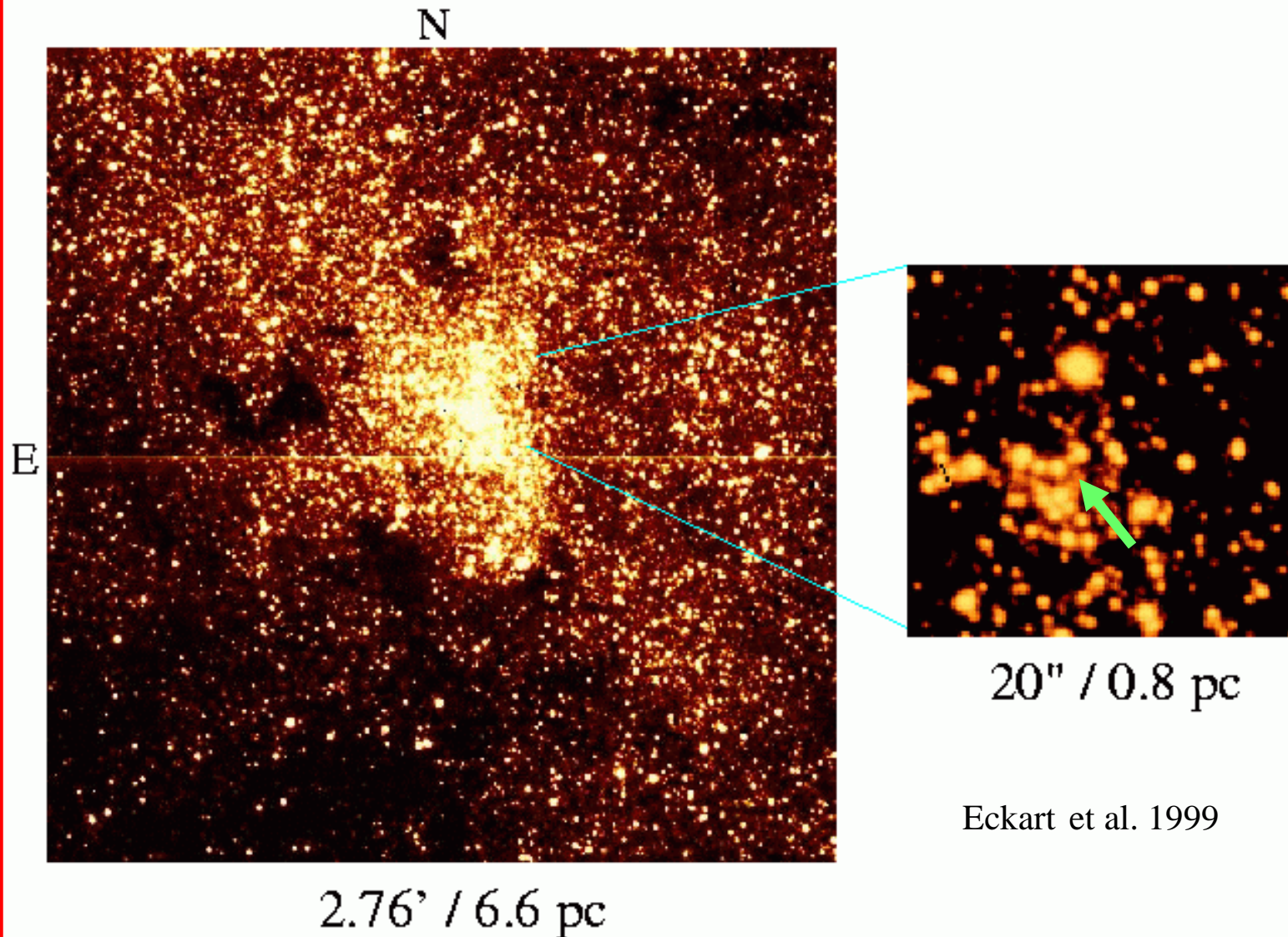


First 2.2 μ m scans through the GC

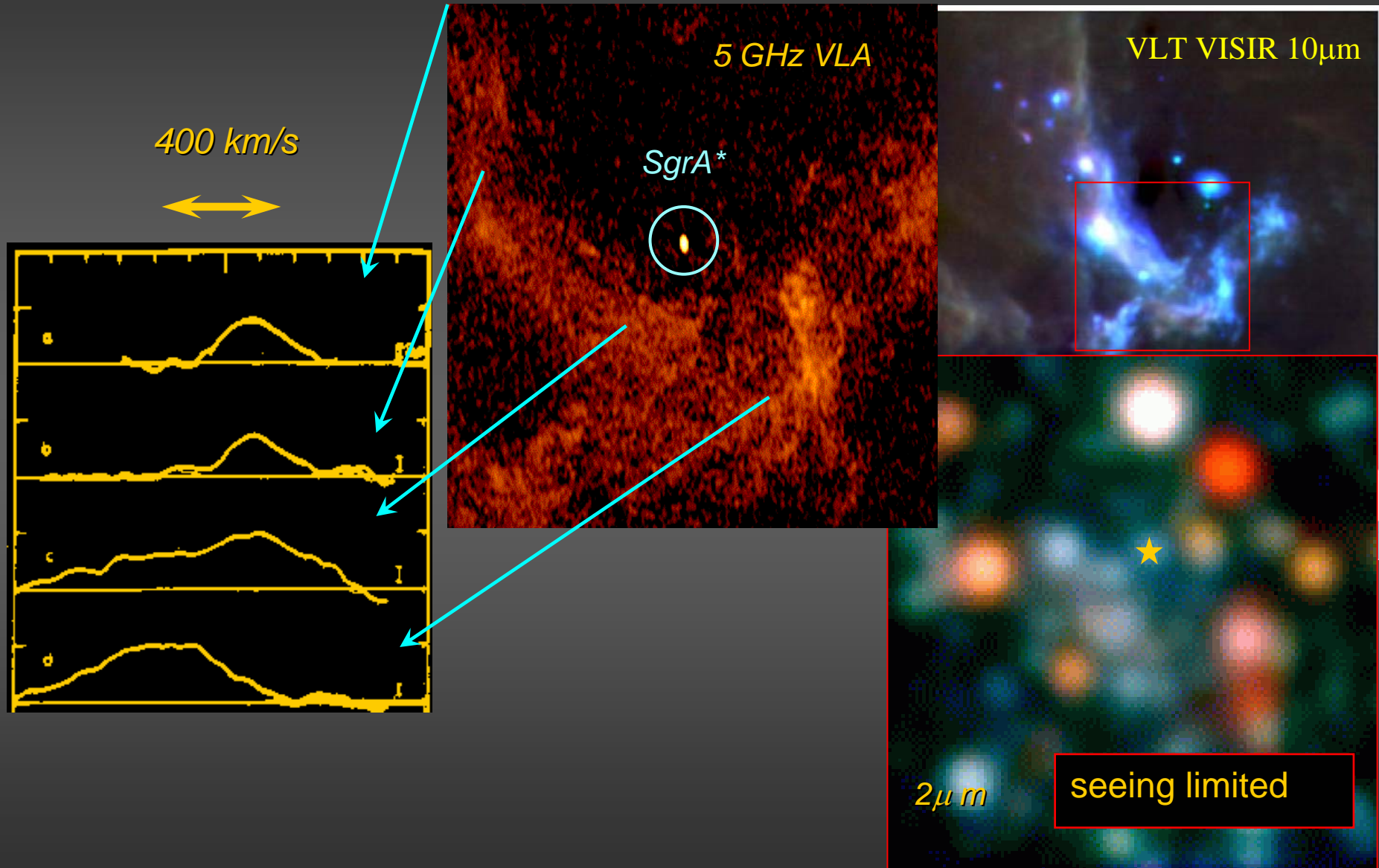


R.A. single detector strip-chart scans (Becklin & Nagebauer 1968)

K-band exposure with ISAAC with VLT/UT1



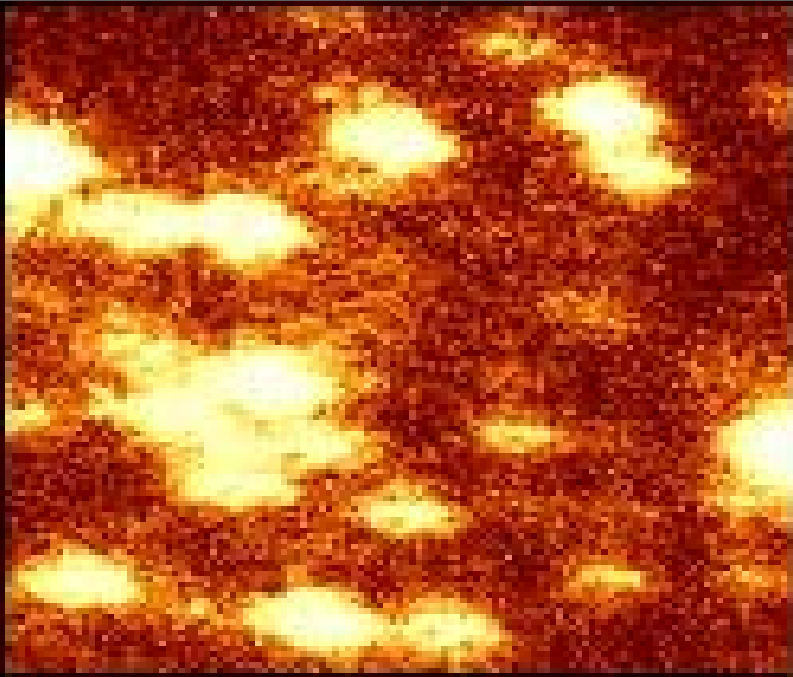
The Galactic Center



Wollman et al. 1977, Lacy et al. 1979, 1980, Lo et al. 1983, DePoy and Sharp 1991

Speckle Interferometry

Via short exposures (typically 100 ms) the influence of the atmosphere on the image can be recorded and corrected for.



SHARP NTT short exposures

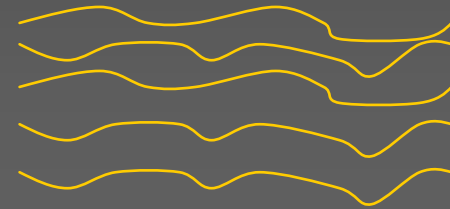
star



vakuum



atmosphere



telescope

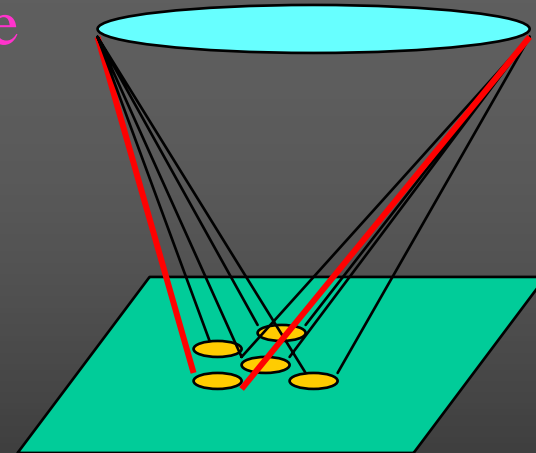
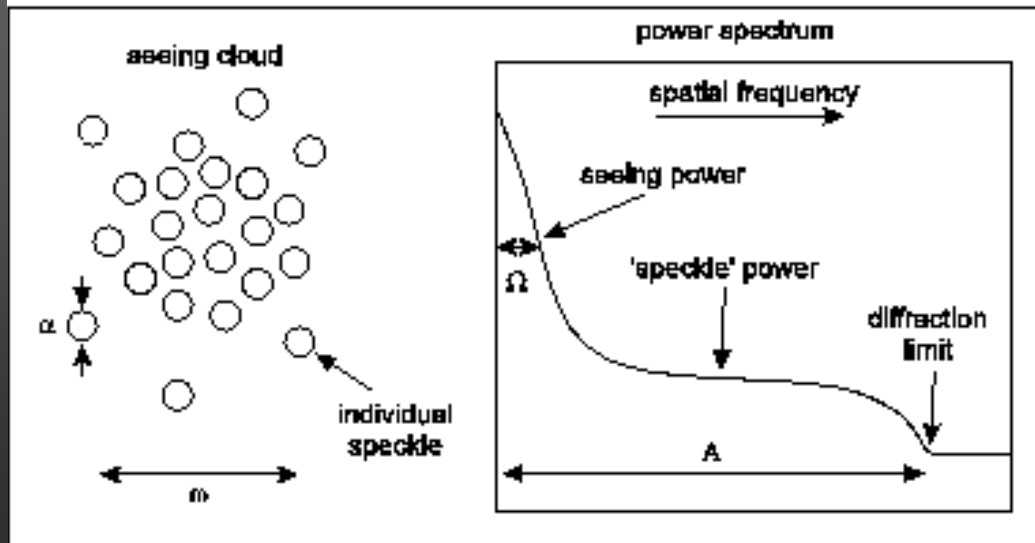
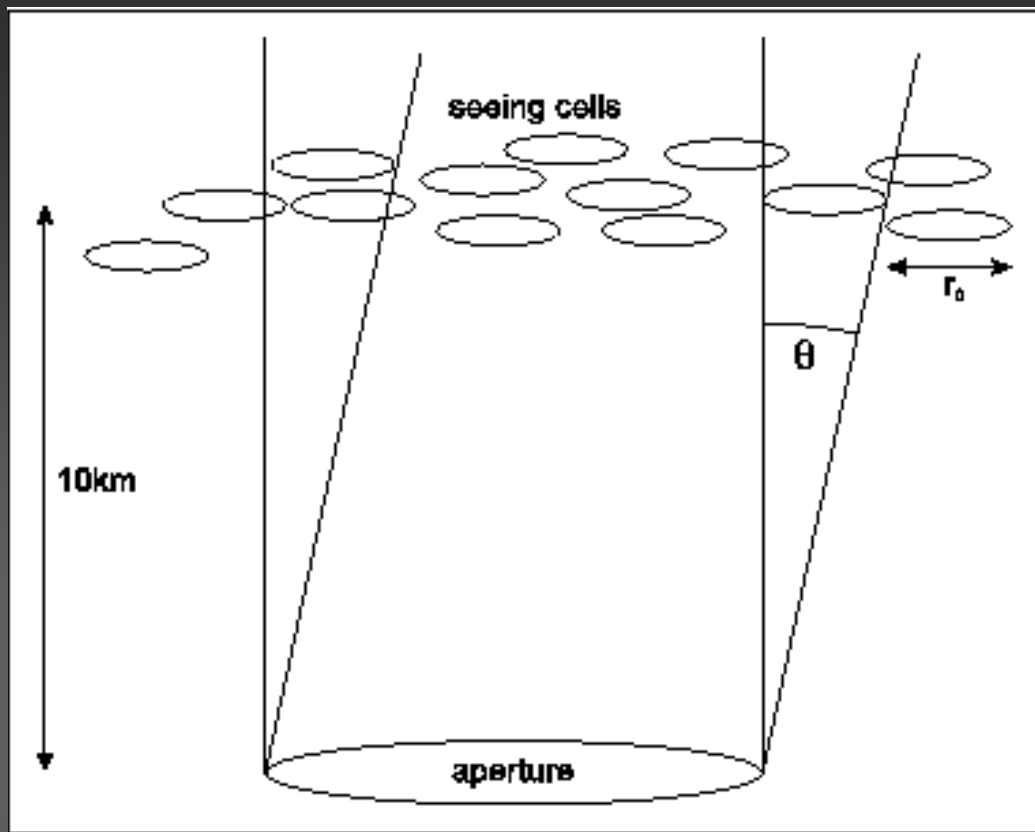


image plane
of the camera

Image Formation

The apparent diameter of a seeing cell determines the size of the isoplanatic patch



Speckles can be regarded as distorted images of the object at the telescope's diffraction limit

Image Formation

image plane

$$I(x, y) = O(x, y) * P(x, y)$$

image is object
convolved with PSF

Fourier plane

$$i(u, v) = o(u, v) p(u, v)$$

$$|\langle i(u, v) \rangle|^2 = o^2(u, v) |\langle T(u, v) \rangle|^2$$

long exposure
power spectrum

$$|\langle i \rangle|^2 = |\langle a e^{i\phi} \rangle|^2$$

$$\langle |i(u, v)|^2 \rangle = o^2(u, v) \langle |T(u, v)|^2 \rangle$$

short exposure
power spectrum

$$\langle |i|^2 \rangle = \langle i^* \times i \rangle = \langle a^2 \rangle \langle e^{-i\phi} e^{i\phi} \rangle = \langle a^2 \rangle$$

information at high
spatial frequencies
is preserved!

Seeing

$$\langle T(u, v) \rangle = T_s(u, v) T^*(u, v)$$

$$w^2 = u^2 + v^2$$

$$T_s(\omega) \approx \exp\left(-3.44 \frac{\lambda |w|^{5/3}}{r_0}\right)$$

$$r_0 \propto \lambda^{6/5} \times (\cos(\gamma))^{3/5}$$

$$\omega \approx \lambda / r_0$$

$$\omega \propto \lambda^{-1/5}$$

The seeing is better in the
Infrared wavelength domain!!

Telescope transfer function: T^*
(autocorrelation of aperture)

Seeing transfer function: T_s

assuming a Kolmogorov power
law for the atmospheric turbulence

r_0 Fried size of turbulent cells
 γ zenith angle

angular diameter of a
(Fried) seeing cell

Also: γ should be small!
Go to Chile!!

$$I(x, y) = O(x, y) * P(x, y) + N(x, y)$$

Shift-and-Add Algorithm

$$S(x, y) = \frac{1}{M} \sum_{m=1}^M I_m(x + x_m, y + y_m)$$

I : image ; O : object
P : PSF ; N : noise

$$S(x, y) = \frac{1}{M} \left(O(x, y) * \sum_{m=1}^M P_m(x + x_m, y + y_m) + \sum_{m=1}^M N_m(x + x_m, y + y_m) \right)$$

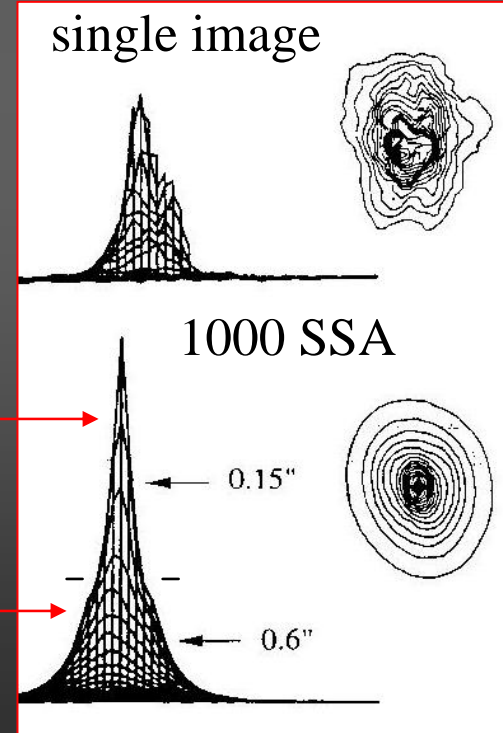
$$S(x, y) = \frac{1}{M} (O(x, y) * P_s(x, y) + N_s(x, y))$$

diffraction limited part

$$R \propto \lambda / D$$

seeing limited part

$$R \propto \lambda / r_0$$



Lucy Deconvolution

$$\Psi_1 = I$$

$$\Phi_i = \Psi_i \otimes P$$

$$R = (I / \Phi_i) * P$$

$$\Psi_{i+1} = \Psi_i \times R$$

deconvolved
image

diffraction limited part

$$R \propto \lambda / D$$

seeing limited part

$$R \propto \lambda / r_0$$

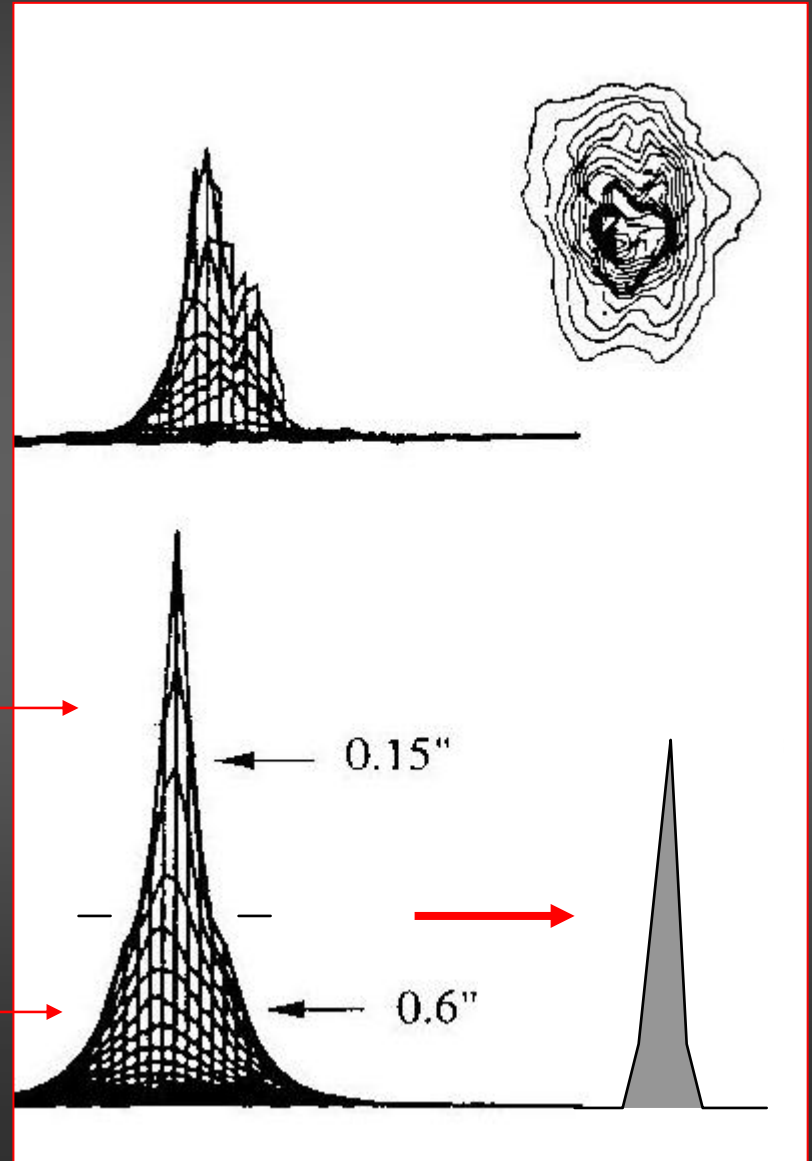
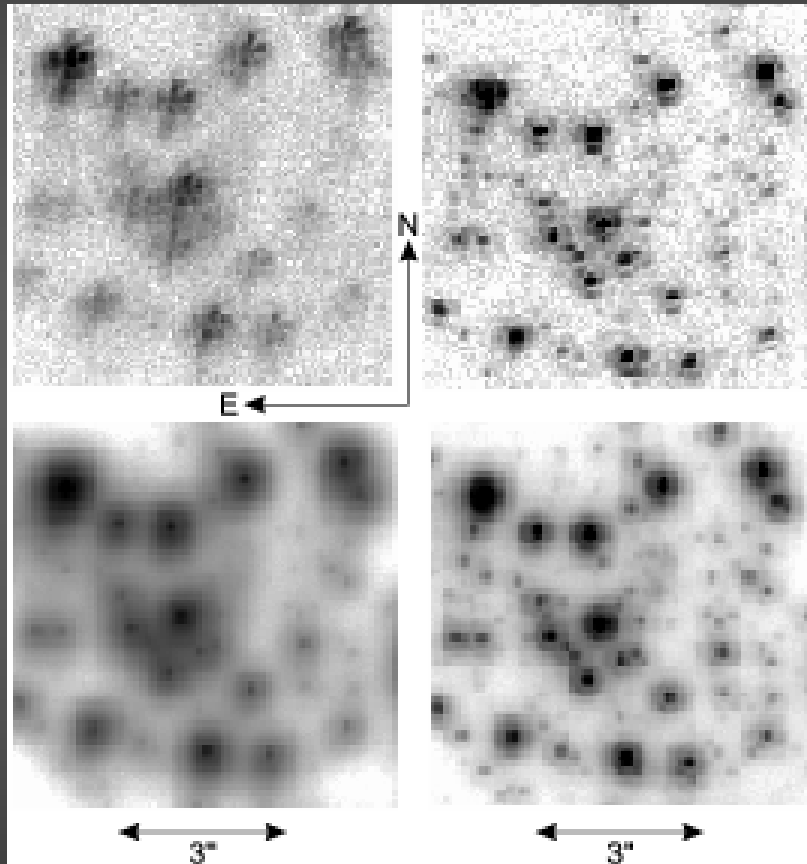
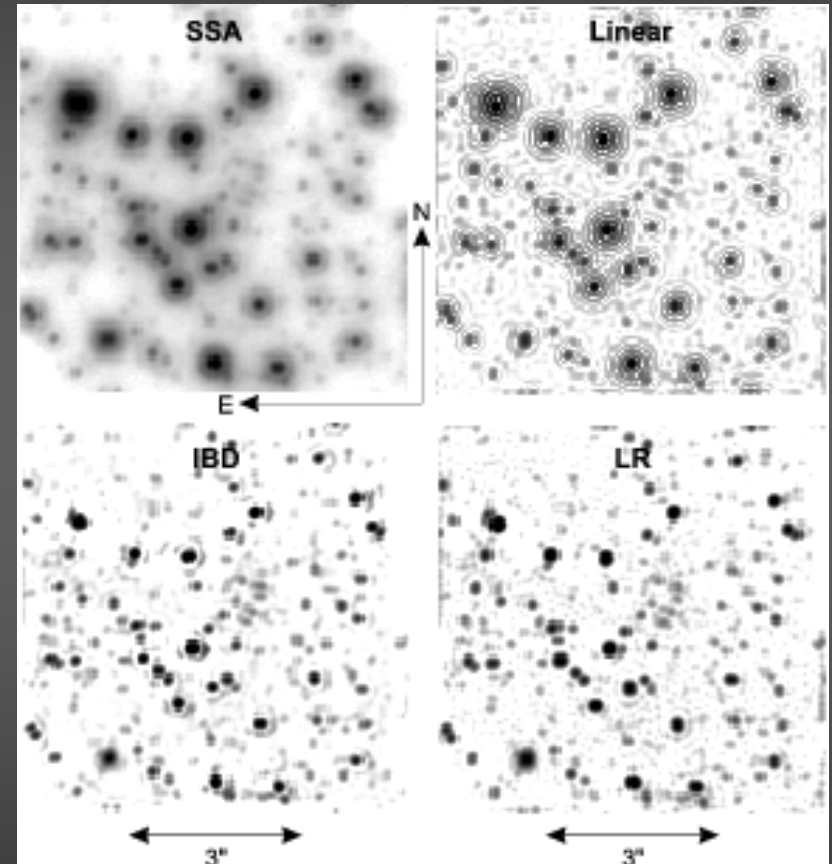


Image Reconstruction



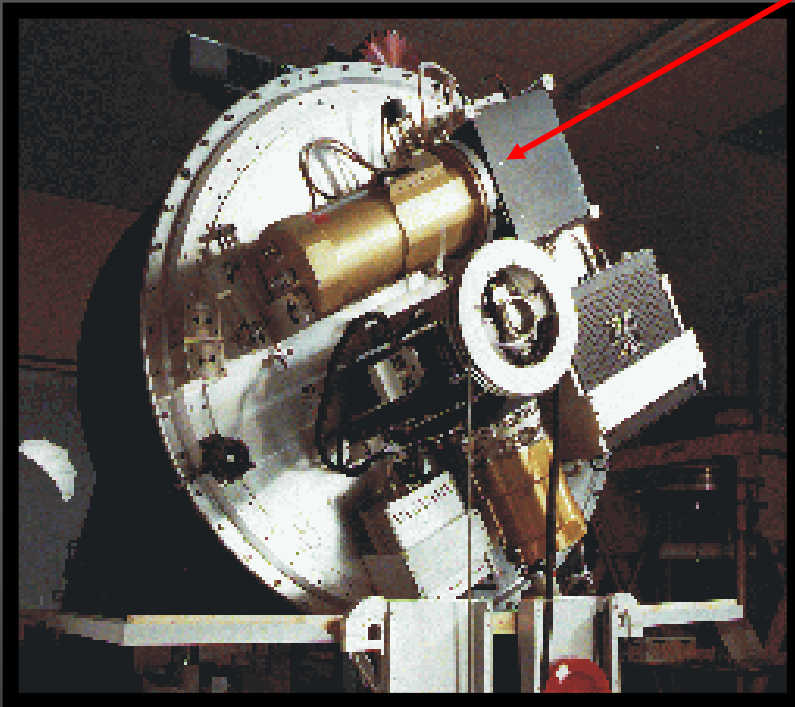
average and excellent speckle image;
average (15% Strehl) and best (30% Strehl)
SSA result of 100 images



Deconvolution methods: SSA, Linear,
Blind deconvolution, Lucy-Richardson

NTT Speckle Interferometry and Adaptive Optics at the VLT UT4

Proper motions: SHARP I + NAOS/CONICA



ESO NTT La Silla since 1992

Keck since ~1995

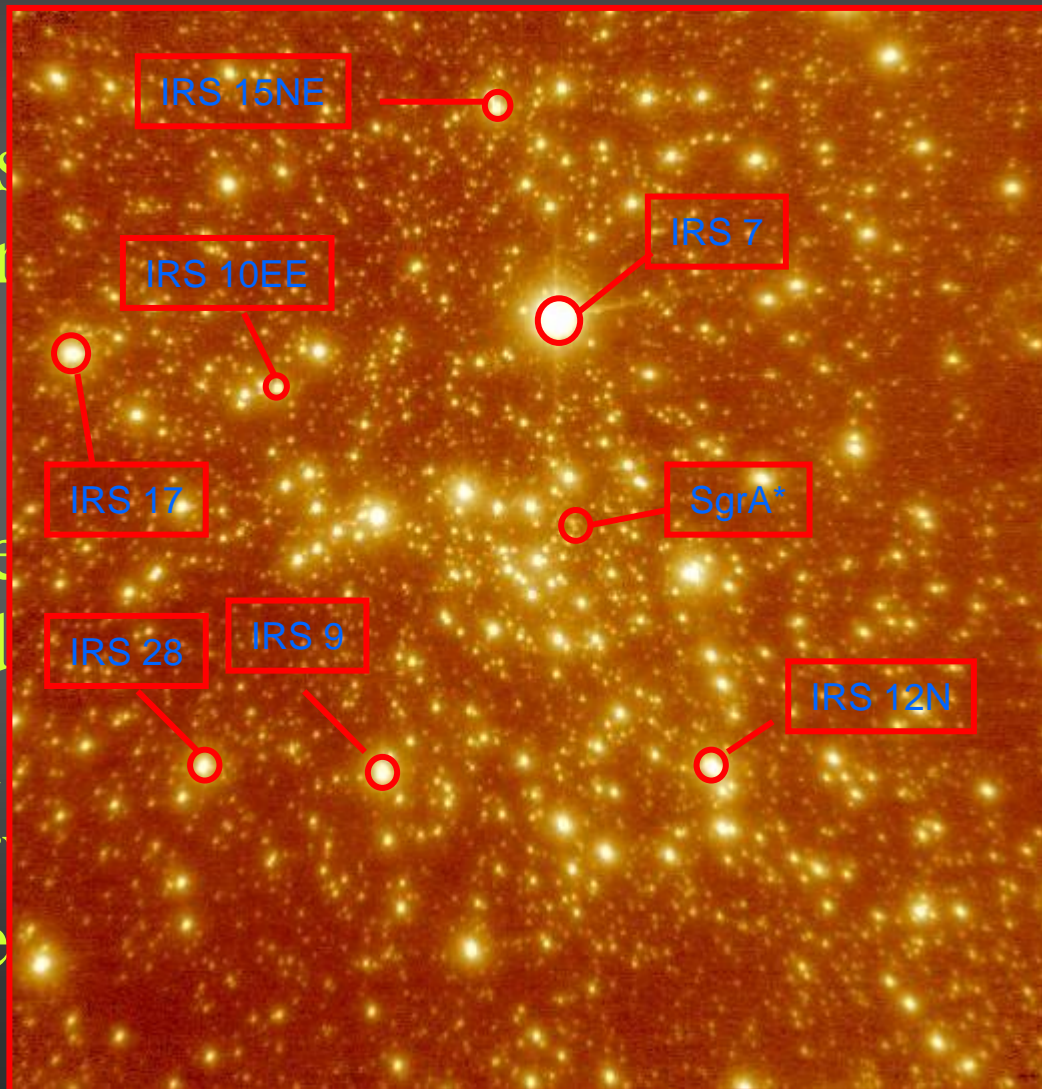


ESO VLT UT4 Paranal since 2002

proper motions from imaging

Proper motions

- First star cluster with proper motions from radio observations
- Stars in all directions from SgrA*
- From observations, proper motions



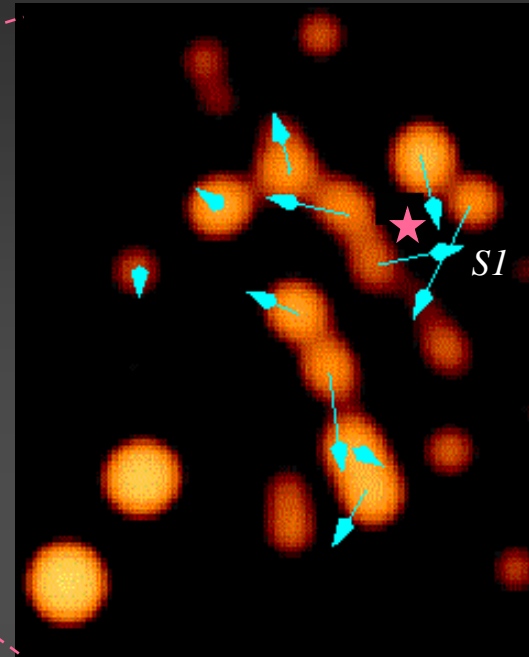
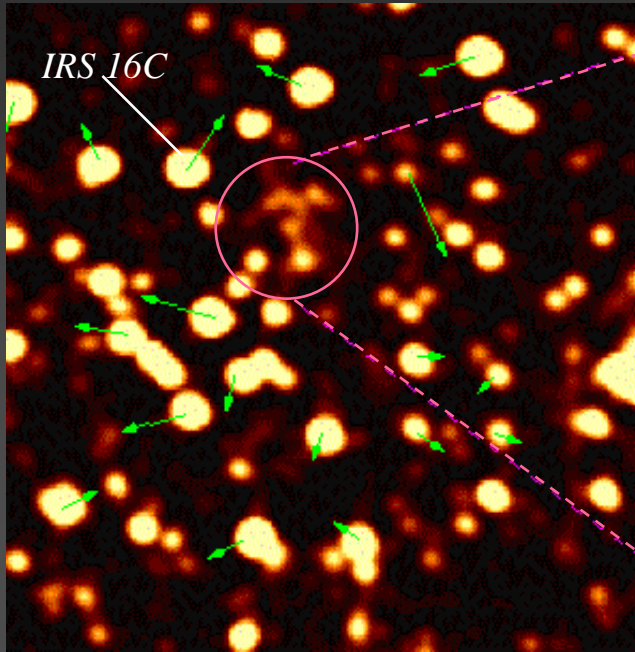
from

in all
n

es of
gives

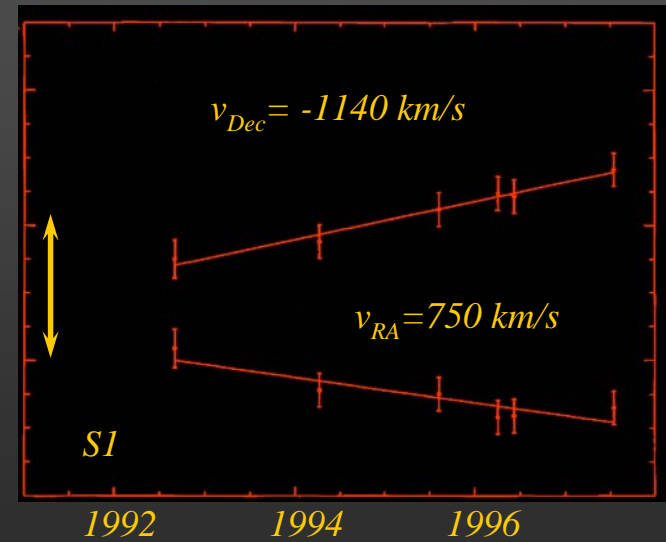
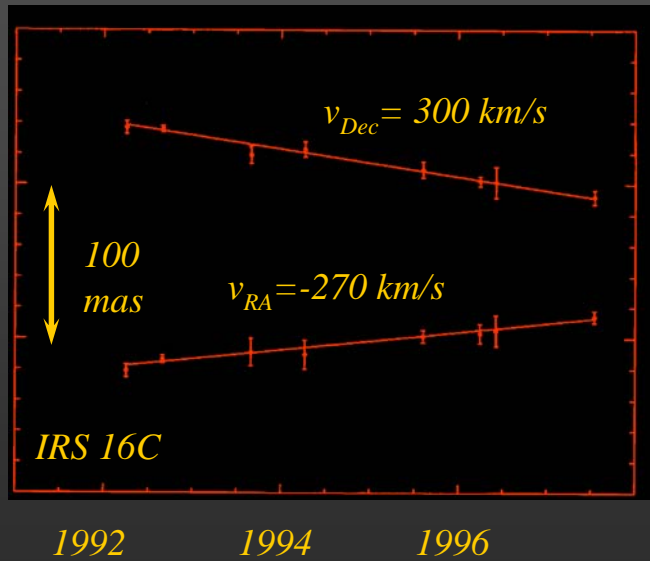
Radio/NIR Restframe:
Reid et al. 2003
Menten et al. 1998

Stellar Proper Motions



*Eckart und
Genzel 96,97,
Genzel et al.
1997*

relative Position



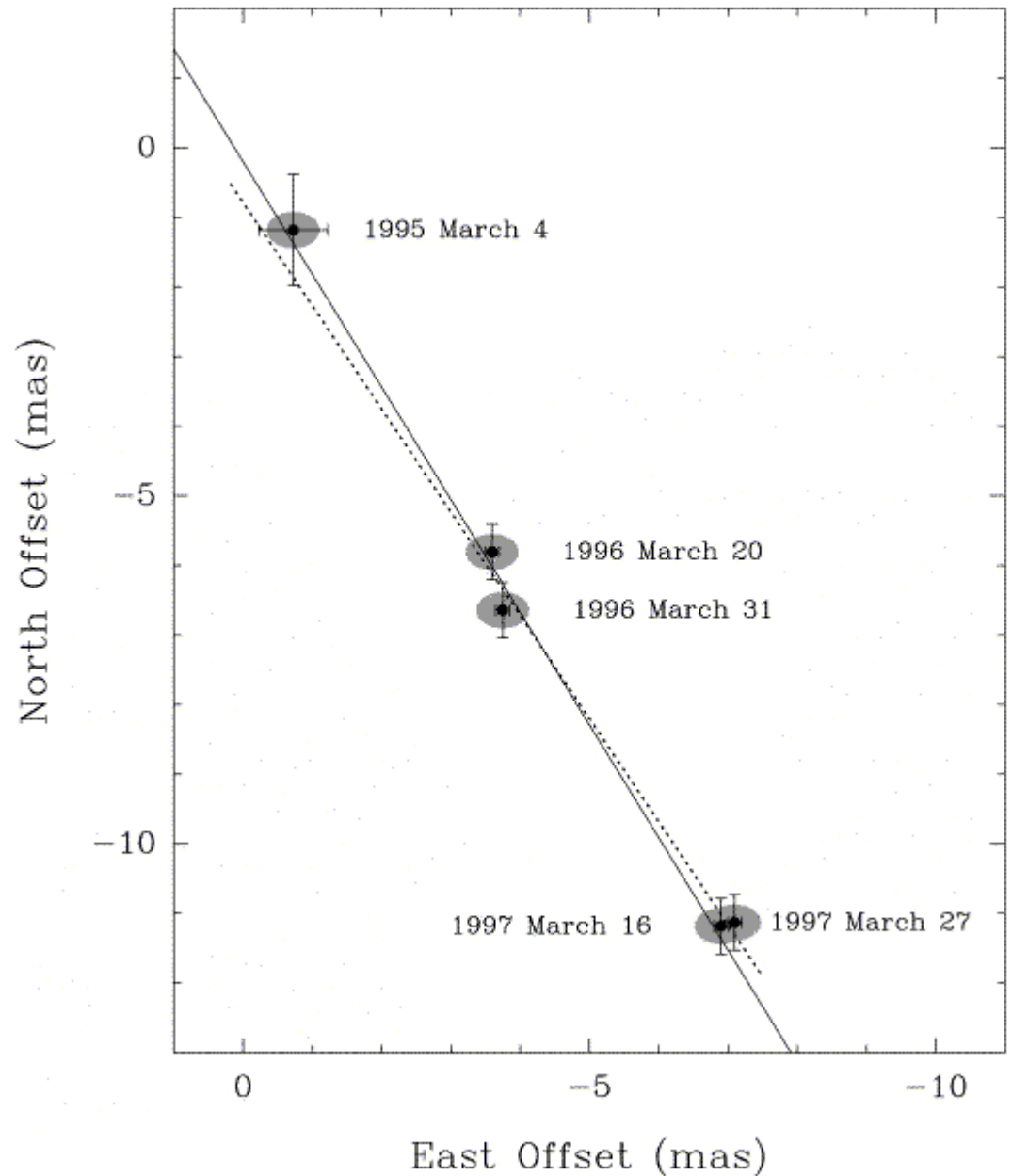
The Galactic Center

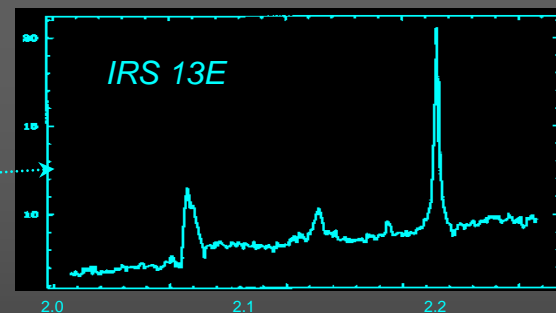
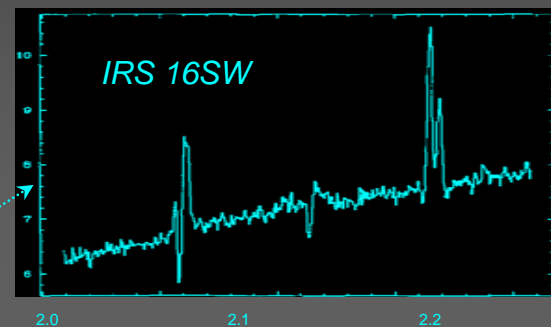
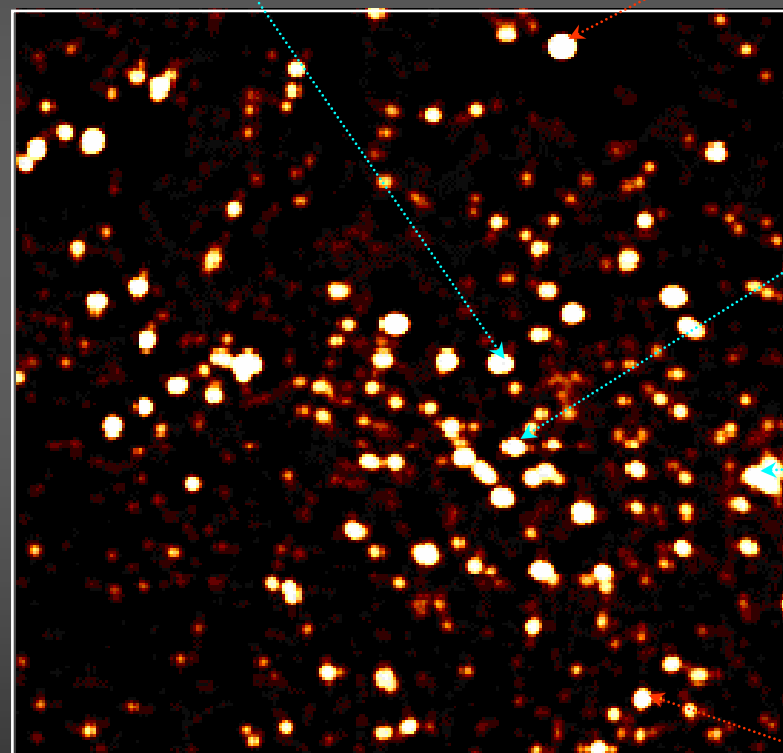
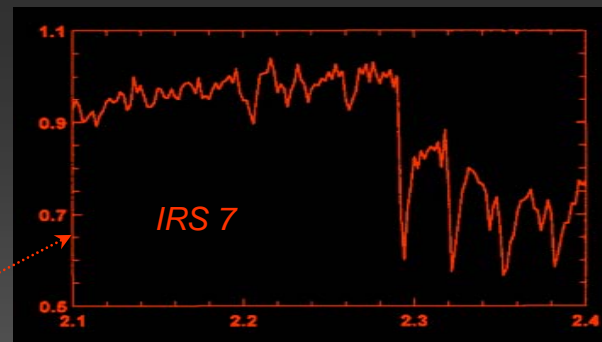
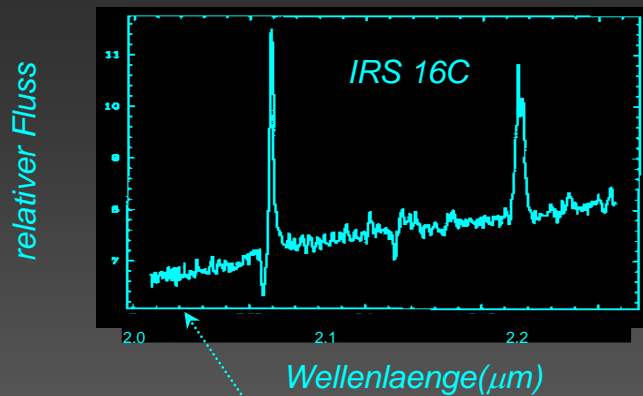
VLBA measurements of the SgrA* proper motion give 5.9 mas/yr almost entirely in the Galactic plane consistent with the suns motion of 219 km/s at 8 kpc.

The upper limit on the intrinsic proper motion of 20 km/s indicates a lower limit to the SgrA* mass of 1000 M_{sun}

Reid et al. 1999 ApJ 524, 816

Backer et al. 1996

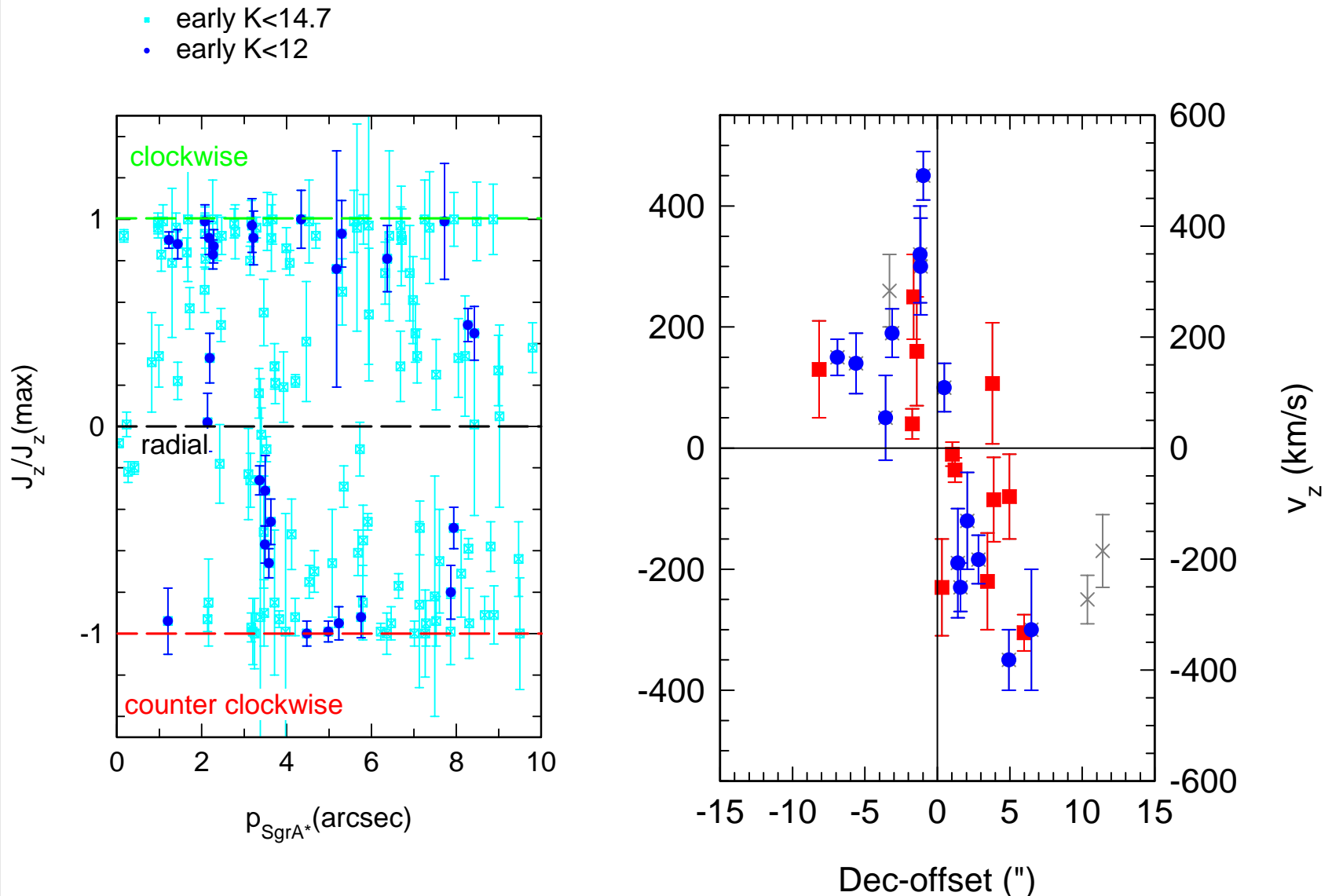




5"

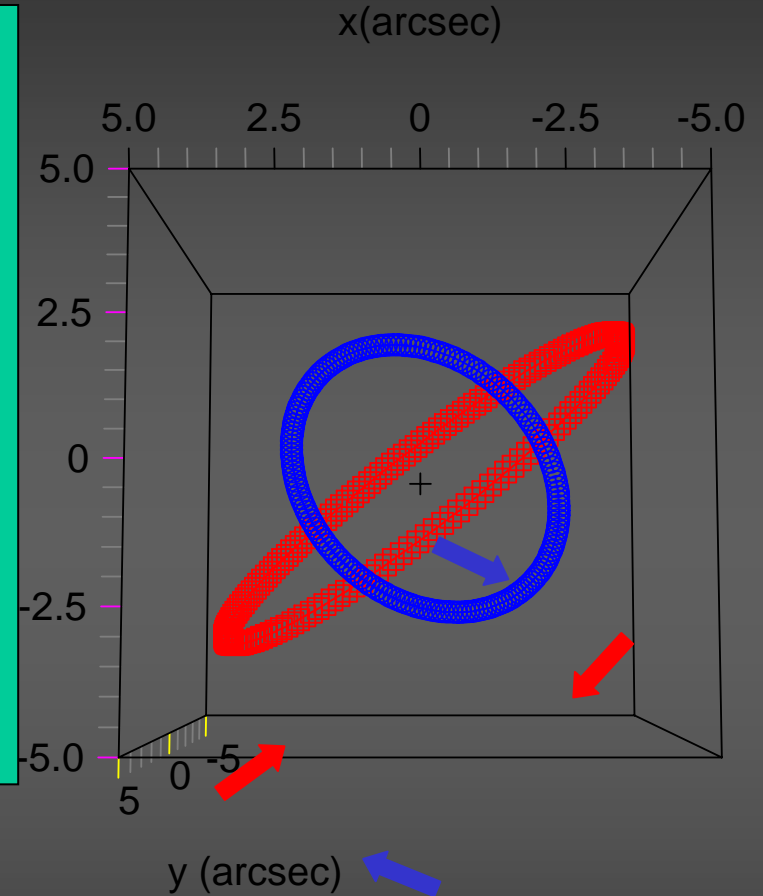
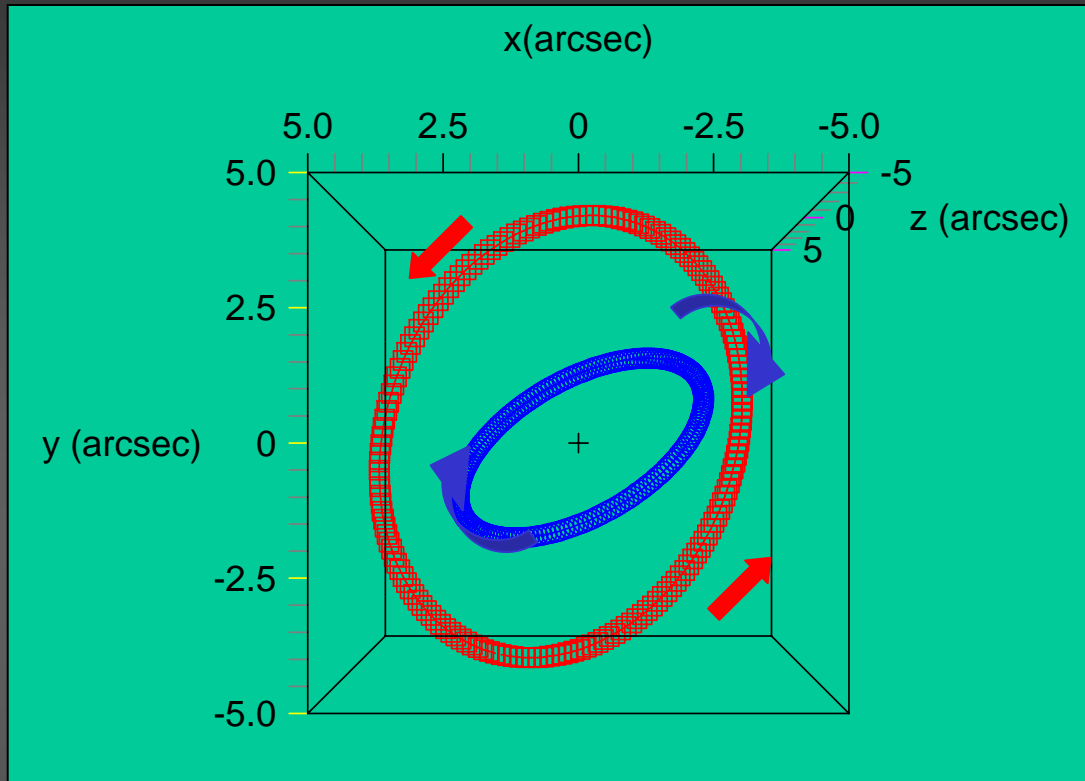
radial velocities from stellar spectroscopy

Overall rotation of early type stars



Genzel et al. 2003, *Ap.J.* (astro-ph 0305423), Ott et al. 2004 (1000 proper motions, 200 3Dvels)

Rotating disks of early type stars



SPIFFI spectroscopy:
The two disks have *very similar short-lived stellar populations* (LBV, Wolf-Rayet...)

→ **Coeval formation**

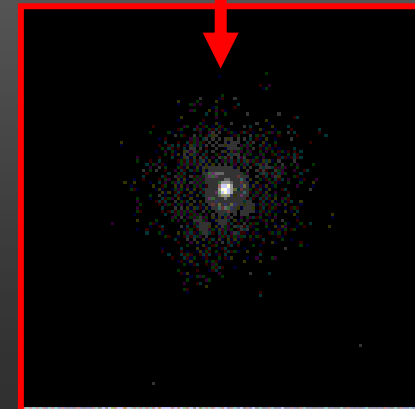
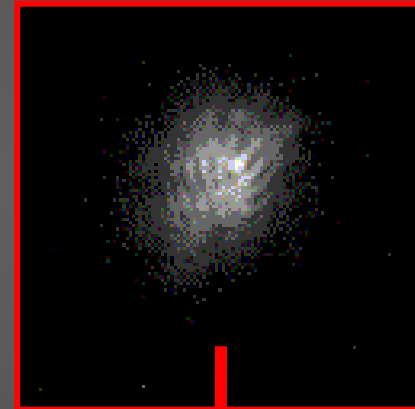
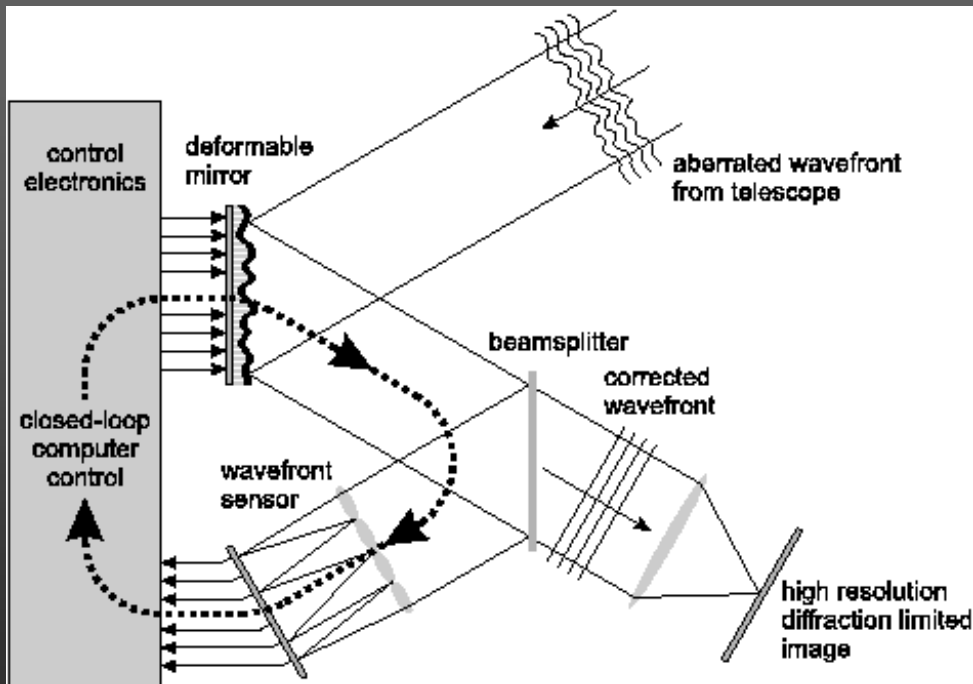
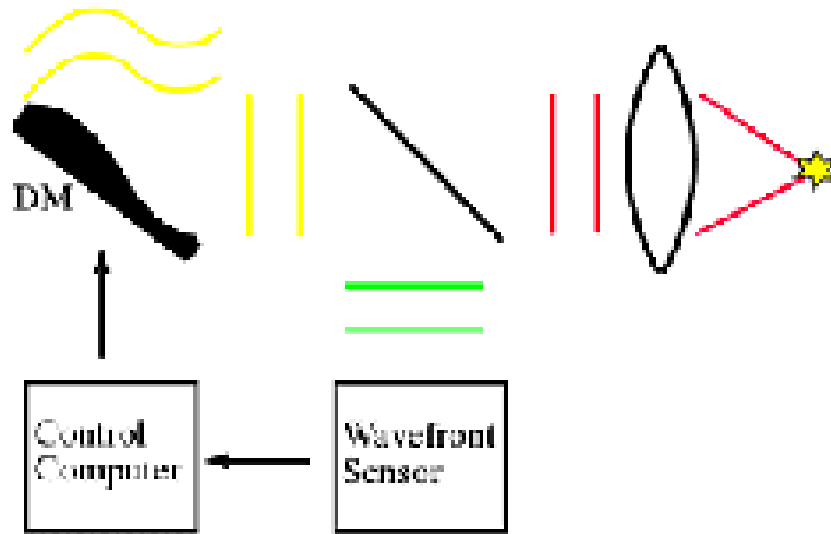
Genzel et al. 2003, Ap.J. 2003 (astro-ph 0305423)

Levin & Beloborodov, Ap.J. 2003

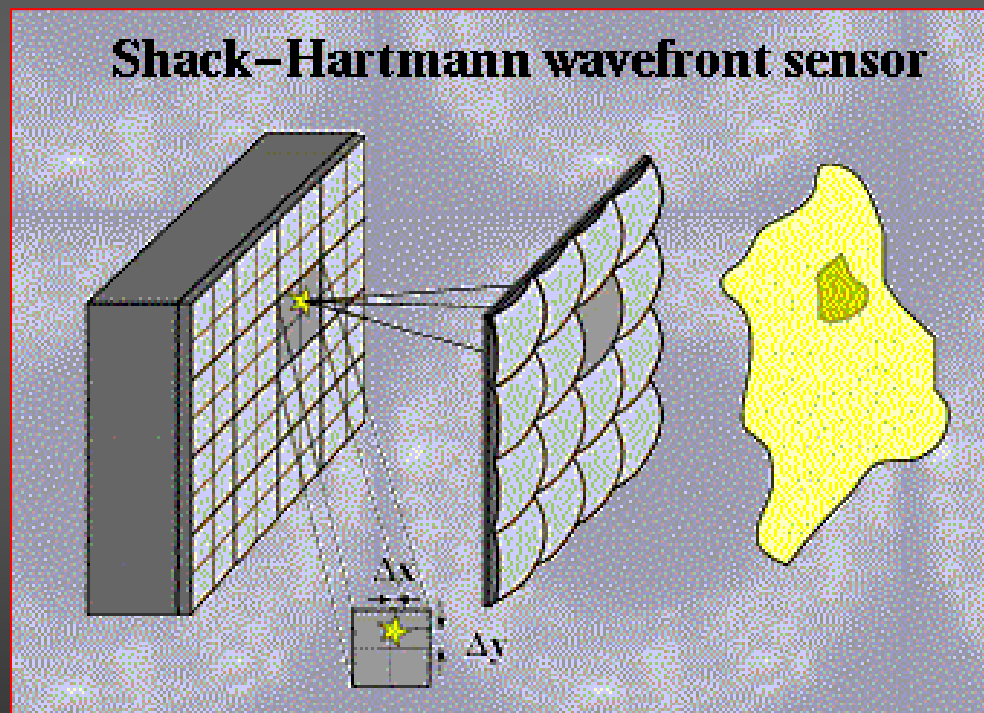
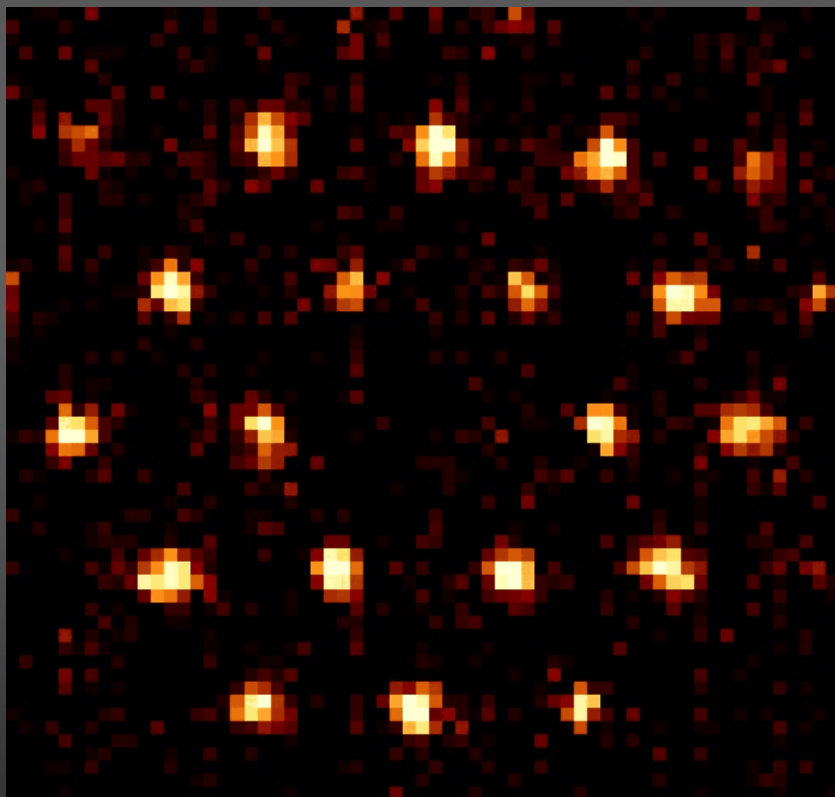
Towards the central arcsecond

Adaptive Optics

distorted wavefront is measured online and straightened via a deformable mirror



Adaptive Optics



Adaptive Optics

Across the aperture the wavefront sensor delivers $m=1 \dots M/2$ positions and M measured gradients of the wavefront ϕ represented via $k=1 \dots K$ Zernicke polynomials as orthogonal wavefront modes:

$$\phi = \sum_{k=1}^K a_k Z_k(x, y)$$

Gradients are then defined via:

$$\left. \frac{\partial \phi}{\partial x} \right|_m = \sum_{k=1}^K a_k \left. \frac{\partial Z_k(x, y)}{\partial x} \right|_m$$

$$\left. \frac{\partial \phi}{\partial y} \right|_m = \sum_{k=1}^K a_k \left. \frac{\partial Z_k(x, y)}{\partial y} \right|_m$$

s are the gradients

a are the modal coefficients

B is the corresponding matrix

$$s = [B]a$$

In detail the quantities in
are given by:

$$s = [B]a$$

Adaptive Optics

$$s = \begin{pmatrix} \left. \frac{\partial \phi}{\partial x} \right|_1 \\ \dots \\ \left. \frac{\partial \phi}{\partial x} \right|_{\frac{M}{2}} \\ \left. \frac{\partial \phi}{\partial y} \right|_1 \\ \dots \\ \left. \frac{\partial \phi}{\partial y} \right|_{\frac{M}{2}} \end{pmatrix}$$

$$a = \begin{pmatrix} a|_1 \\ \dots \\ a|_{\frac{M}{2}} \\ a|_1 \\ \dots \\ a|_{\frac{M}{2}} \end{pmatrix}$$

$$[B] = \begin{pmatrix} \mu_{1,1} & \mu_{2,1} & \dots & \mu_{K,1} \\ \dots & \dots & \dots & \dots \\ \mu_{1,\frac{M}{2}} & \mu_{2,\frac{M}{2}} & \dots & \mu_{K,\frac{M}{2}} \\ \xi_{1,1} & \xi_{2,1} & \dots & \xi_{K,1} \\ \dots & \dots & \dots & \dots \\ \xi_{1,\frac{M}{2}} & \xi_{2,\frac{M}{2}} & \dots & \xi_{K,\frac{M}{2}} \end{pmatrix}$$

with matrix elements:

The model coefficients
are obtained by inverting
the matrix and calculating:

$$\mu_{k,m} = \left. \frac{\partial Z_k(x, y)}{\partial x} \right|_m$$

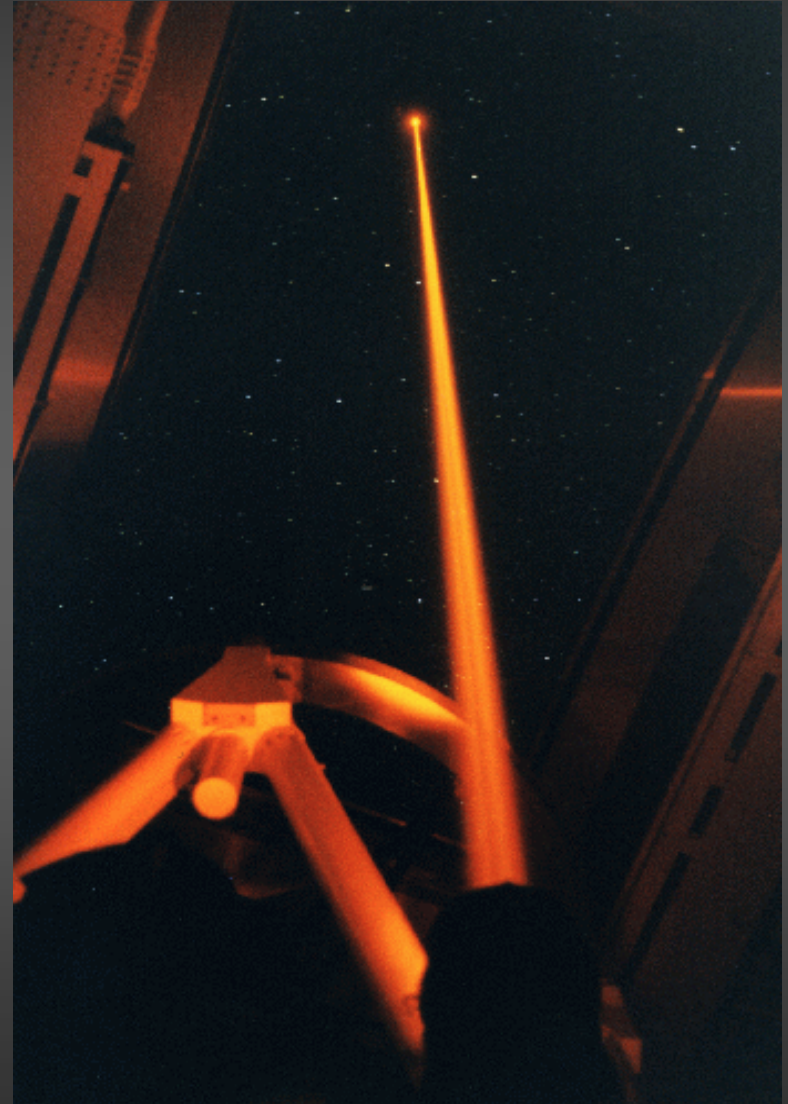
$$\xi_{k,m} = \left. \frac{\partial Z_k(x, y)}{\partial y} \right|_m$$

$$a = [(B^T B)^{-1} B^T] s$$

Calibration with an internal light source gives the
mirror response matrix $[G]$ and the actuator commands g :

$$g = [G]a$$

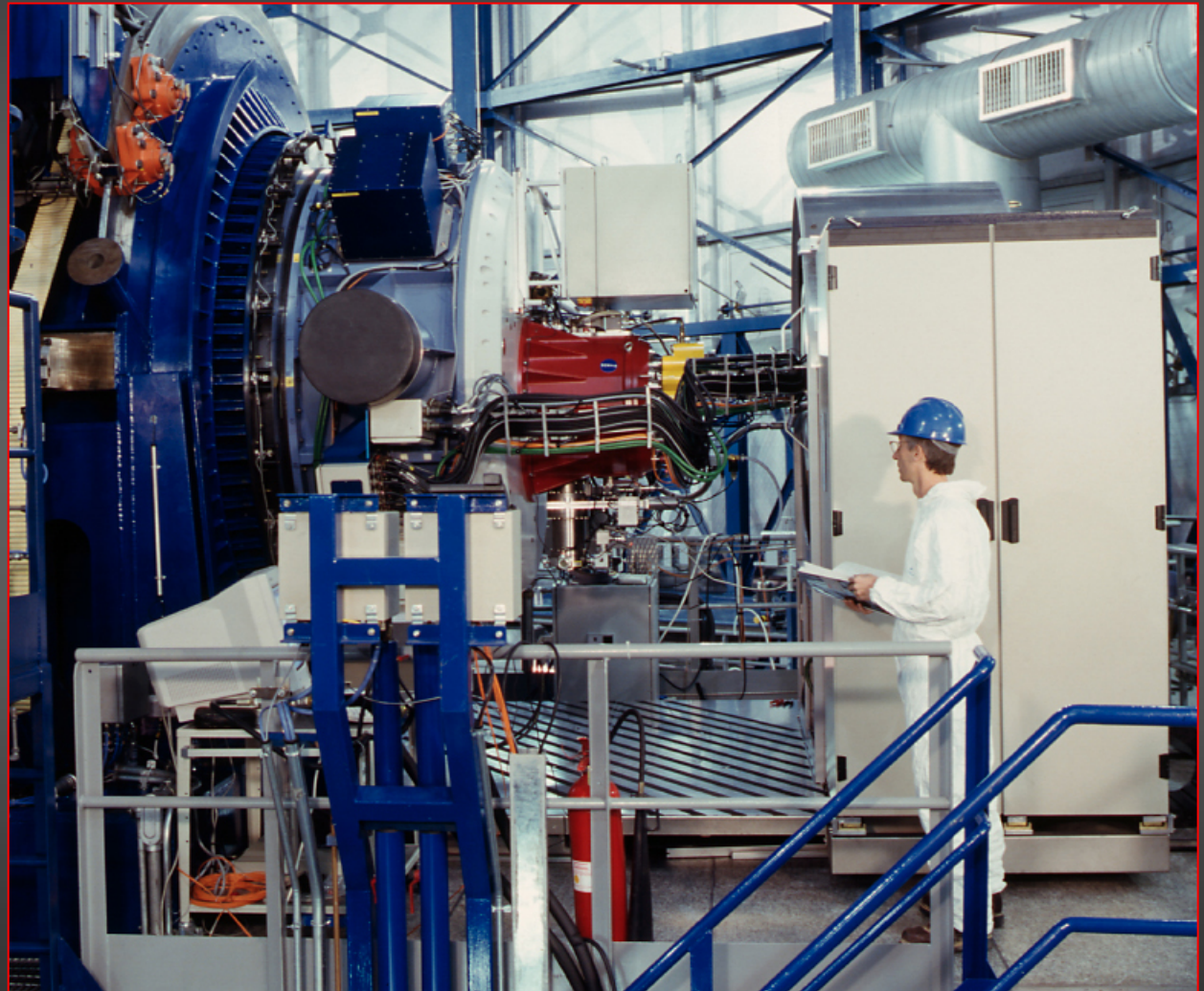
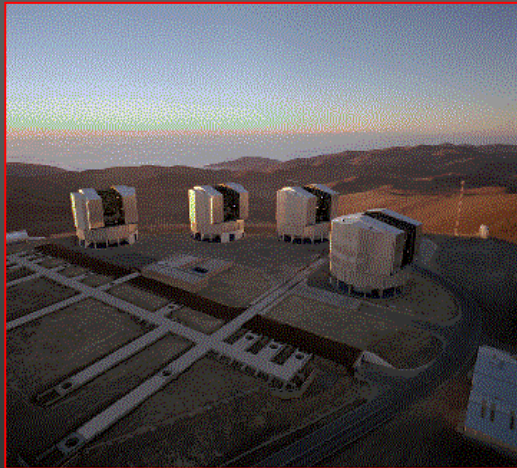
Adaptive Optics



MPE laser guide star at the ALFA Calar Alto AO-System

Adaptive Optics at ESO Paranal

CONICA at
the VLT UT4



Adaptive Optics at ESO Paranal



First Light of the VLT Laser Guide Star

ESO PR Photo 07a/06 (23 February 2006)

© ESO



An Artificial Star Above Paranal

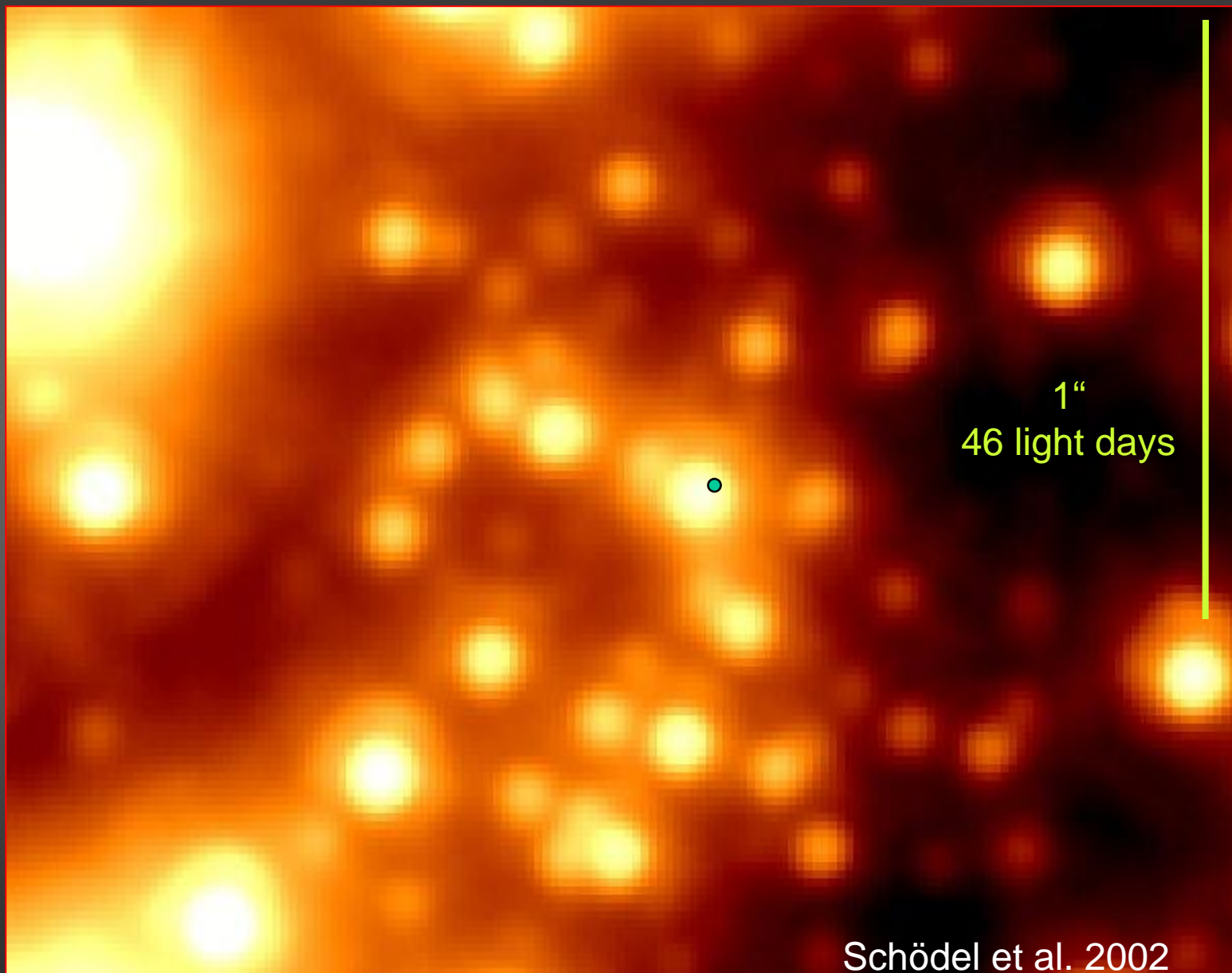
ESO PR Photo 07b/06 (23 February 2006)

© ESO



28 Jan. 2006; 8 W into a fiber

Adaptive Optics at the VLT in Chile

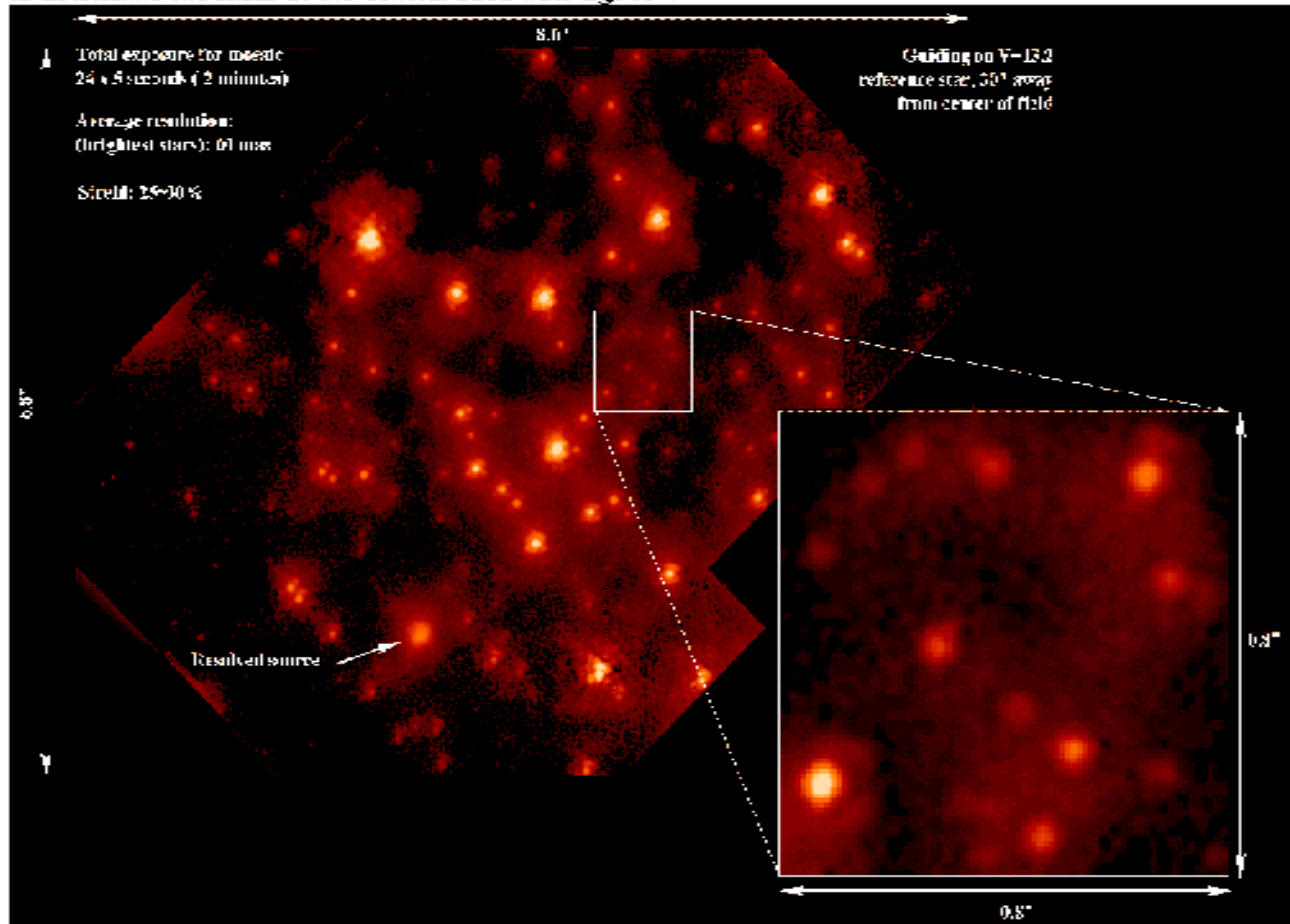


Keck II AO image of the GC

Adaptive Optics at Keck

Galactic Center Keck Adaptive Optics

Mosaic of 24 images (total integration time: 120 seconds), this image shows the very central area of our own galaxy, the Milky Way. It was obtained on May 26th, 1999. The central arcsecond (inset) will help to determine the mass of the central black hole Sgr A*.



Position of the central mass
from accelerations

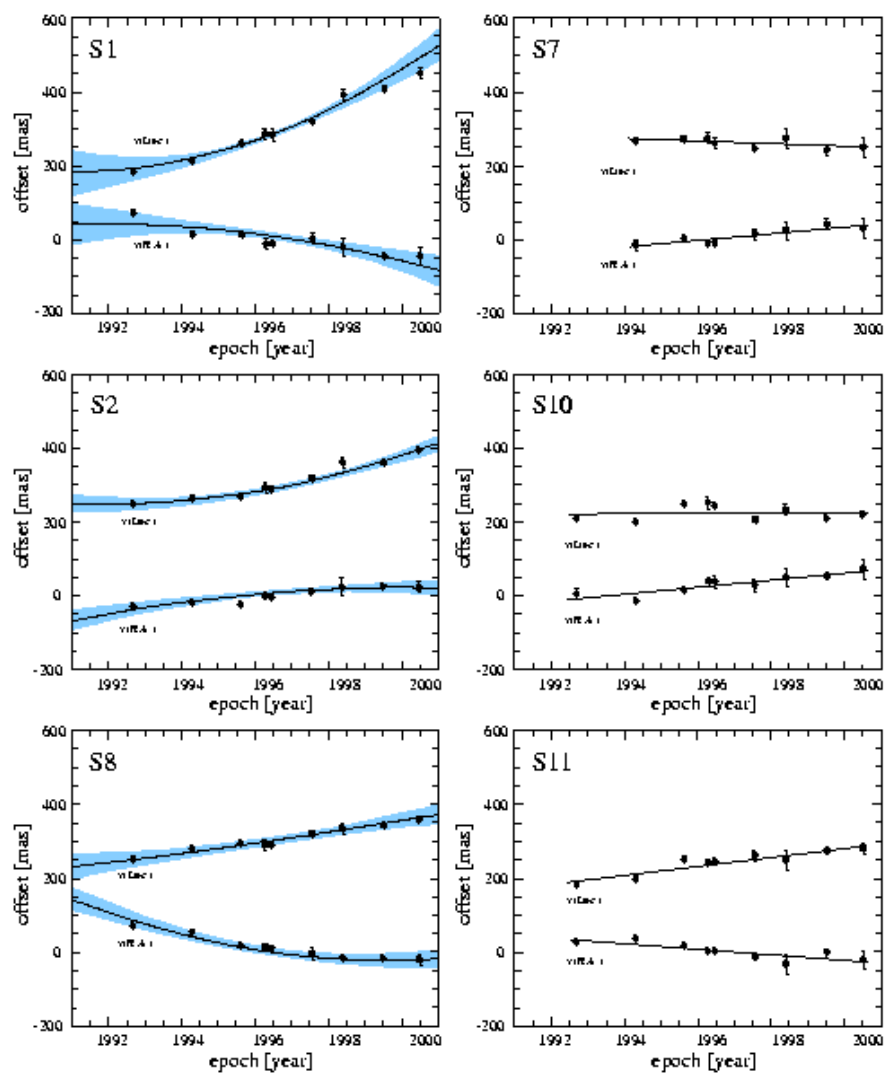
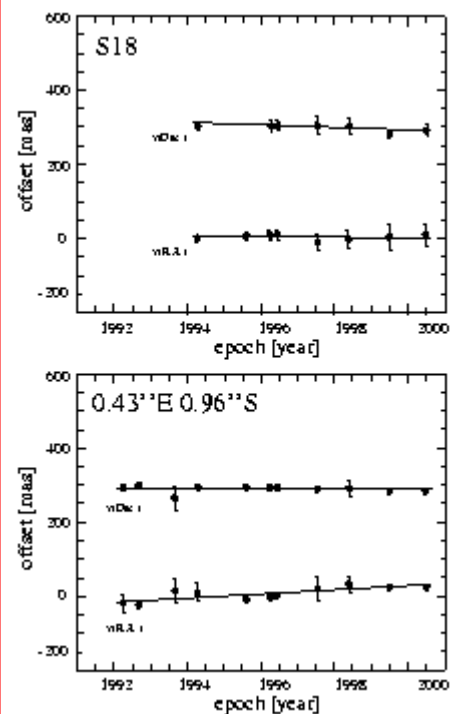


Fig.1



The Galactic Center

Newton's law:

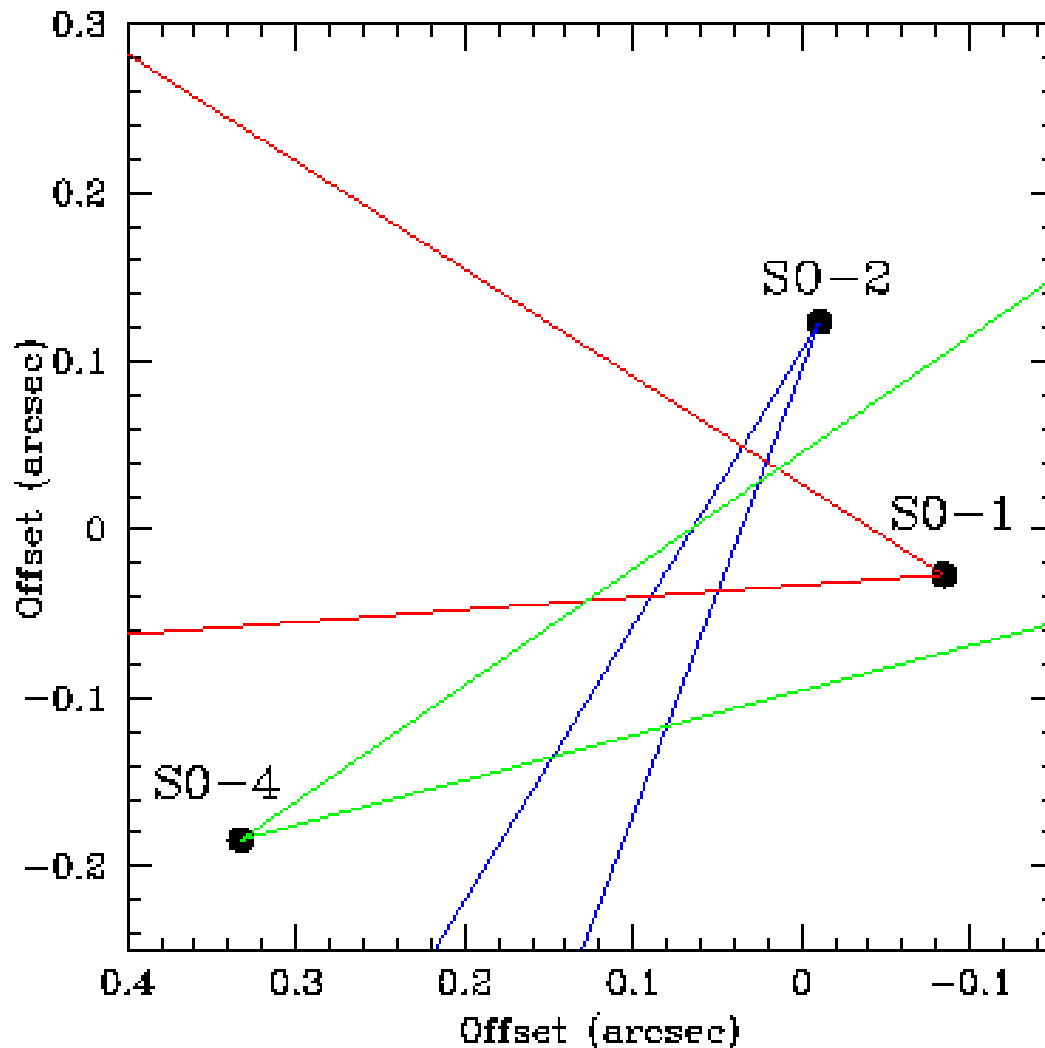
$$\vec{F} = m\vec{a} = -G \frac{Mm}{r^2} \frac{\vec{r}}{r}$$

Acceleration vector points towards mass center!

Mass estimate from accelerations:

$$M \cos^3(\vartheta) = 8681 \frac{a[\text{mas} / \text{yr}^2] r^2[\text{pc}]}{G}$$

The Galactic Center



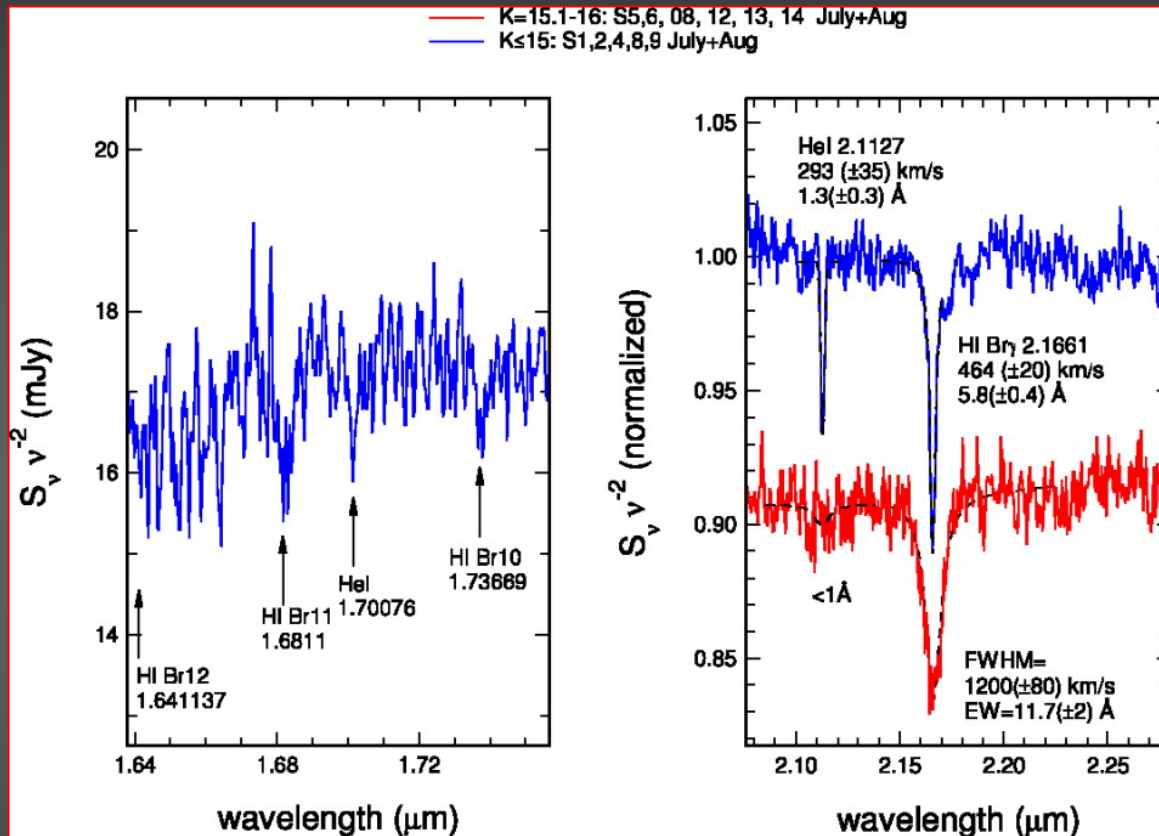
Acceleration vectors

SgrA* is included in the acceleration error cones of S1, S2, and S8.

Ghez , Morris, Becklin, Kremenek, & Tanner 2000, Nature 407, 349; astro-ph/0009339

Orbits of the central stars
from multiple positions and velocities

High Velocity B-Stars in the Central Arcsecond



B0-B2 V stars

Br γ FWHM 460 km/s

HeI FWHM 293 km/s

$R_{\text{inst}} \sim 80$ km/s

$\langle v_{\text{rot}} \sin(i) \rangle = 0.55$ FWHM

= 154 (± 19) km/s

Gathier, Lamers & Snow (1981): 130 km/s

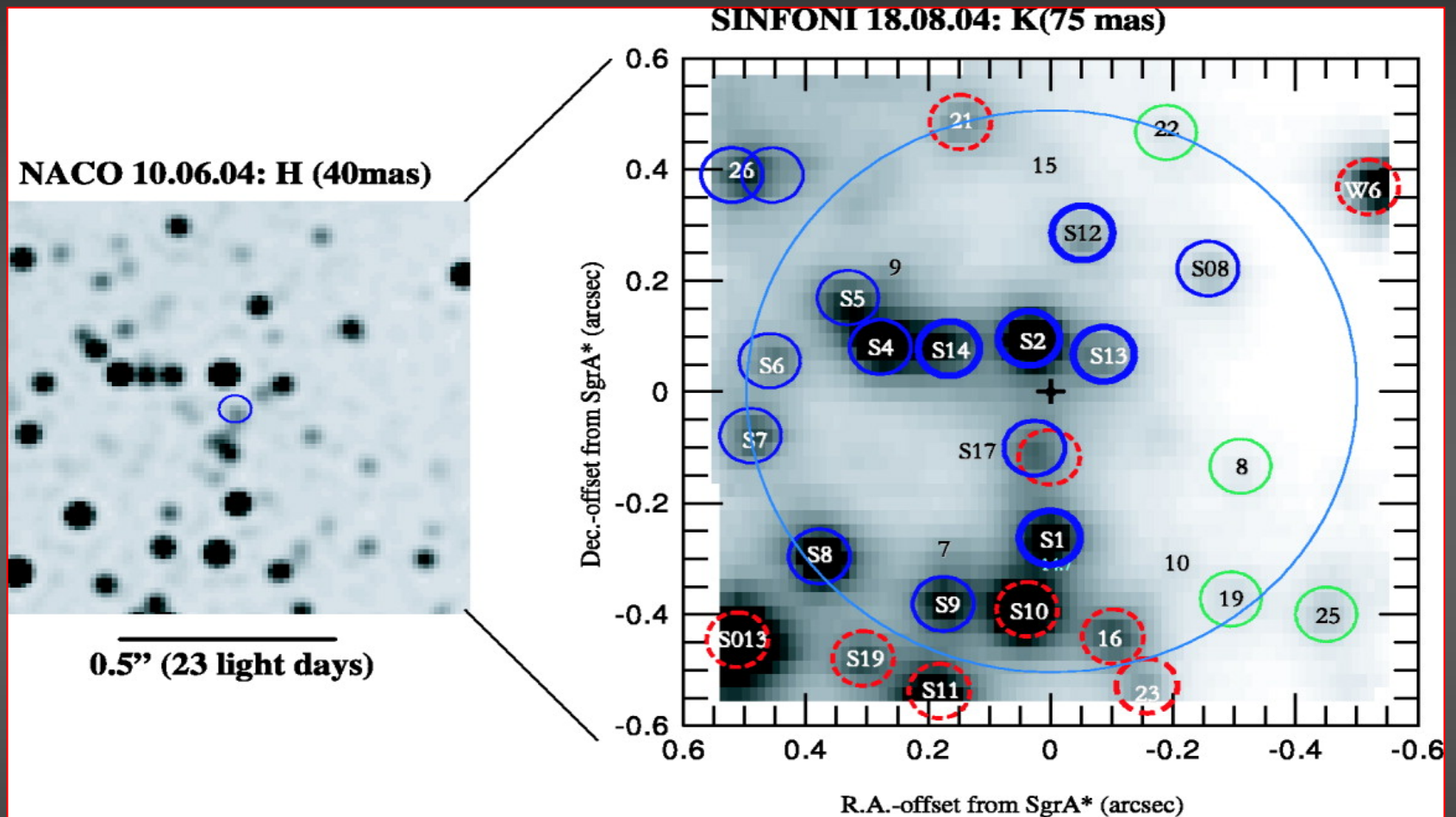
B4-9V stars

Br γ FWHM 1200 km/s

Eisenhauer et al. 2005

S-stars are normally rotating B stars

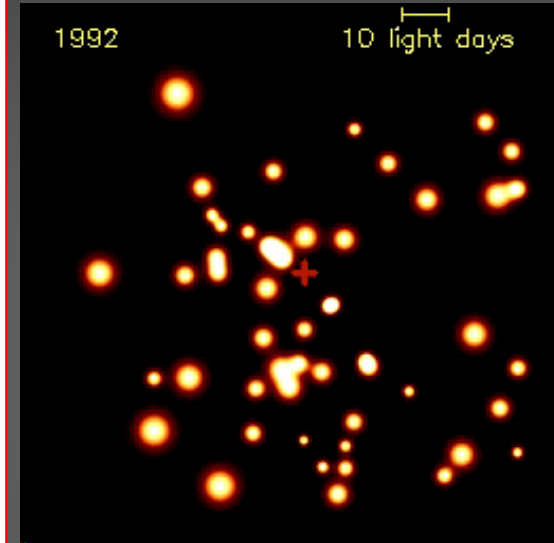
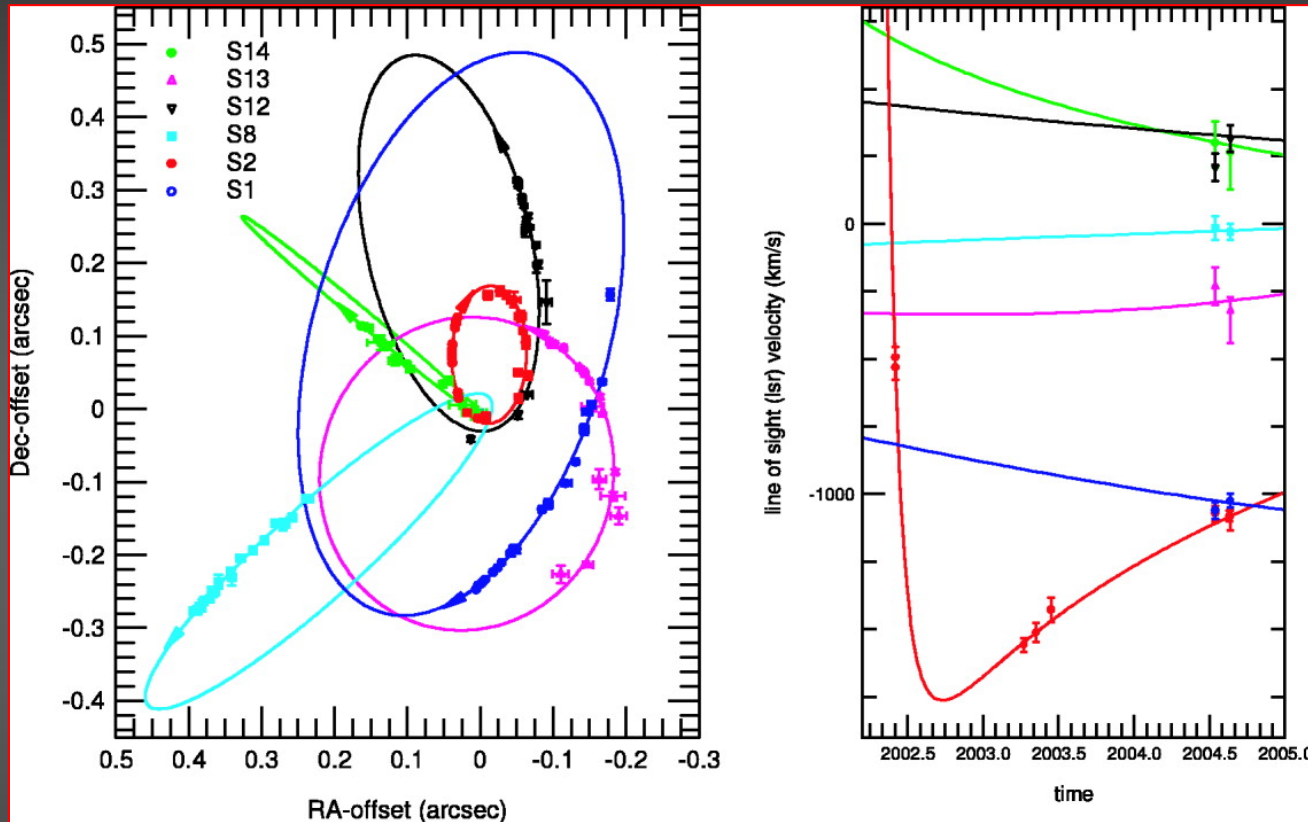
High Velocity Early Type Stars in the Central Arcsecond



Eisenhauer et al. 2005

- late type
- early type
- uncertain but not late type

Orbits of High Velocity Stars in the Central Arcsecond



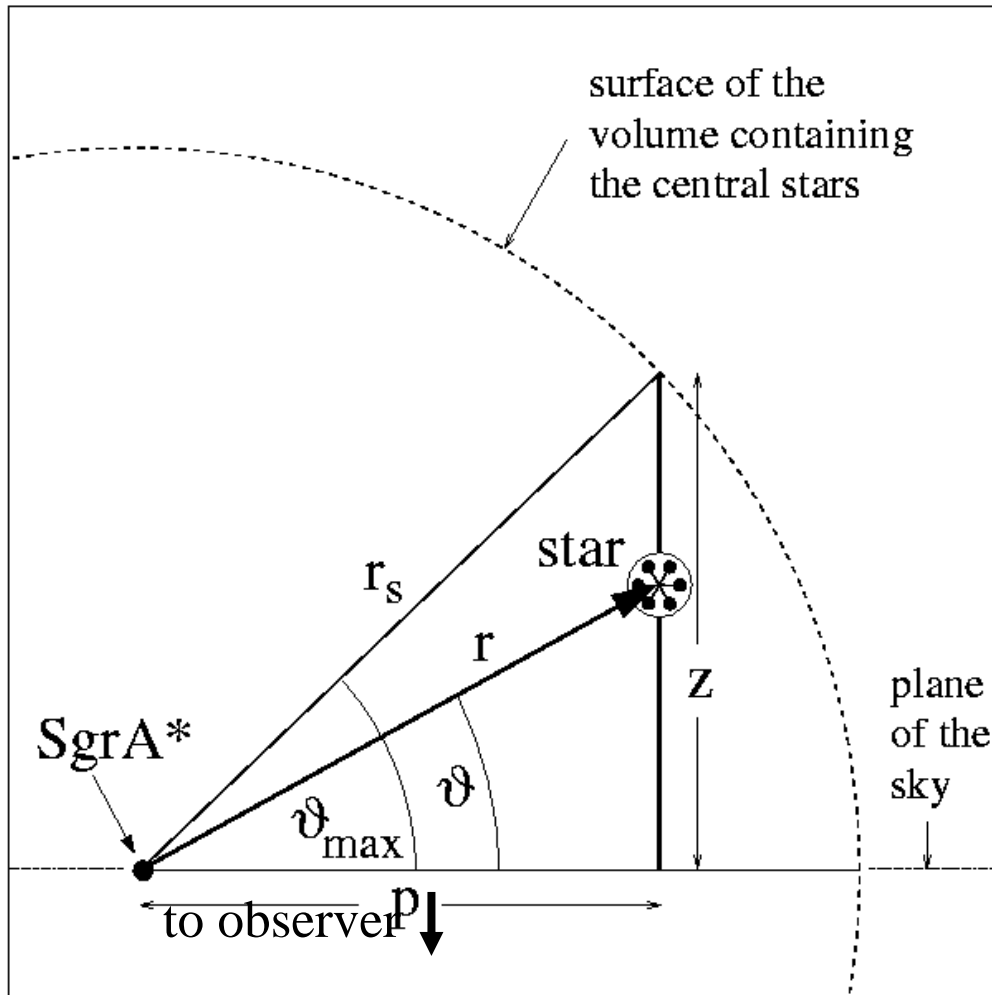
Eckart et al. 2002 (S2 is bound; first elements)
 Schödel et al. 2002, 2003 (first detailed elements)
 Ghez et al 2003 (detailed elements)
 Eisenhauer 2005 (improved elements and distance)

*Mass of the BH at the position of SgrA**

Mass and mass distribution

Enclosed mass estimate
from accelerations

The Galactic Center



Geometry for stars
at the Galactic Center:

Projection of the
acceleration vector
onto the plane of the
sky in which $SgrA^*$
is located.

$$P(V > v_{star}, R) =$$

$$1 - P(V < v_{star}, R) =$$

$$1 - \frac{1}{\sigma} \int_0^{v_{star}} v \times \exp\left(-v^2 / (2\sigma^2)\right) dv$$

$S1, S2, S8$ are within
a 15 mpc ($0.4''$) radius
sphere around $SgrA^*$

The Galactic Center

Newton's law:

$$\vec{F} = m\vec{a} = -G \frac{Mm}{r^2} \frac{\vec{r}}{r}$$

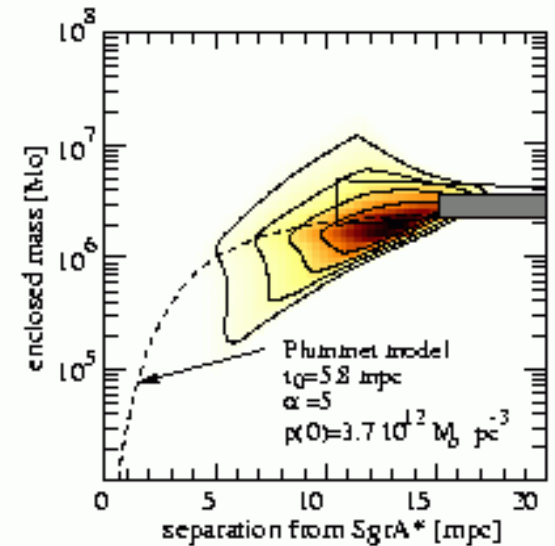
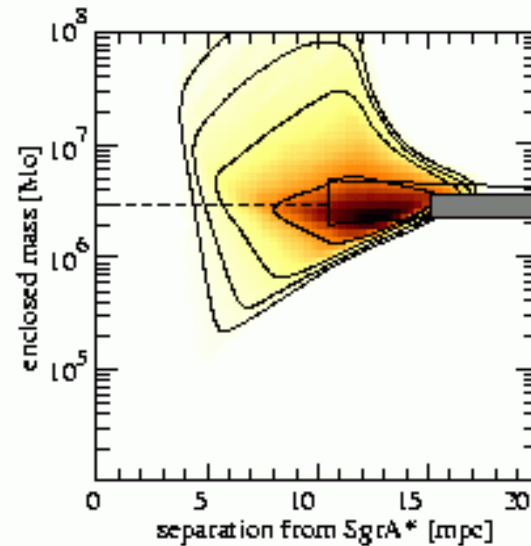
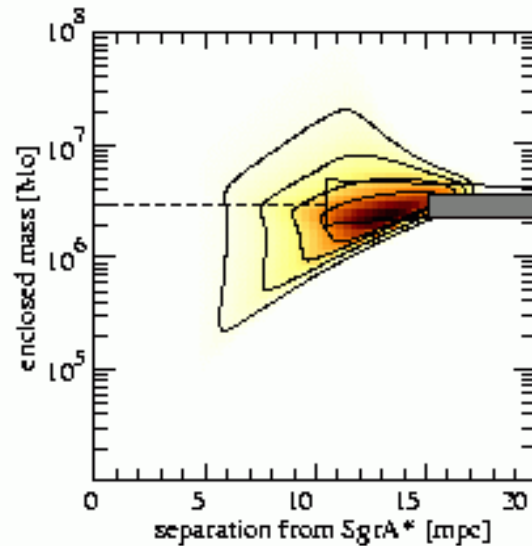
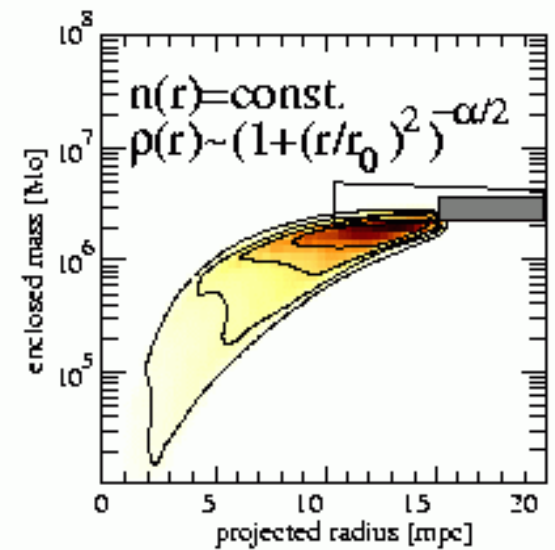
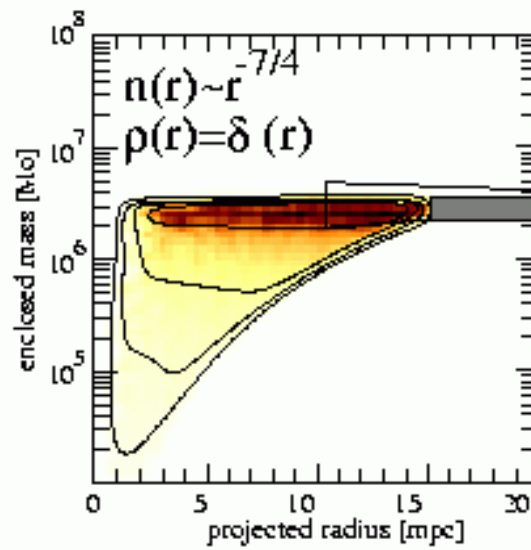
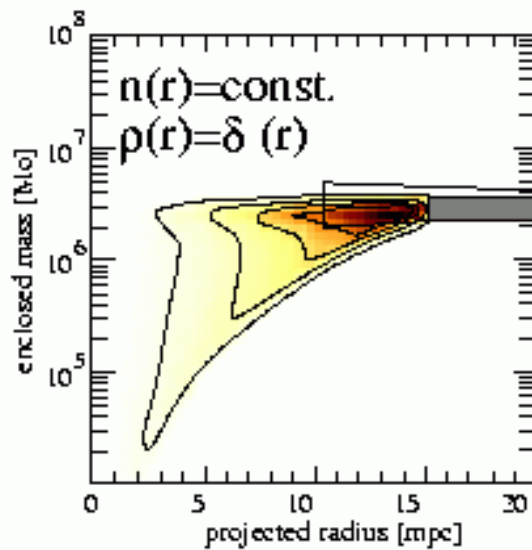
Acceleration vector points towards mass center!

Mass estimate from accelerations:

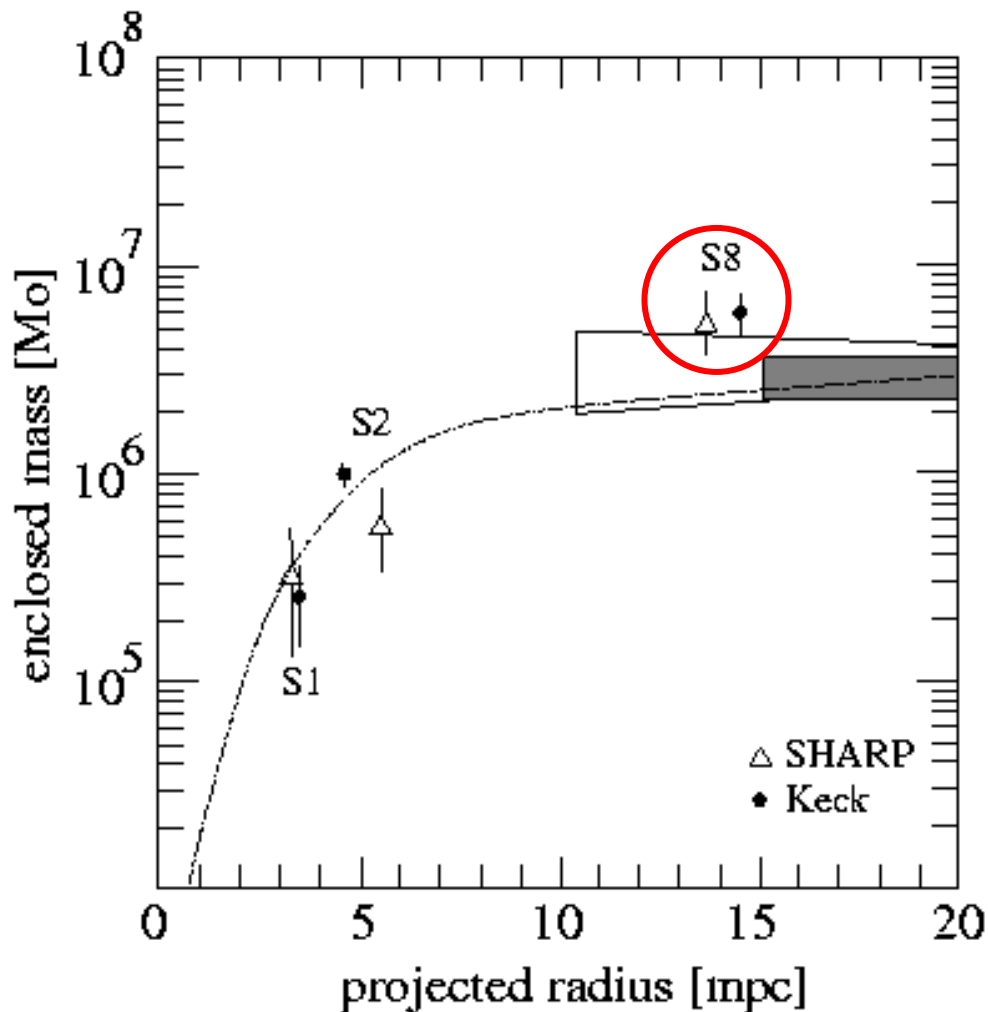
$$M \cos^3(\vartheta) = 8681 \frac{a[\text{mas} / \text{yr}^2] r^2[\text{pc}]}{G}$$

The Galactic Center

Statistical deprojection of the radii and accelerations for a volume of $0.4'' \pm 0.1''$



The Galactic Center

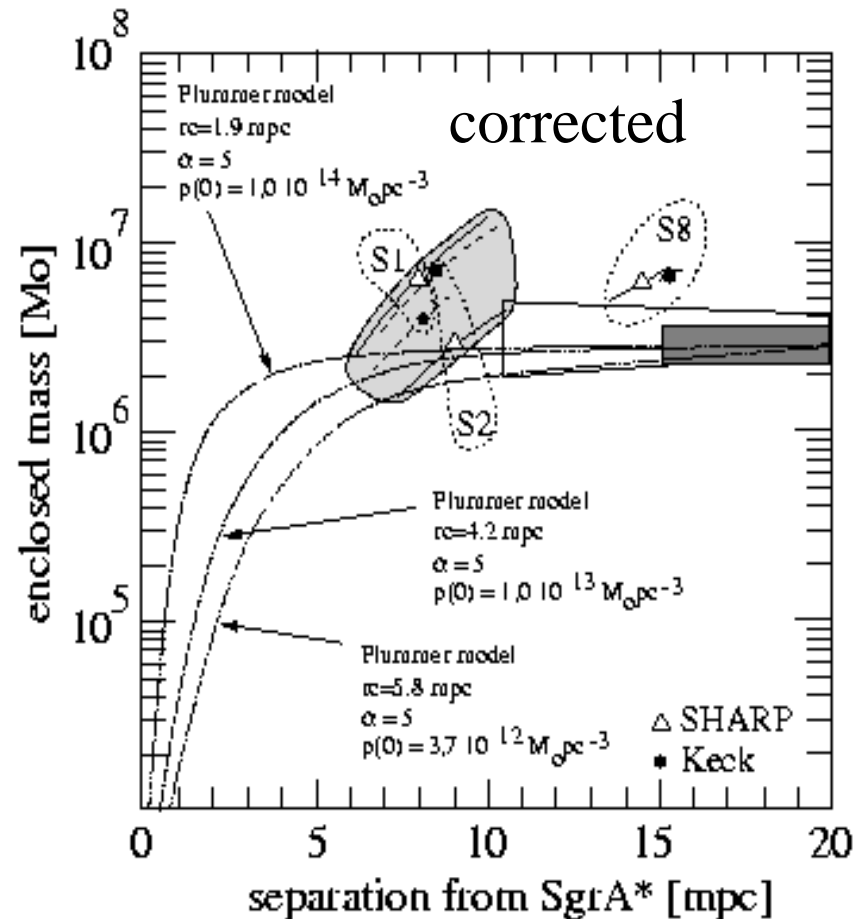
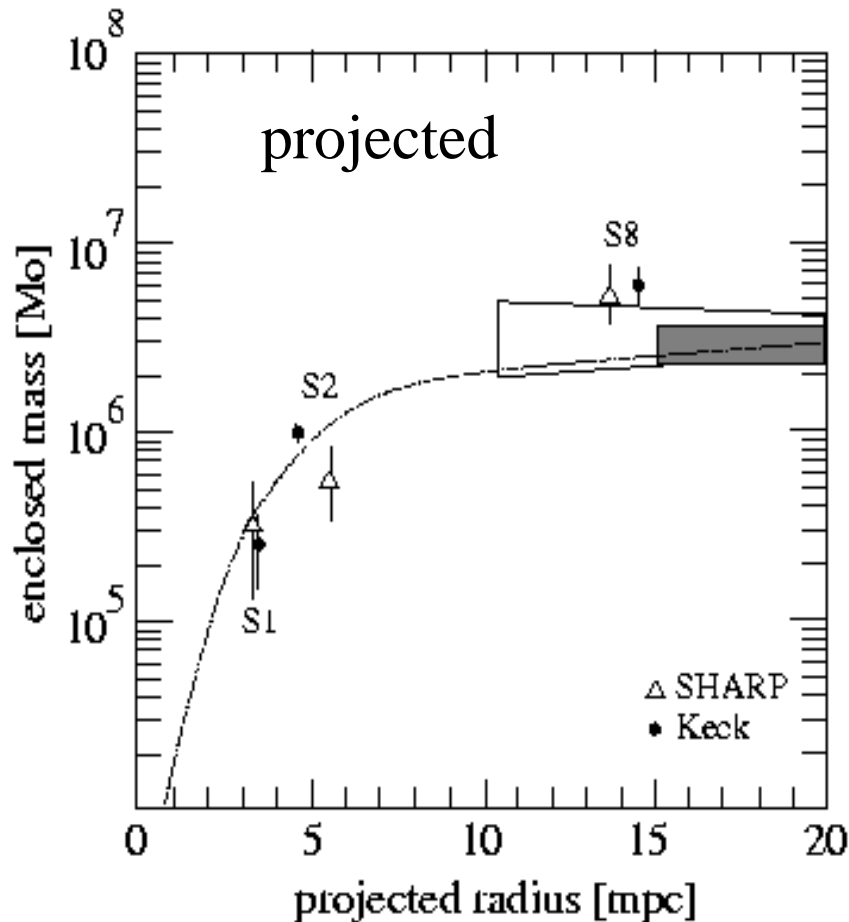


Projected enclosed mass estimates from projected radii and accelerations. These numbers are only **lower limits** of the actual enclosed mass!!

The enclosed mass estimate from the acceleration of S8 is currently too high.

The Galactic Center

Enclosed mass estimate based on accelerations



Mass Estimators

Enclosed Mass: First Order Estimates

Mass enclosed within projected radius p , assuming that the stars are just bound i.e. on ellipses:

$$E_{kin} = \frac{1}{2}mv^2 < G \frac{Mm}{p}$$

The minimum enclosed mass is then:

$$M_{\min}(< p) \geq \frac{v_{sky}^2 p}{2G}$$

For individual stars (few hundred km/s @ a few 10mpc distance) one then get of the order of 1000.000 solar masses.

Enclosed Mass: Mass Estimators

The mass estimator derived from the virial theorem assumes a homogenous distribution of stars and an isotropic velocity field:

$$M_{\text{virial}} = \frac{3\pi}{2G} \frac{\sum_i w(i) v_i^2}{\sum_i w(i) / p_i}$$

The mass estimator derived by Bahcall & Tremaine assumes that the stars are on isotropic orbits that are dominated by a central mass:

$$M_{BT} = \frac{16}{\pi G \sum_i w(i)} \sum_i w(i) p_i v_i^2$$

For the inner most ensemble of stars both estimators result in approximately 3 million solar masses with <10 mpc.

Jean's Method

Form the collisionless Boltzmann equation

Jeans mass

$$\frac{\partial f}{\partial t} + v \nabla f + \nabla \Phi \frac{\partial f}{\partial v} = 0$$

With the stellar phase space density

$$f = f(t, r, v)$$

and a spherical system with

$$\sigma_{\phi}^2(r) = \sigma_g^2(r)$$

One can deduce the Jeans Equation :

$$\Phi = \frac{GM(r)}{r} = v_{rot}^2(r) - \sigma_r^2(r) \left\langle \frac{d \ln(n(r))}{d \ln(r)} + \frac{d \ln(\sigma_r(r))}{d \ln(r)} + 2\beta \right\rangle$$

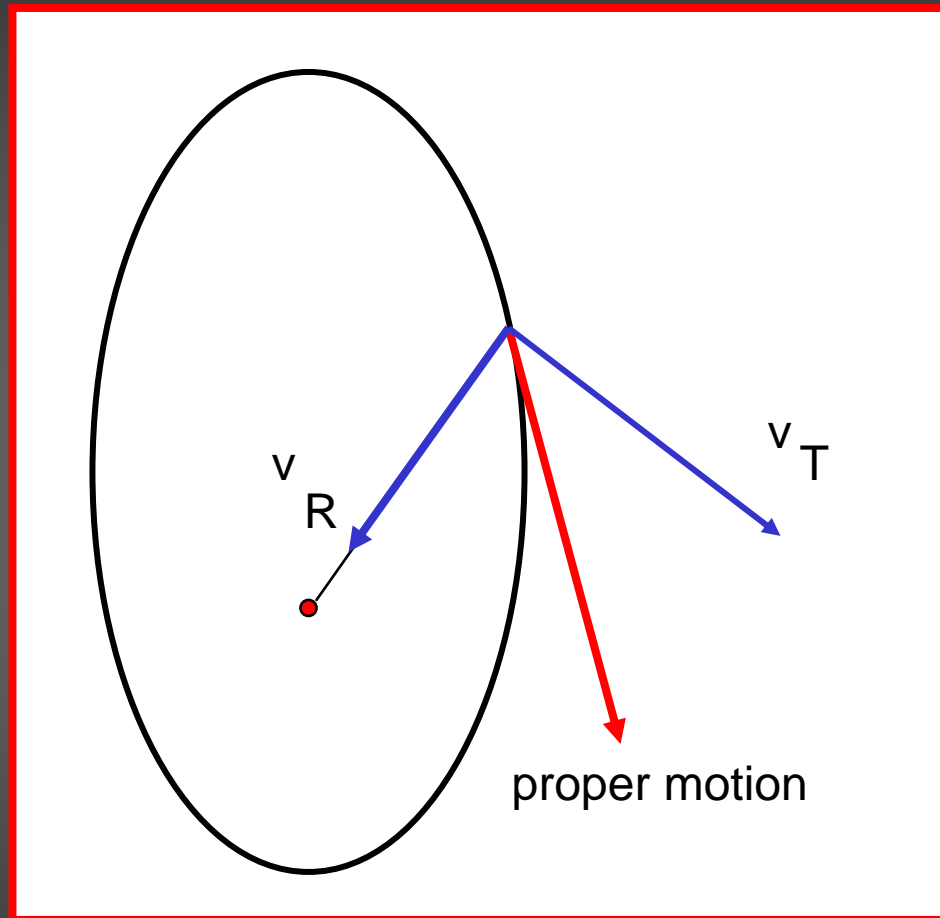
The Jeans-Mass

$$M(r) = f(v_{rot}(r), \sigma_r(r), n_r(r), \beta)$$

Contains β as a measure for the anisotropy of the (3-dimensional) velocity field:

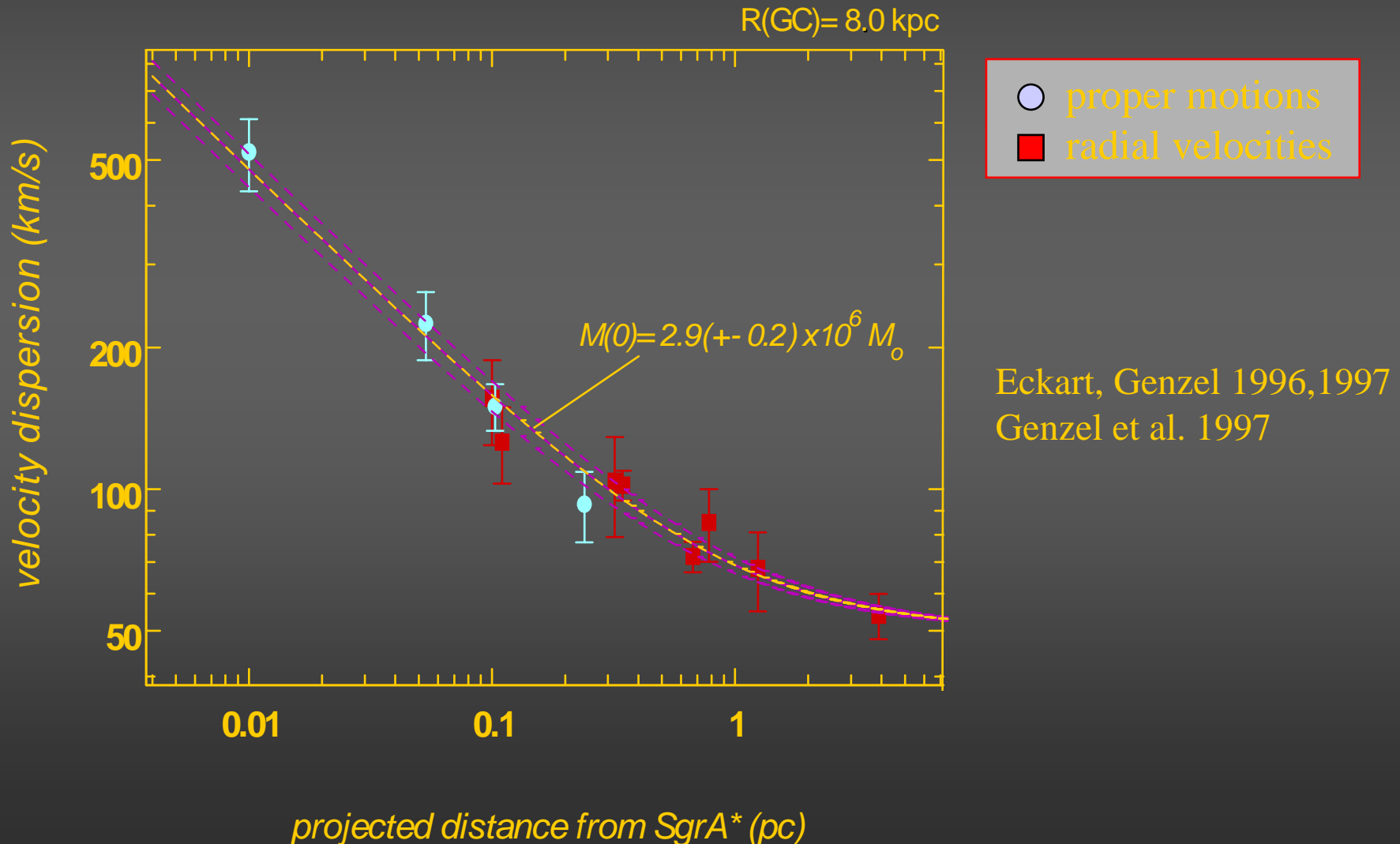
$$\beta = 1 - \frac{\sigma_g^2(r)}{\sigma_r^2(r)}$$

The Galactic Center

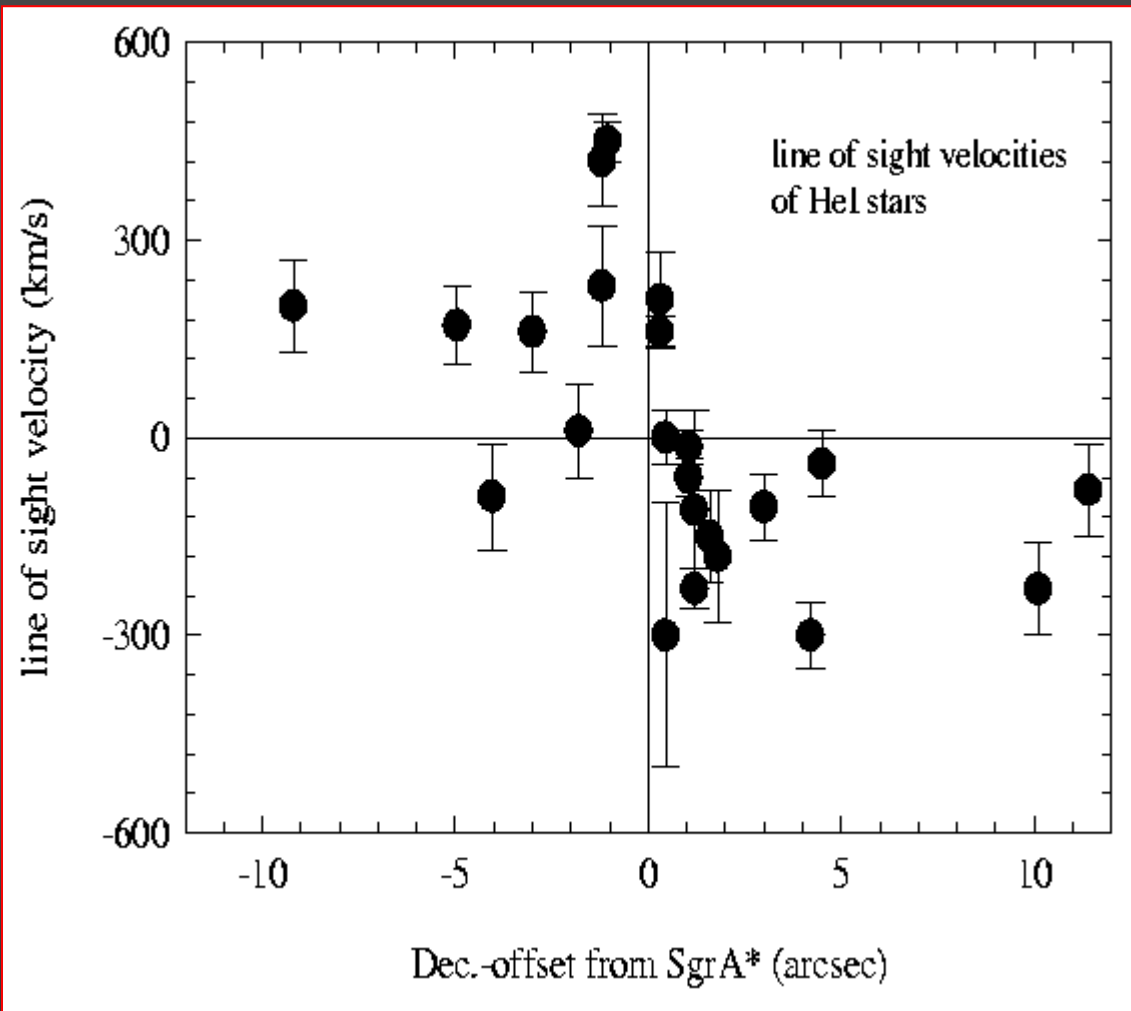


The observable projected velocity vector can be decomposed into velocity vectors in tangential T and radial R direction in the plane of the sky.

*Velocity as a function of separation from SgrA**



Counter rotation of the central stellar cluster in radial velocities

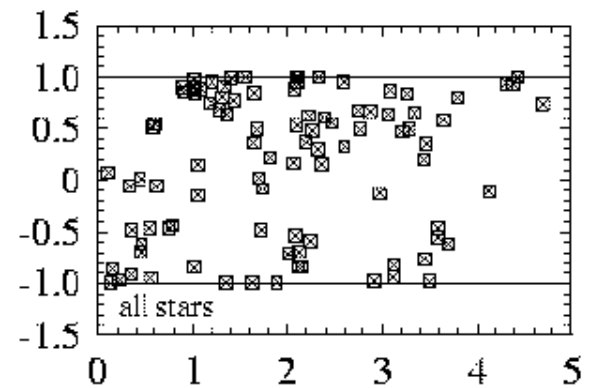
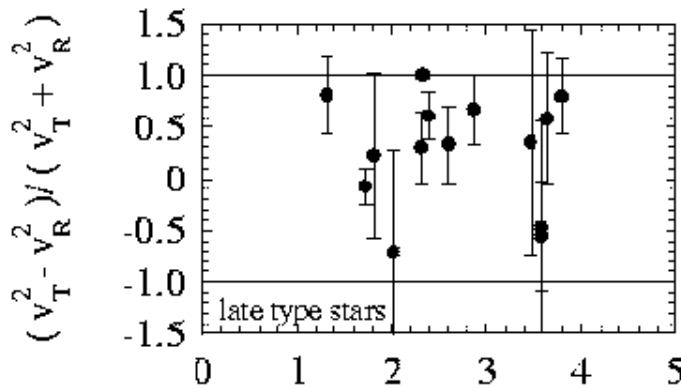
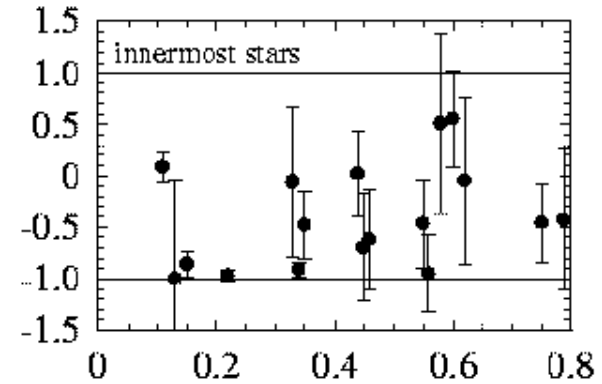
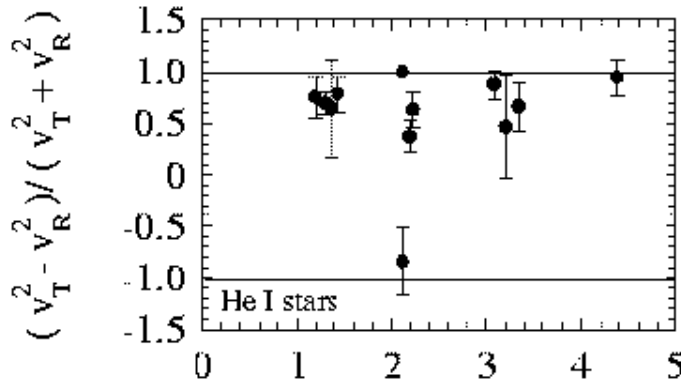


The Galactic Center

Indications for anisotropies in the proper motion velocity field

Genzel, Pichon, Eckart,
Gerhard, Ott, 2000,
MNRAS 317, 348

$$\gamma = (v_T^2 - v_R^2) / (v_T^2 + v_R^2)$$



offset from SgrA* (arcsecs)

offset from SgrA* (arcsecs)

The Galactic Center

$$\langle \beta \rangle = 1 - \frac{\langle \sigma_t^2 \rangle}{\langle \sigma_r^2 \rangle} = 3 \frac{\langle \sigma_R^2 \rangle - \langle \sigma_T^2 \rangle}{3\langle \sigma_R^2 \rangle - \langle \sigma_T^2 \rangle}$$

The anisotropy measure β is defined via 3-dimensional velocity dispersions (tangential t and radial r). It has, however, been shown how it is linked to observable projected velocity dispersions of motions in tangential T and radial R direction in the orbits projected onto the plane of the sky (Leonard & Merritt 1989).

The Galactic Center

The projected velocity dispersion $\sigma(R)$ and surface density $\Sigma(R)$ are linked to the 3-dimensional quantities $n(r)$ and $\sigma(r)$ via Abel integral equations.

$$\Sigma(R) = 2 \int_r^\infty n(r) r dr / \sqrt{(r^2 - R^2)}$$

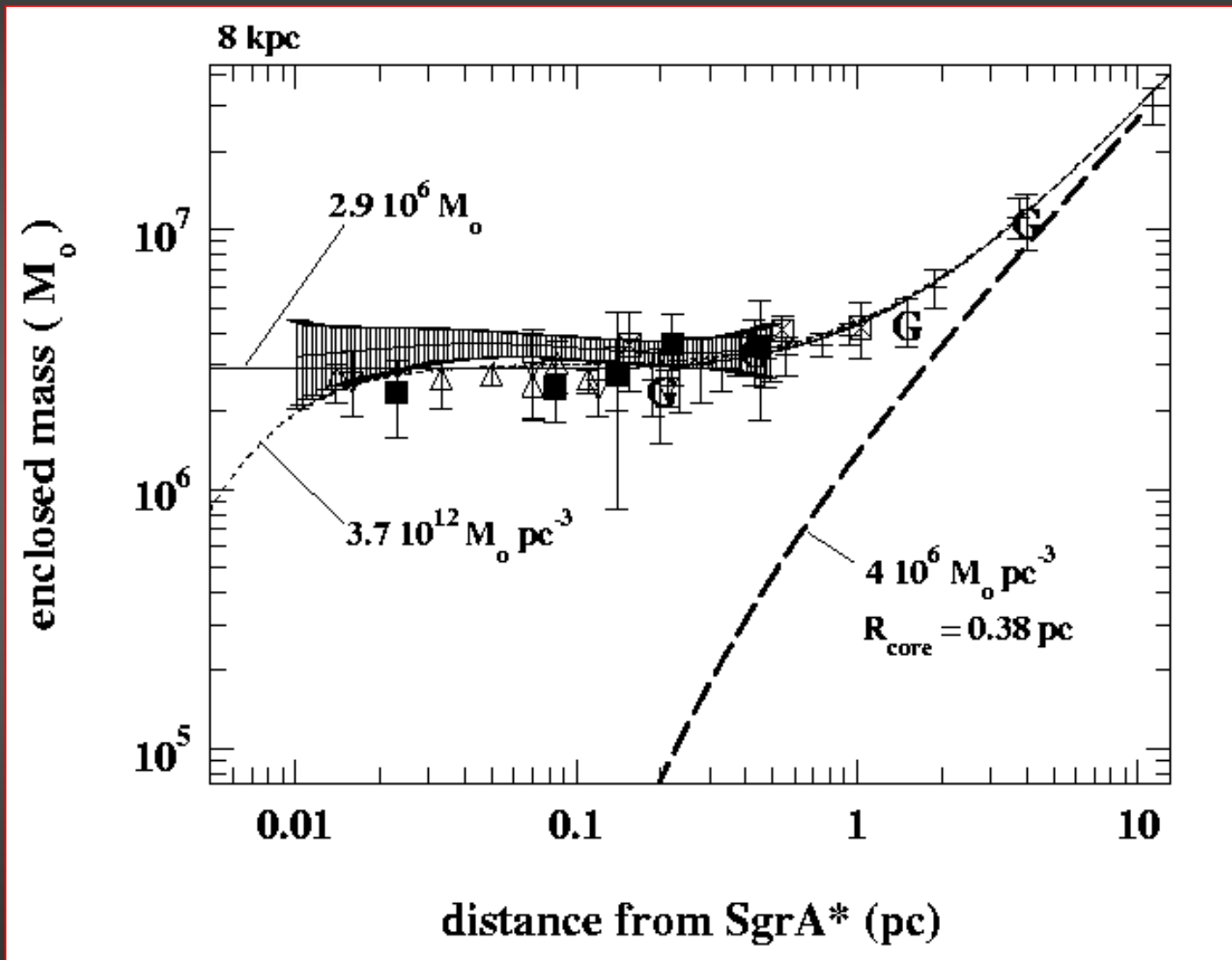
$$\Sigma(R) \sigma_R(R)^2 = \int_r^\infty n(r) \sigma_r(r)^2 r dr / \sqrt{(r^2 - R^2)}$$

The 3-dimensional quantities $n(r)$ and $\sigma(r)$ can be modeled via analytical expressions in the target space to fit the data in the observer space via the Abel integral equations .

$$n(r) = (\Sigma_o / r_o) [1 + (r / r_o)^\alpha]^{-1}$$

$$\sigma_r(r)^2 = \sigma(\infty)^2 + \sigma(r_0)^2 (r / r_0)^{-2\varepsilon}$$

Enclosed mass towards the center of the Galaxy



The Galactic Center

With a spherical potential

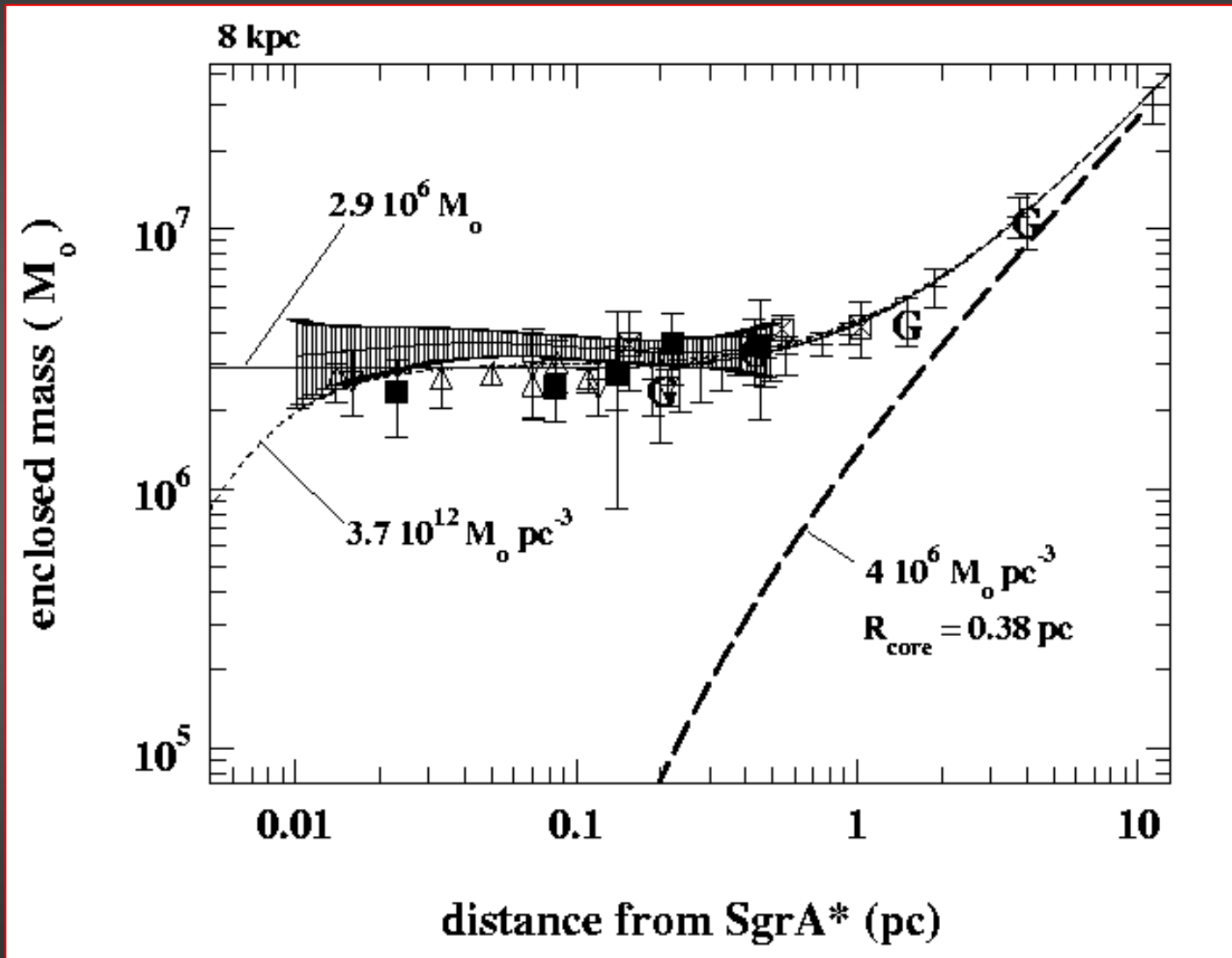
$$\Phi = -\frac{GM}{\sqrt{(r^2 + b^2)}}$$

one finds for spherical stellar systems a volume density

$$\rho = \frac{\rho_0}{(1 + (r/b)^2)^{5/2}}$$

also called Plummer model (Plummer 1911)

Enclosed mass towards the center of the Galaxy



Mass and mass density for SgrA*

With

follows

$$M_{SgrA*} \approx 3.0 \times 10^6 M_o$$

$$\rho_{SgrA*} \geq 4 \times 10^{12} M_o pc^{-3}$$

This has to be compared with the mass density of a
3 Millionen Mo black hole within a Schwarzschild
sphere of 8×10^{-4} cm diameter:

$$\rho_{SgrA*} \geq 4.4 \times 10^{25} M_o pc^{-3}$$

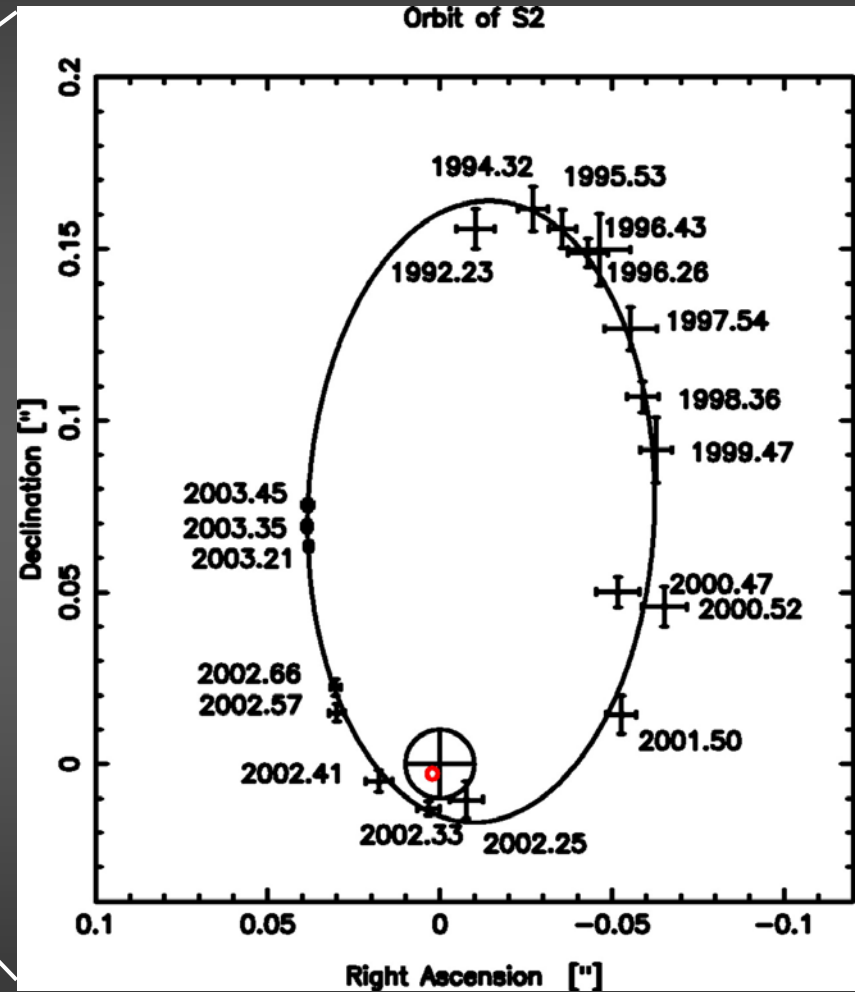
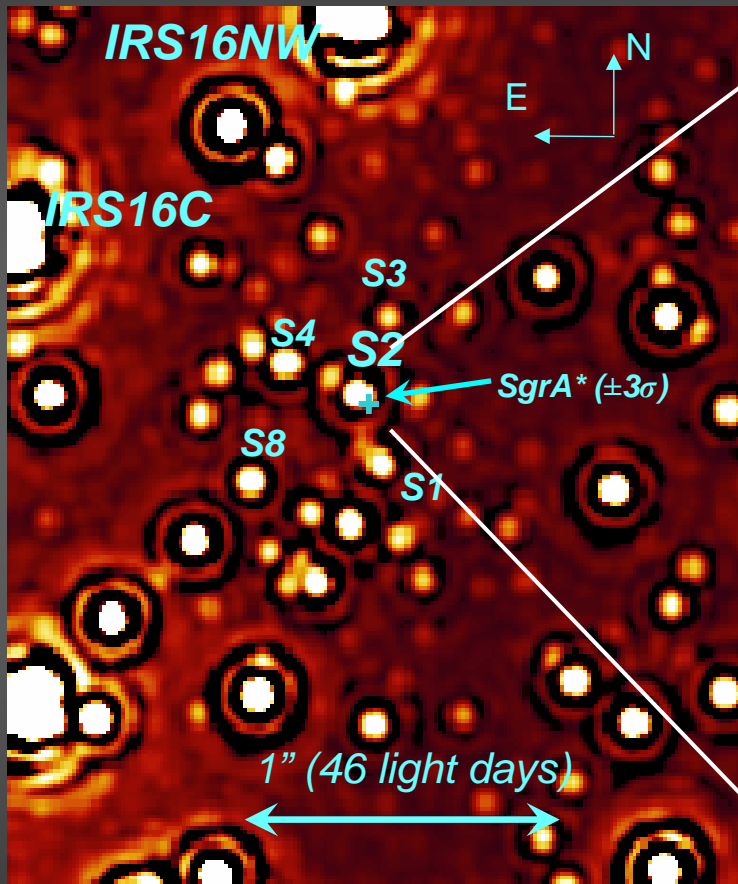
Derived from stellar
statistics within the central
few arcseconds.

Genzel, Eckart, Ott, Eisenhauer 1997
Ghez, Klein, Morris, Becklin 1998
Eckart, Ott, Genzel 1999
Genzel et al. 2000

Mass from the S2 Orbit

Mass and mass density from a single star!

The Orbit of S2 near SgrA*



Schödel, Genzel, Eckart, Ott, Reid, Alexander et al., *Nature* 419, 694, 2002
 Eisenhauer et al. 2004, *ApJ* 597, L121, 2004

Enclosed Mass from S2 Orbit

Kepler's laws give

$$M_{S2} = \frac{4\pi^2}{G} \frac{a^3}{T^2}$$

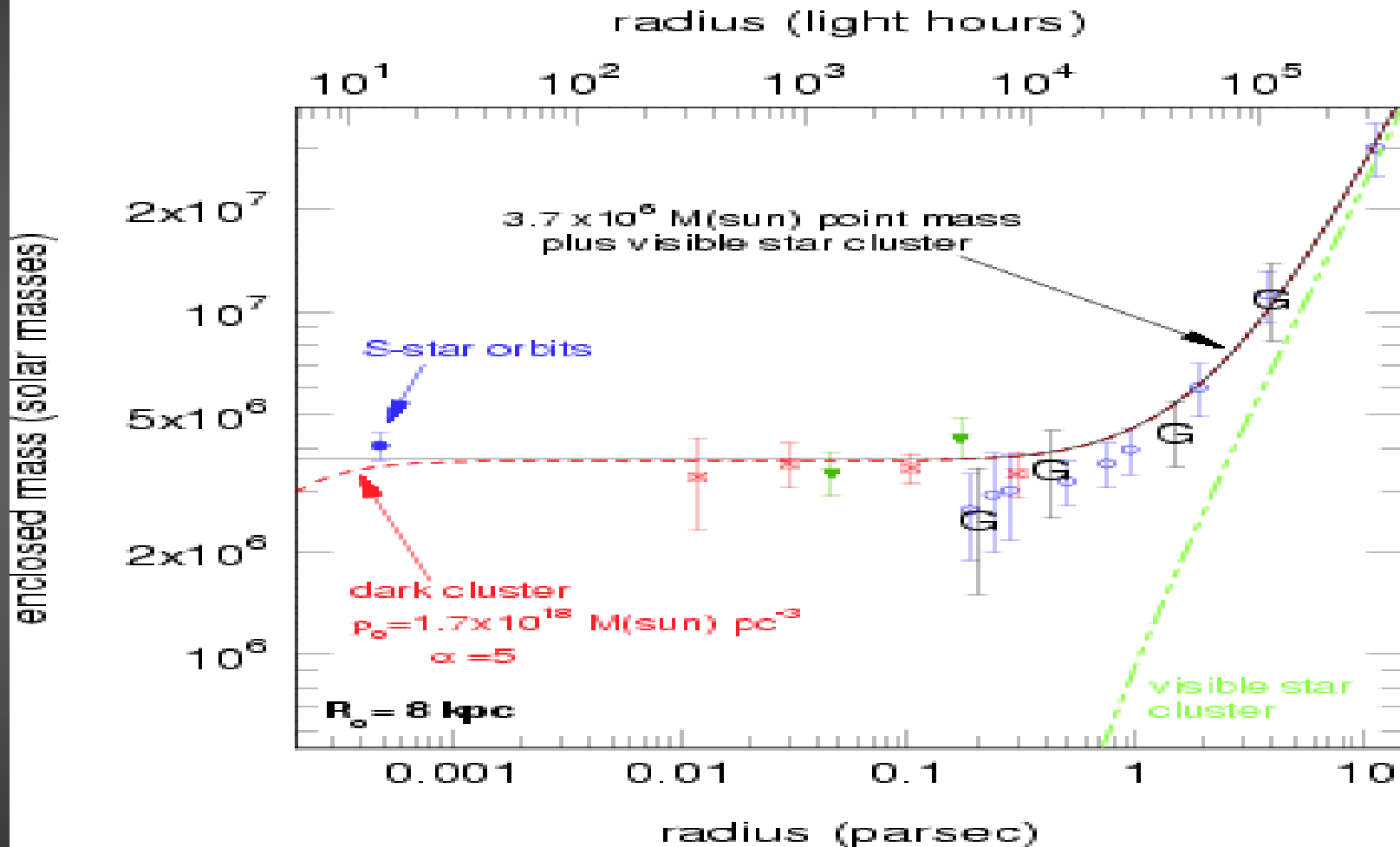
For an orbital period T and a semi major axes a .

For S2 this results into:

$$M_{SgrA*} \approx (3.61 \pm 0.32) \times 10^6 M_{\odot}$$

One can solve for the distance at the same time: 7.62 ± 0.32 kpc

Unresolved Enclosed mass



see Genzel et al. 1996, 2000, Eckart et al. 2002, Schödel et al. 2002, 2003

Mass and mass density for SgrA* from the Recent S2 Orbit

$$M_{SgrA*} \approx (3.6 \pm 0.3) \times 10^6 M_{\odot}$$

$$\rho_{SgrA*} \geq 10^{17} M_{\odot} pc^{-3}$$

This has to be compared with the mass density of a
3 Millionen M_{\odot} black hole within a Schwarzschild
sphere of 8×10^{11} cm diameter:

$$\rho_{SgrA*} \geq 4.4 \times 10^{25} M_{\odot} pc^{-3}$$

Schödel et al. 2002

Eckart et al. 2002

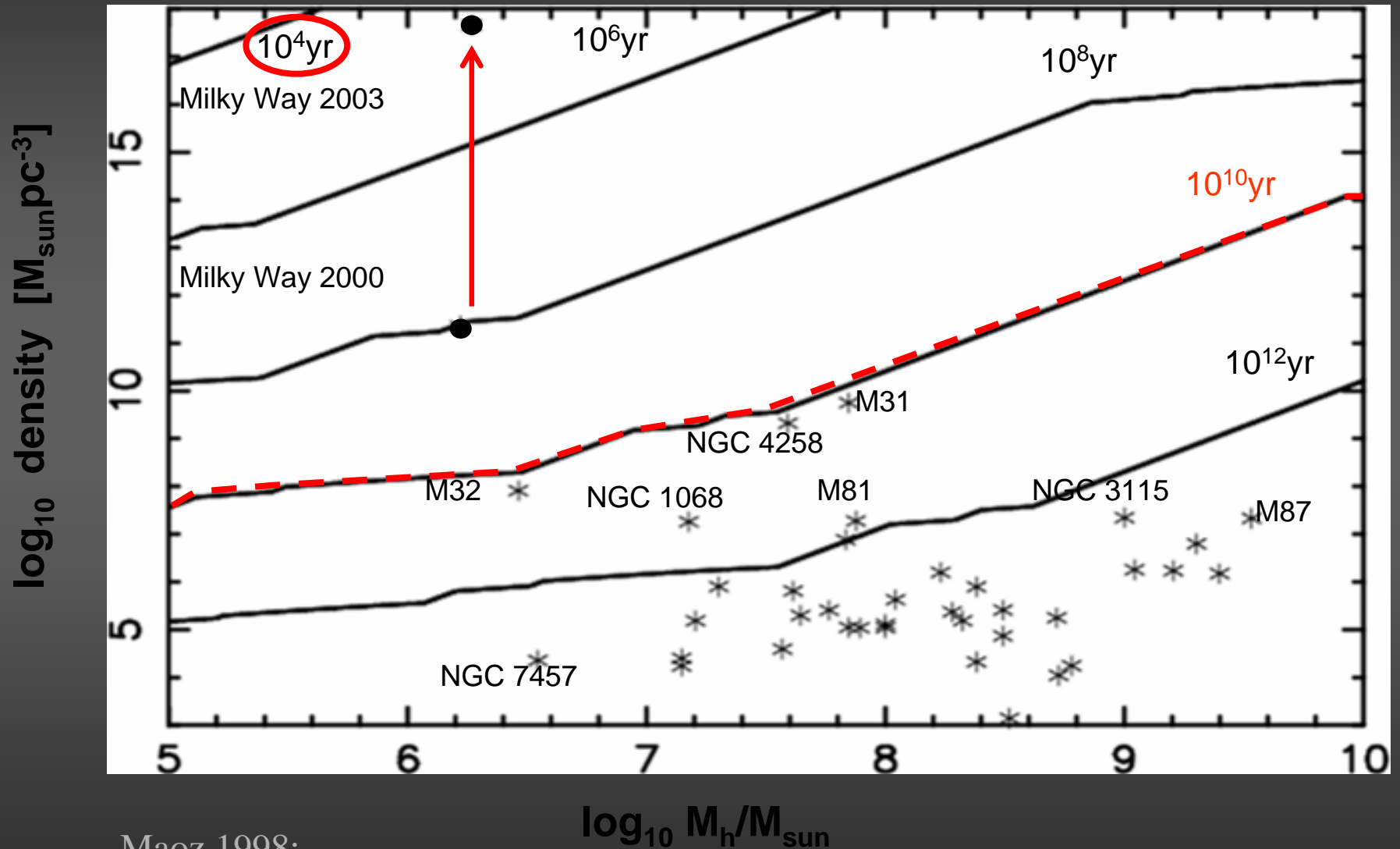
Genzel, Eckart, Ott, Eisenhauer 1997

Ghez, Klein, Morris, Becklin 1998

Eckart, Ott, Genzel 1999

Genzel et al. 2000

Stability of Enclosed Masses



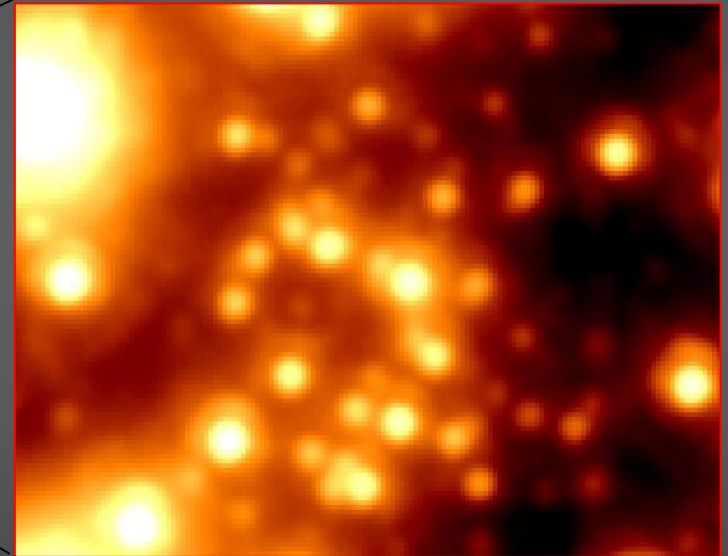
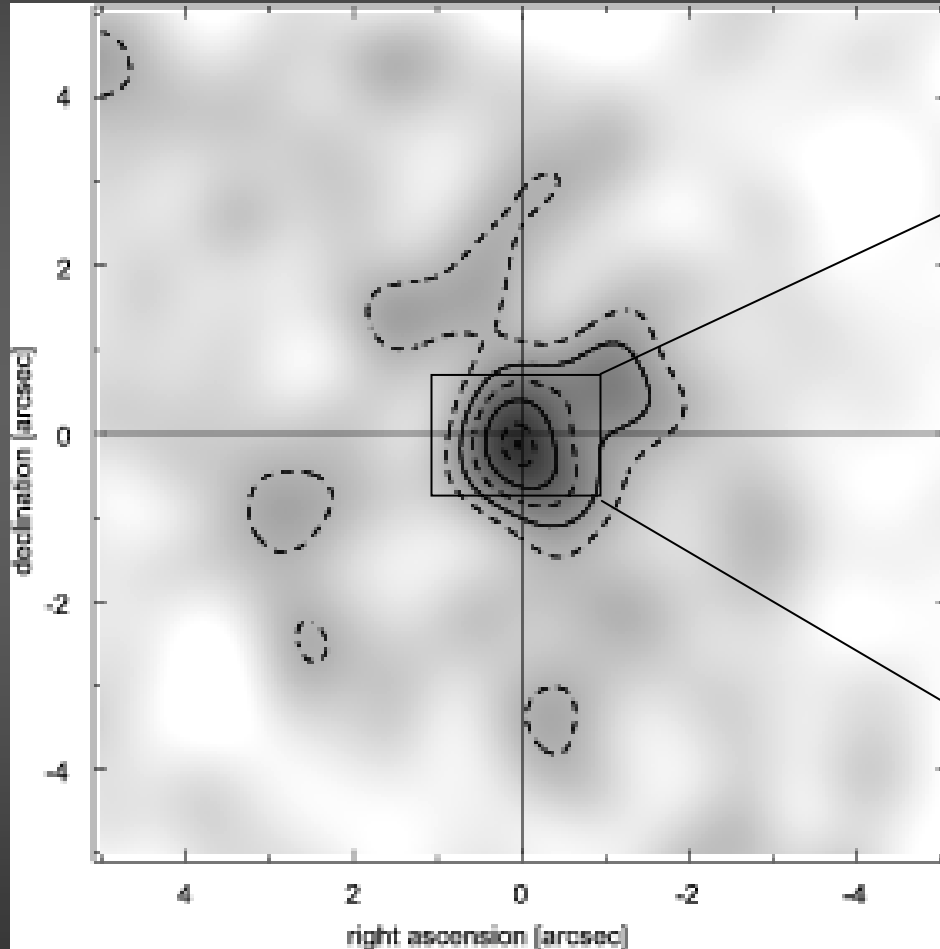
Maoz 1998;

Eckart, Schödel & Straubmeier 2004

Stellar Mass of the Cusp

Distribution of stars: The central cusp

- More than 90 sources can be detected in the central arcsecond in H-Band NACO/VLT images!
- A stellar cusp is clearly detected.

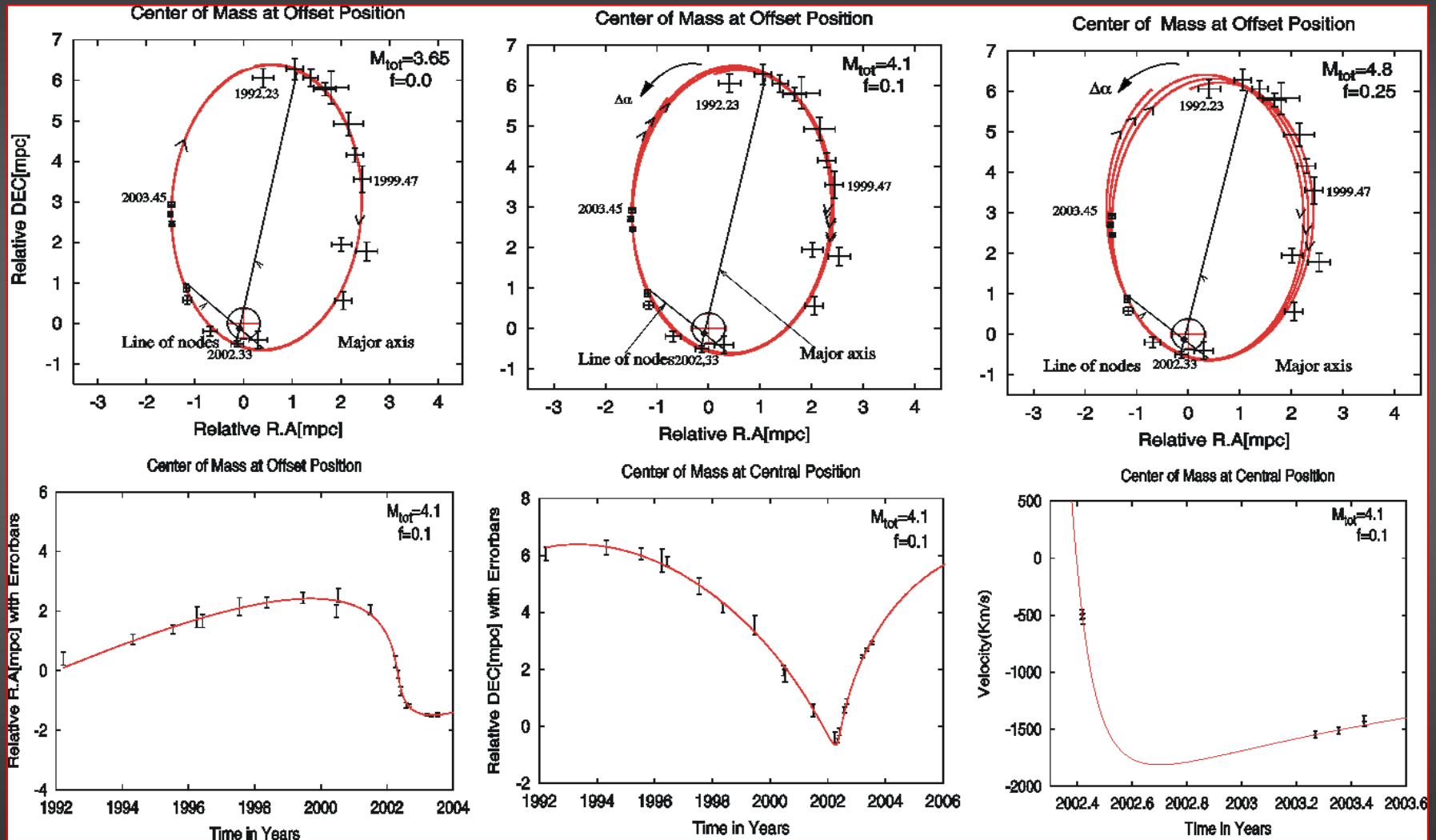


1"/46 light days

surface number density of stars
excess above mean density by 2, 3, 4, 5, 6.3 σ

Schödel et al. 2003
Eckart, Schödel, Straubmeier 2005

Weighing the central cusp



Mouawad, Eckart et al. 2003, 2005
 Rubilar & Eckart A&A, 2001

cusp mass limit $\sim 10^{**5} M_{solar}$

End of Part I

Standard Accretion Theory

A convenient way to describe the emission from the surroundings of a black hole is the so called Eddington luminosity.

The Eddington limit on the luminosity L of an object of mass M is set by the balance of gravity and radiation pressure in the object's envelope in the case of spherical accretion.

At a distance r from the center of the object the energy flux is

$$f = \frac{L}{4\pi r^2}$$

$$\sigma_t f / c$$

with the Thomson cross section

$$\sigma_t$$

Standard Accretion Theory

If the envelope is bound to the object then the radiation pressure is balanced by gravity. For one proton with mass m_p per electron in the fully ionized material of the envelope, the balance condition is:

$$\frac{\sigma_t L}{4\pi c r^2} = \frac{GMm_p}{r^2}$$

The corresponding luminosity is called the Eddington luminosity

$$L_{Edd} = \frac{4\pi GMm_p c}{\sigma_t} = \frac{4\pi c GM}{\kappa}$$

With $\sigma_t = 6.65 \times 10^{-25} \text{ cm}^2$

and $m_p = 1.67 \times 10^{-24} \text{ g}$

the opacity due to electron scattering is

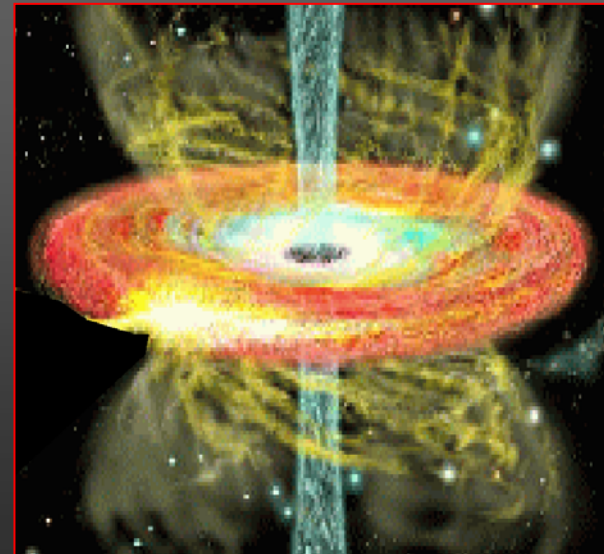
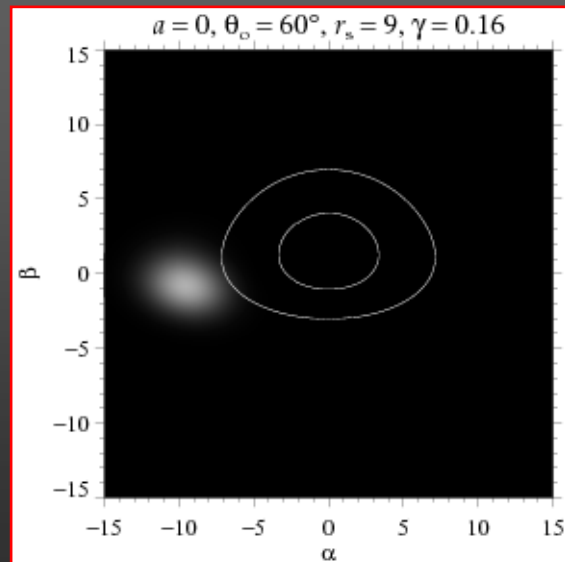
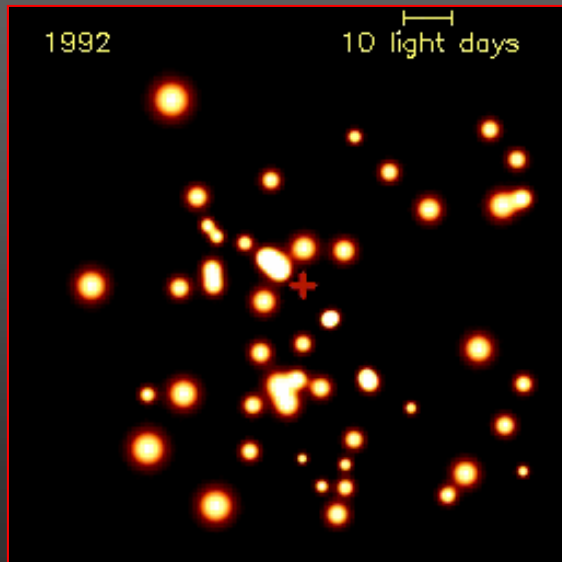
$$\kappa = \frac{\sigma_t}{m_p} = 0.4 \text{ cm}^2 \text{ g}^{-1}$$

SgrA* at the Center of the Milky Way

Observing the X- and γ -ray Sky
Astrophysical Spring School, April 2006

Andreas Eckart

I. Physikalisches Institut der Universität zu Köln



•II.Part

Accretion of matter onto SgrA*

Radio, X-ray variability

NIR/X-ray correlations

Adiabatic expansion

NIR polarization

Disk and jet models

Alternative models for SgrA*

IMBHs

MBHs in external galaxies

Future Experiments

The Accretion of Matter

Standard Accretion Theory

A black hole of mass $M = m M_{\odot}$

accrets at a rate

$$\dot{M} = m \dot{M}_{Edd}$$

Here m is the accretion rate expressed in units \dot{M}_{Edd} , the accretion rate at the Eddington luminosity

$$\dot{M}_{Edd} = \frac{L_{Edd}}{c^2 \eta_{eff}} = \frac{4\pi G (M / M_{\odot})}{\eta_{eff} \kappa c}$$

For $\eta_{eff} = 0.1$ this results in an accretion rate of

$$\dot{M}_{Edd} = 1.39 \times 10^{18} \text{ g s}^{-1} = 2.21 \times 10^{-8} \left(\frac{M}{M_{\odot}} \right) M_{\odot} \text{ yr}^{-1}$$

Standard Accretion Theory

With an estimated total wind mass loss - that could be accreted - of

$$\dot{M} \approx 2 \times 10^{-4} M_{\odot} \text{yr}^{-1}$$

that corresponds to an accretion rate in Eddington units of

$$\dot{m} \approx 1 \times 10^{-3}$$

for a black hole mass of

$$(3 - 4) \times 10^6 M_{\odot}$$

From the 2.2 micron flux of ~2mJy one obtains a specific luminosity of

$$L = \nu L_{\nu} = 2.1 \times 10^{34} \text{erg} / \text{s}$$

This corresponds to an efficiency of converting mass into electromagnetic energy of

$$\eta_{\text{eff}} = 10^{-8} - 10^{-9}$$

Standard Accretion Theory

From the bolometric luminosity of $L \approx 2.1 \times 10^{36} \text{ erg / s}$

one obtains an efficiency of

$$\eta_{\text{eff}} = \frac{L_{\text{bol}}}{\dot{M}_{\text{Edd}} c^2} \approx 5 \times 10^{-6}$$

For the estimated accretion rate this would imply a much larger bolometric luminosity than actually observed:

$$L \approx 0.1 \times \dot{M}_{\text{Edd}} c^2 \approx 4 \times 10^{43} \text{ erg / s}$$

This is larger by a factor of about 10^7

SgrA* is either very inefficiently accreting matter or very little of the matter available for accretion actually reaches the MBH, while the rest is blown away.

Dynamical Model for Accretion

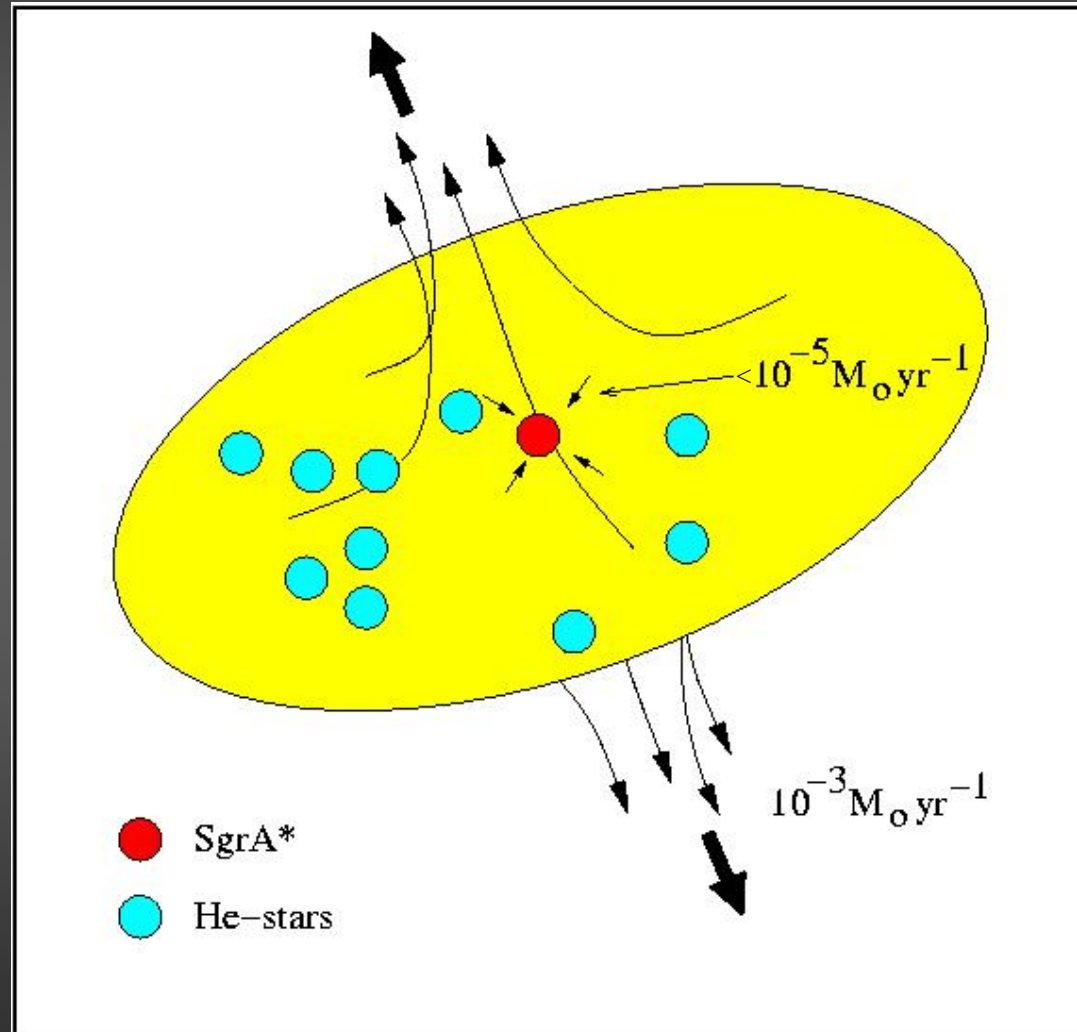
Interaction between the 'starburst' and the black hole

Mass loss from stars $10^{-3} M_{\odot} \text{yr}^{-1}$

radiation efficiency
of SgrA* $\approx 10^{-8}$

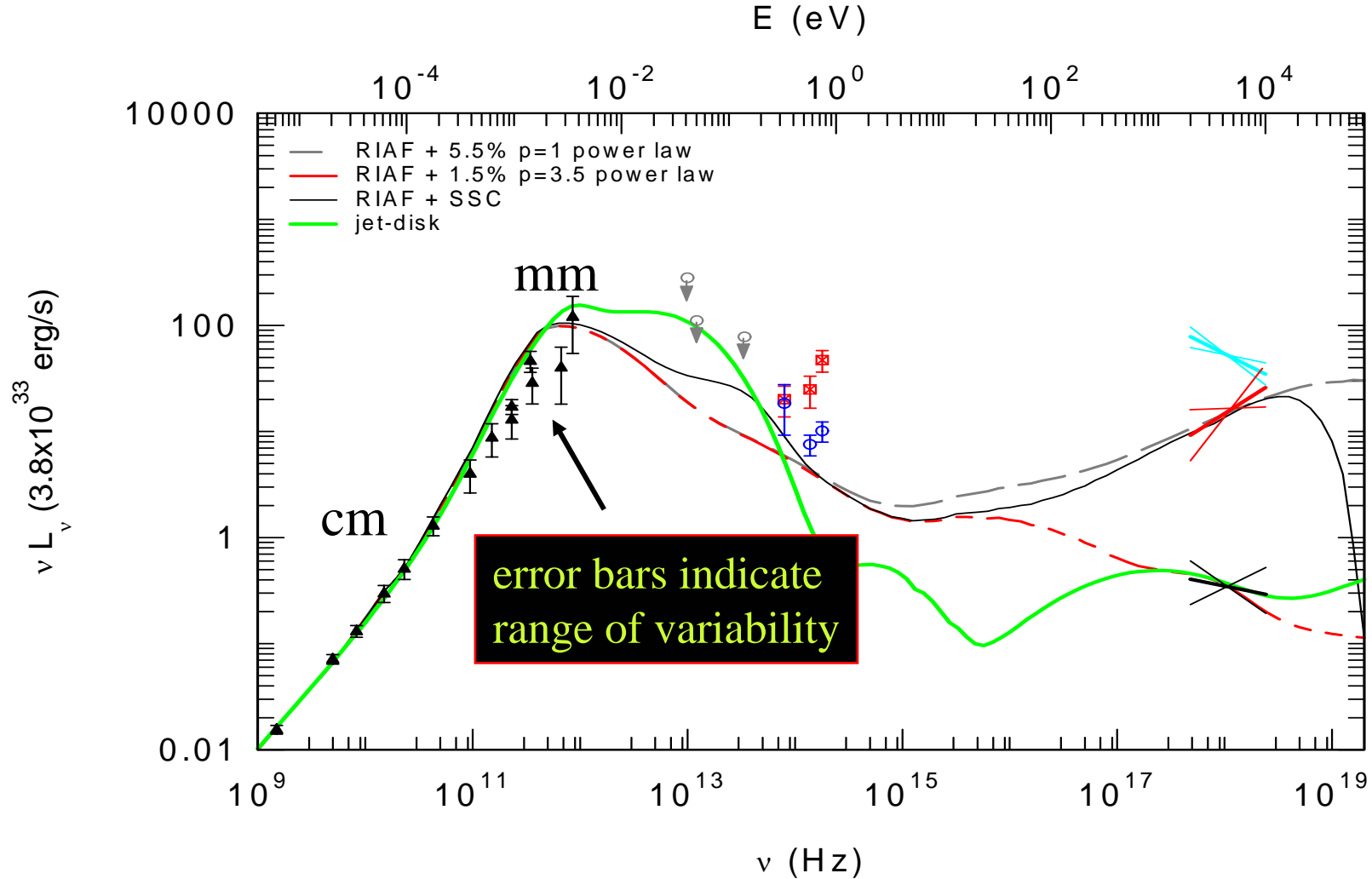
Bower et al. 2003:
RM of linear polarized
flux rules out large
accretion rates

Quataert 2003:
hydrodynamic calculations show
that almost the entire mass gets
blown away in a central wind.
Available for accretion: $10^{-5} M_{\odot} \text{yr}^{-1}$



Radio Variability

Radio Variability



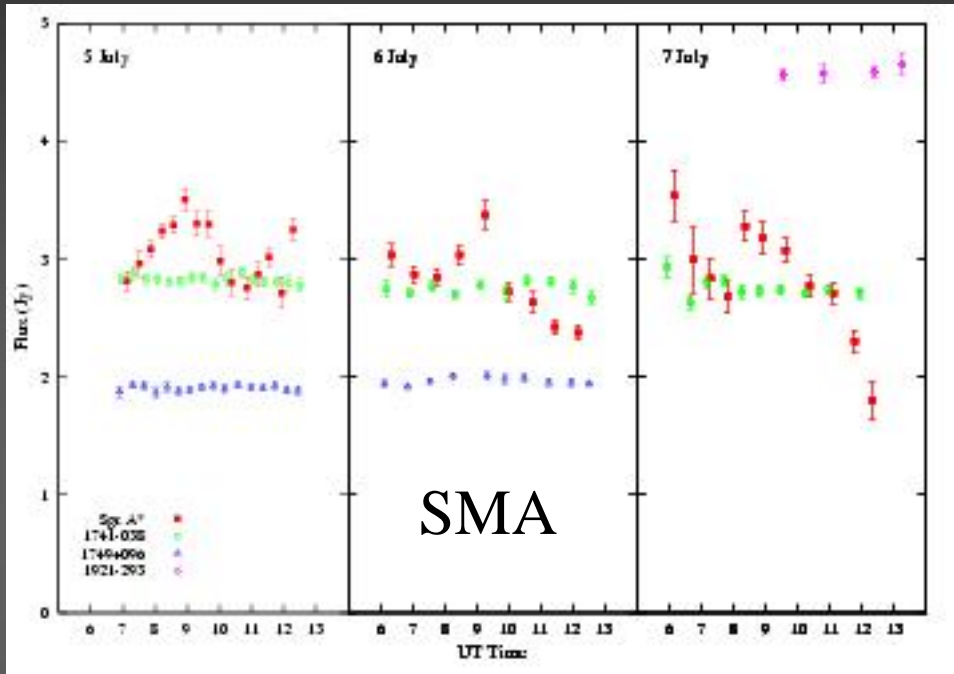
Radio: Zhao, Falcke, Bower, Aitken, et al. 1999-2003

X-ray: Baganoff et al. 2001, 2003, Goldwurm et al. 2003, Porquet et al. 2003,

NIR: Genzel et al. 2003, Ghez et al. 2003

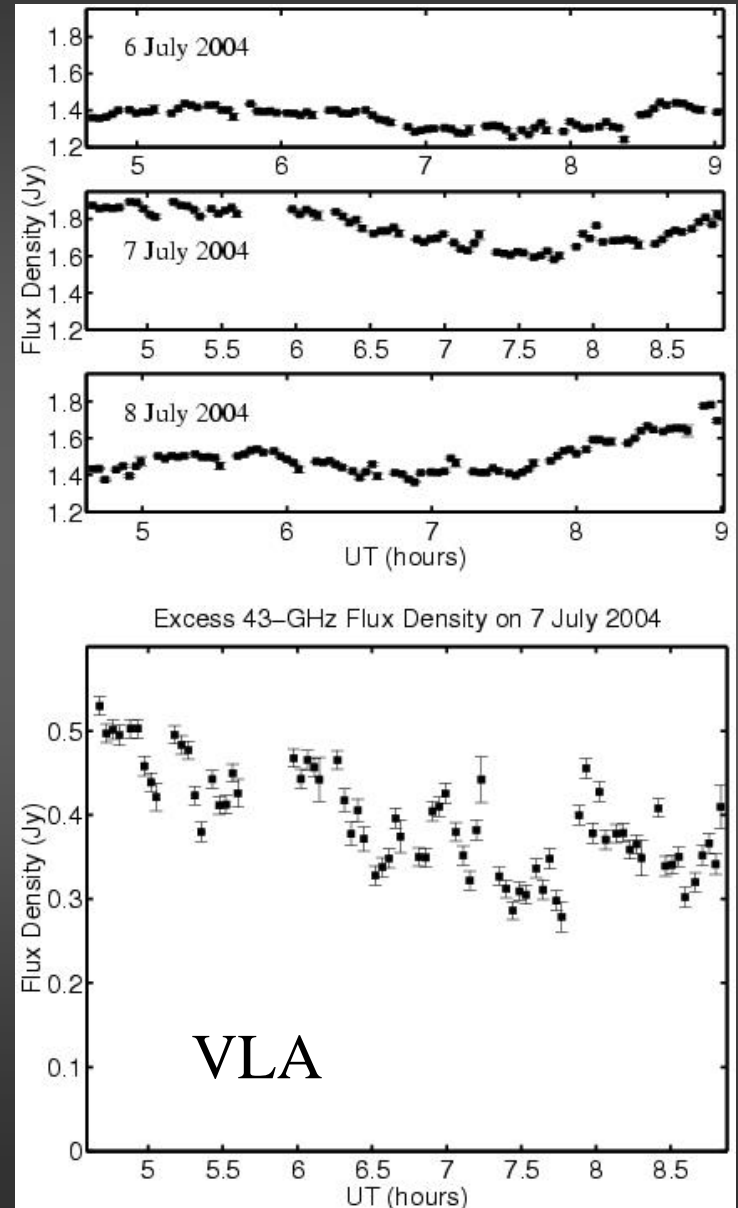
models: Markoff, Falcke, Liu, Melia, Narayan, Quataert, Yuan et al. 1999-2001

mm/sub-mm Monitoring in 2004

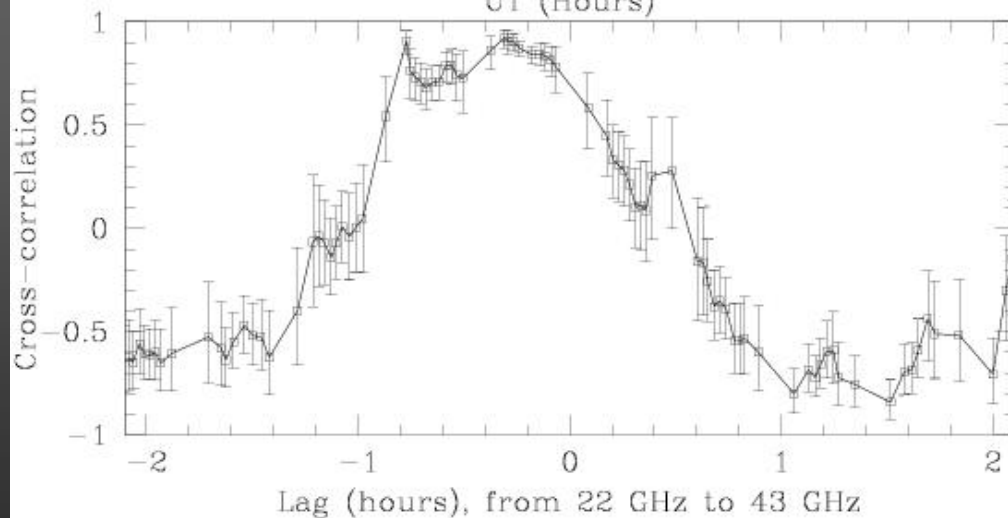
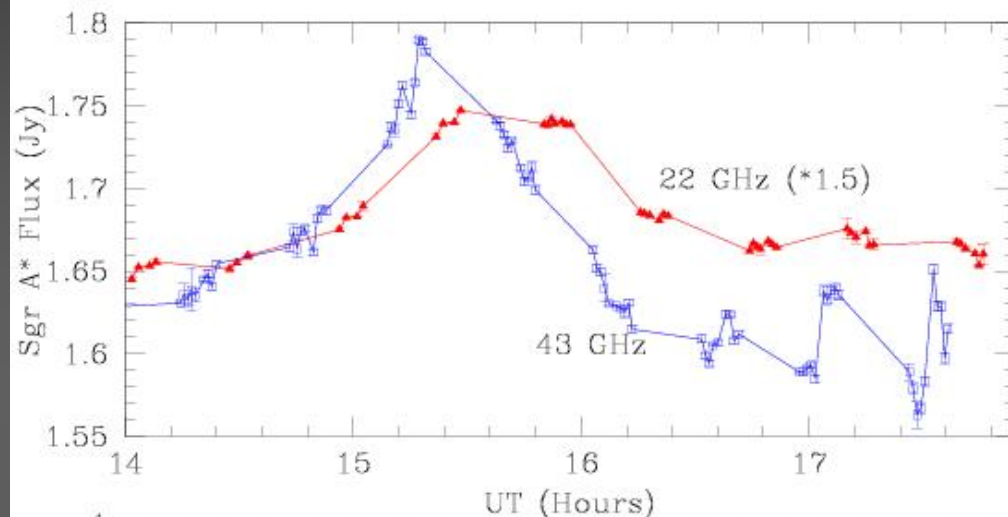


Eckart, Morris, Baganoff,
Bower, Marone et al. 2006 A&A in press

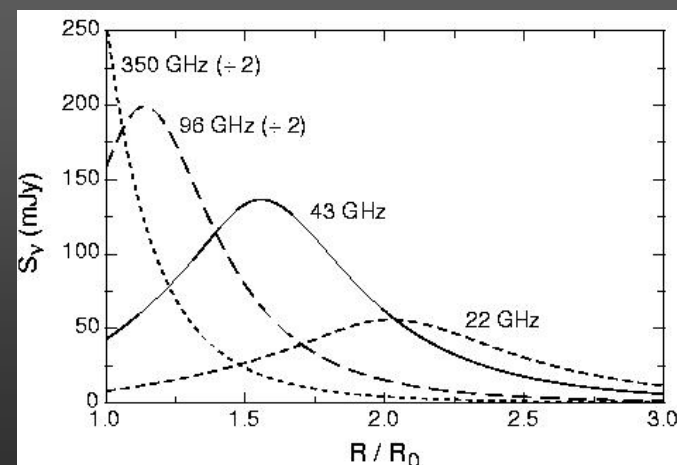
Indication for decaying flux density at
0.7 and 7 mm following an X-ray flare
– consistent with adiabatic expansion



Adiabatic Expansion



Yusef-Zadeh et al. 2006,
Astro-ph/0603685
submitted to ApJ



X-Ray/NIR Variability

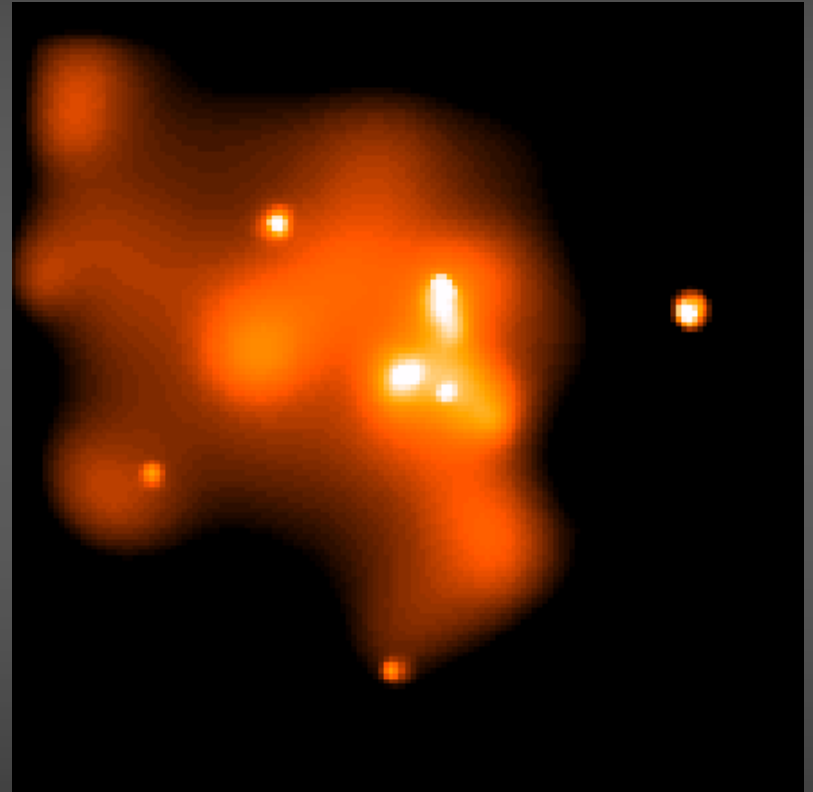
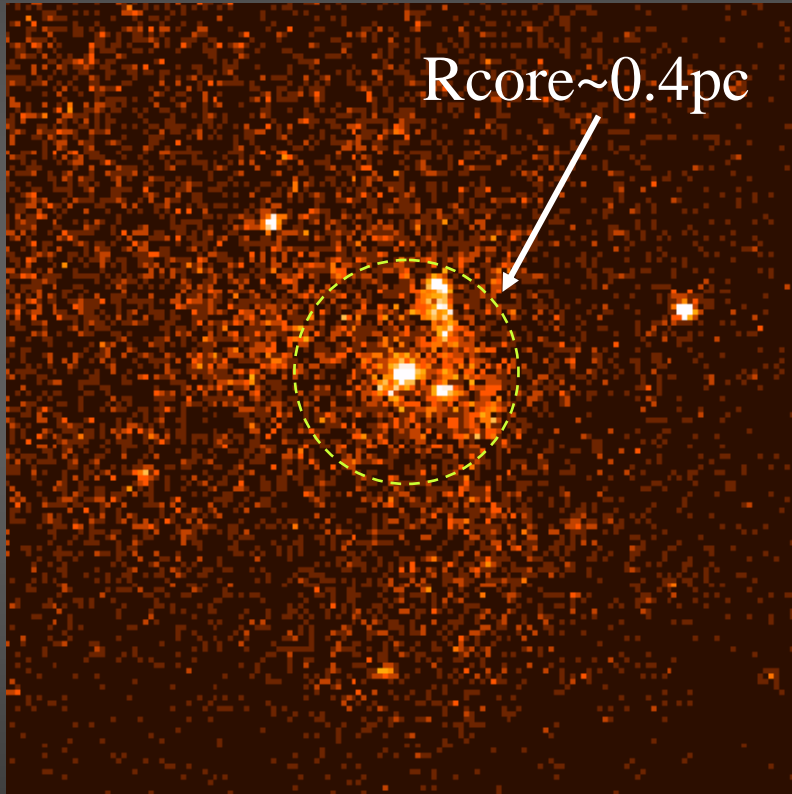
Chandras Image of the Galactic Center

N

0.5-10 keV

$R_{\text{core}} \sim 0.4 \text{ pc}$

E



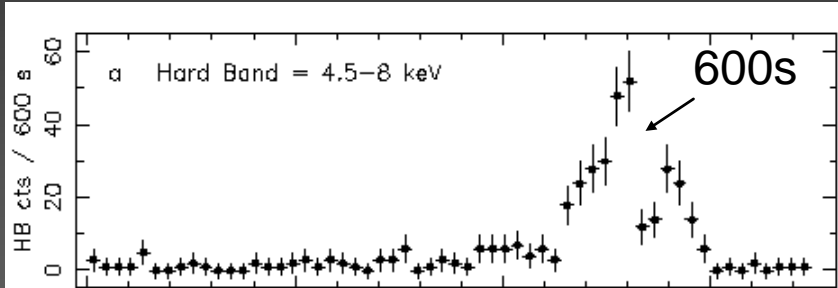
smoothed

← 75"/10 yr →
0.5" resolution

Baganoff et al. Nature 2001

SgrA* burst in October 2000 in the 2-8 keV band

Baganoff et al. 2001, Nature 413, 45



$$R_{S, 3 \times 10^6 M_o} = 9 \times 10^{11} \text{ cm}$$

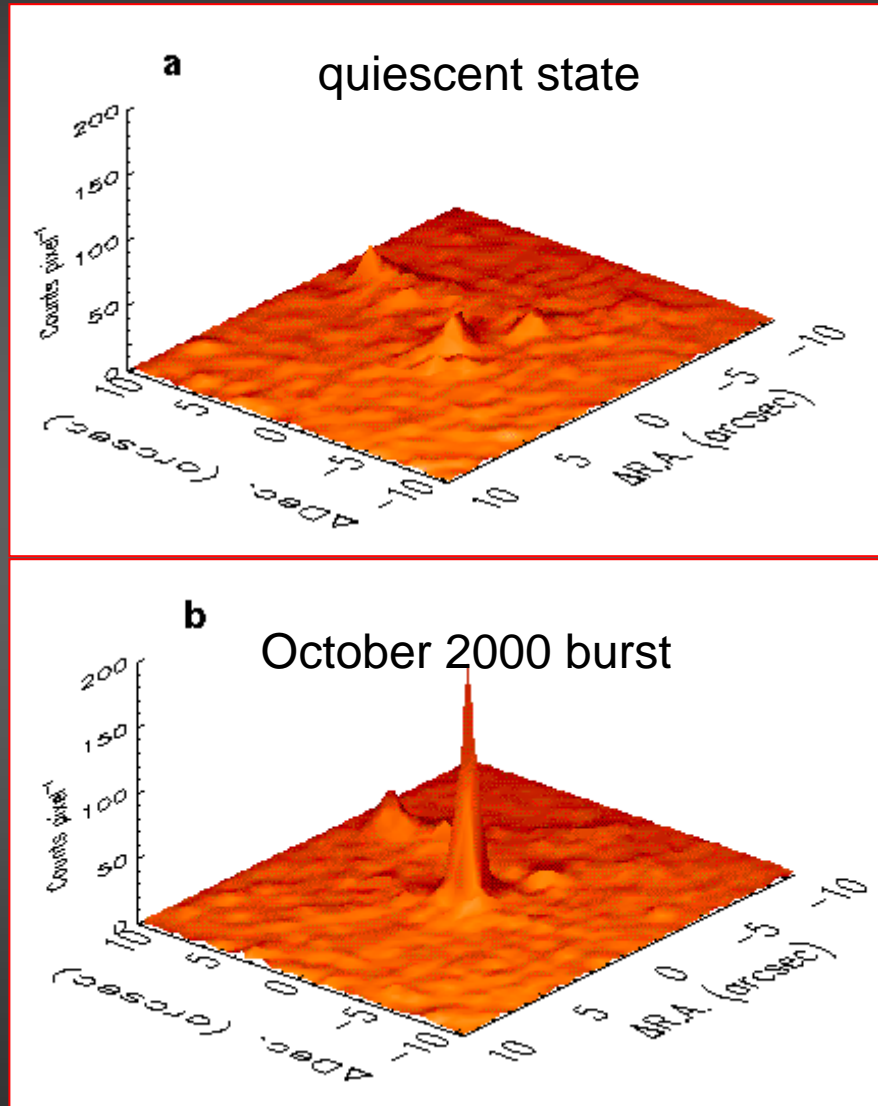
$$2.8h \approx 350R_s$$

$$600s \approx 21R_s$$

$$S_{burst} \approx 50 \times S_{quiescent}$$

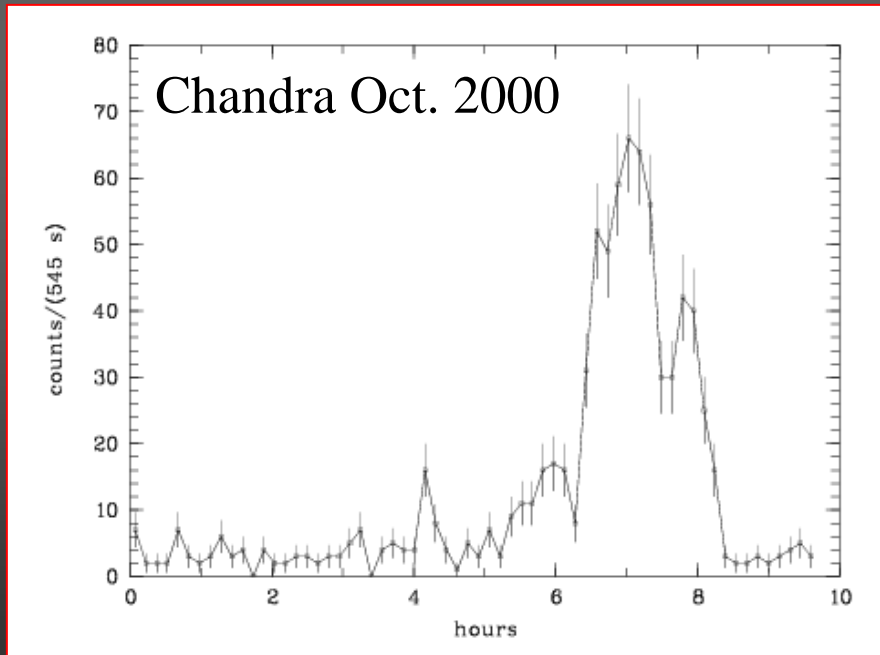
May 2002 Monitoring:

1.2 ± 0.4 flares/day

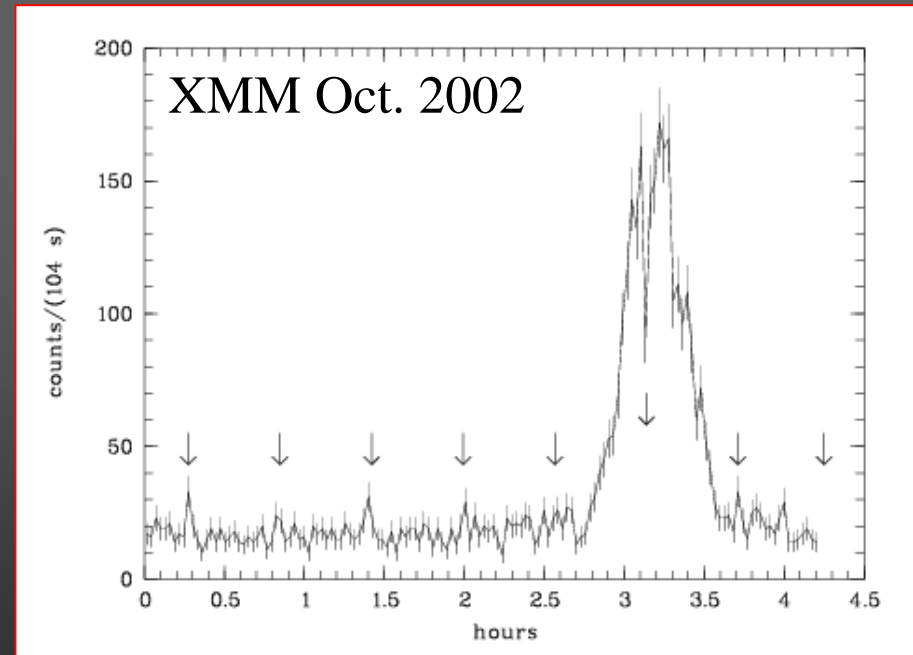


Detection of Cyclic Accretion Disk Modes ?

Analysing the two strongest X-ray bursts Aschenbach et al. 2004 (astro-ph/0401589) report the detection of cyclic modes associated with accretion disks.

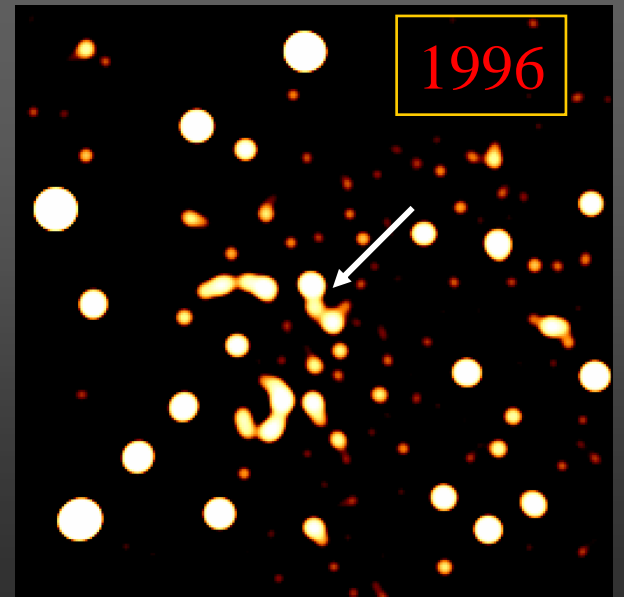
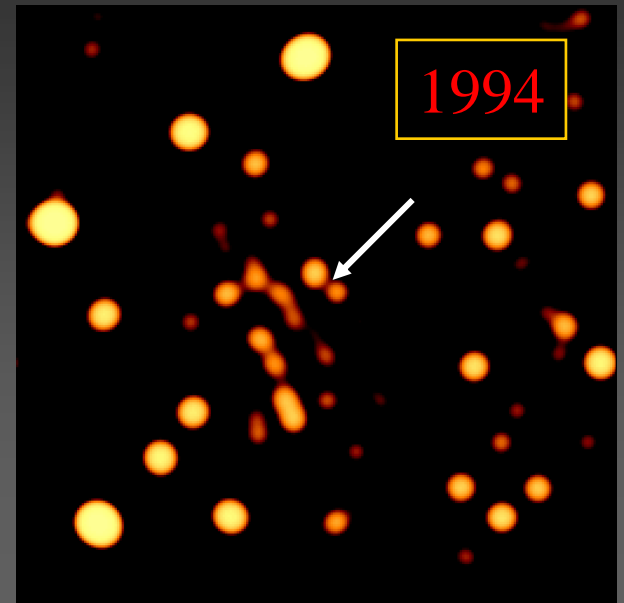
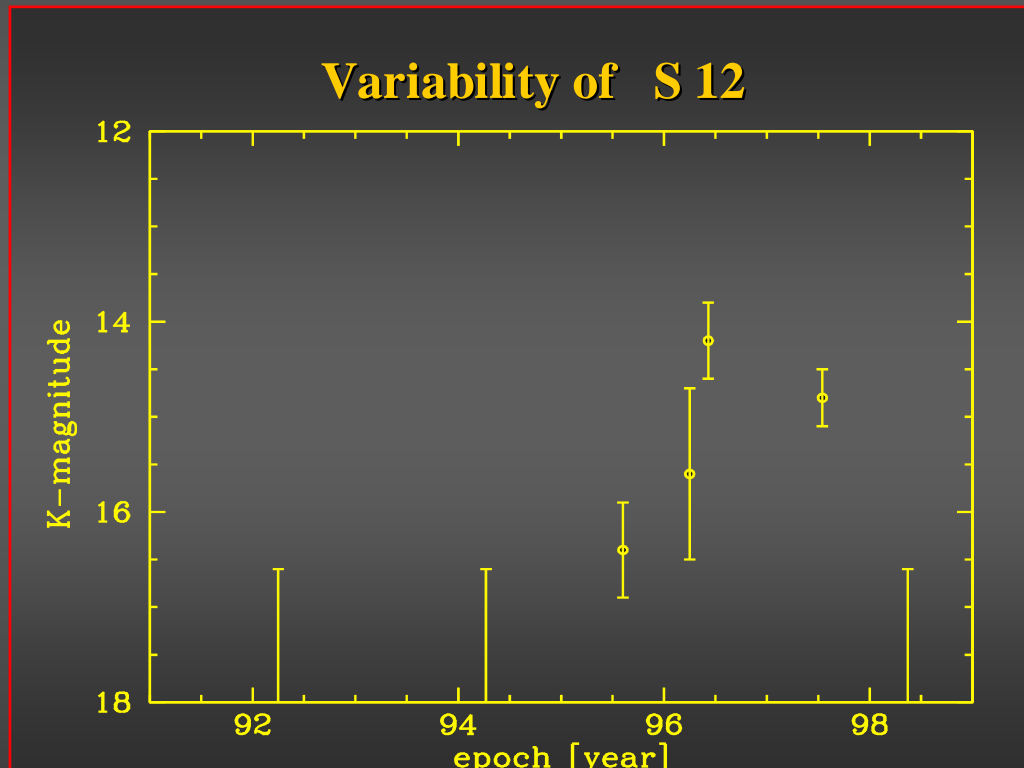


Baganoff et al. 2001



Porquet et al. 2003

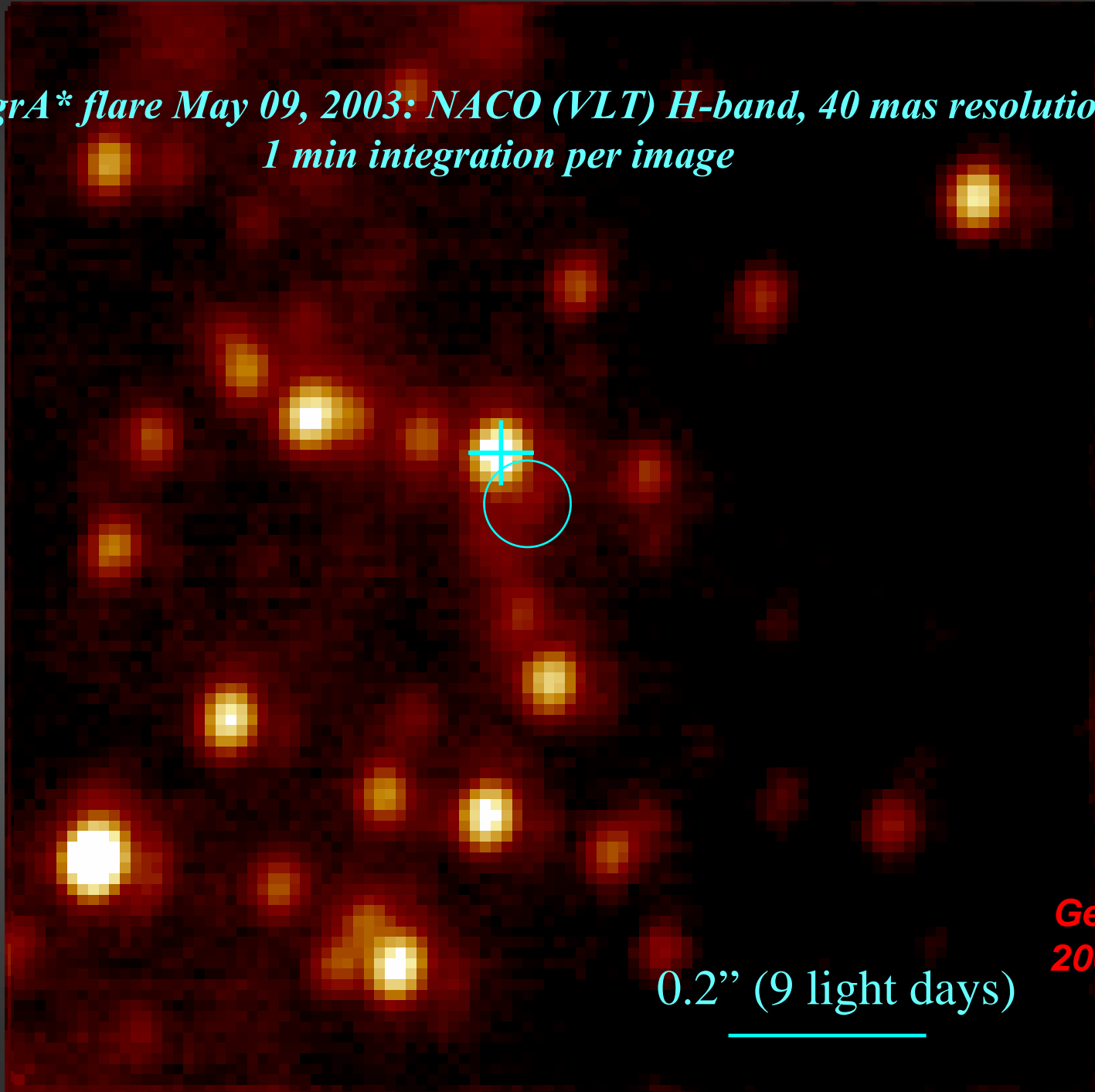
Why is SgrA* so faint?



Genzel et al. 1997, MNRAS 291, 219

Narayan et al. 1998, Ap.J. 492, 554

SgrA flare May 09, 2003: NACO (VLT) H-band, 40 mas resolution,
1 min integration per image*



0.2'' (9 light days)

*Genzel et al.
2003, Nature*

X-Ray/NIR/Radio Correlations

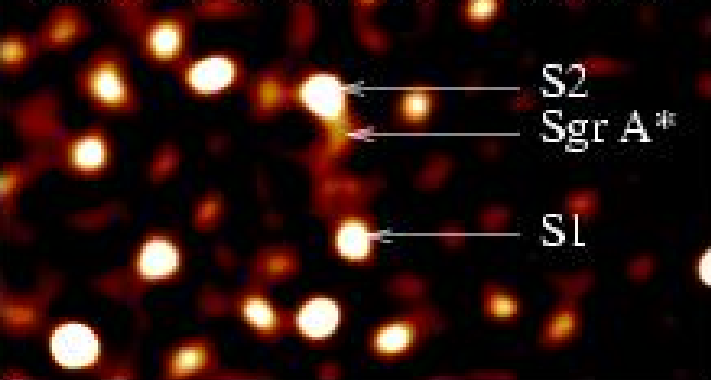
*SgrA**

What is the Emission Mechanism?

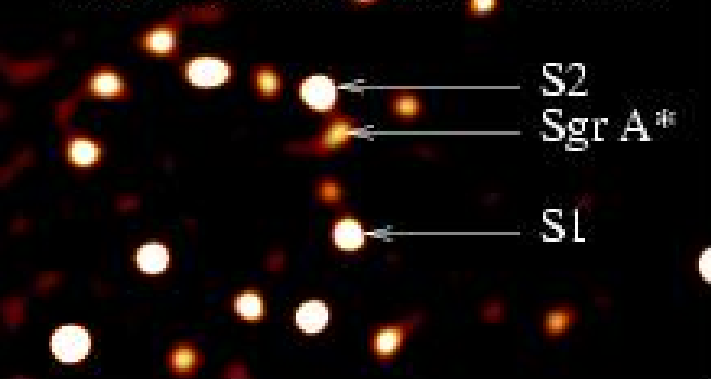
*What is the Nature of the Dark Mass
Concentration at the Center
of the Milky Way?*

*Simultaneous NIR / X-ray
Measurements of Sgr A**
2003

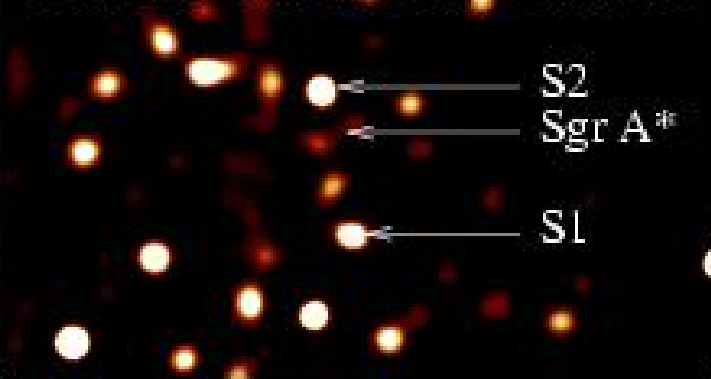
June 19 UT:23h51m–24h00m



June 20 UT:00h15m – 00h

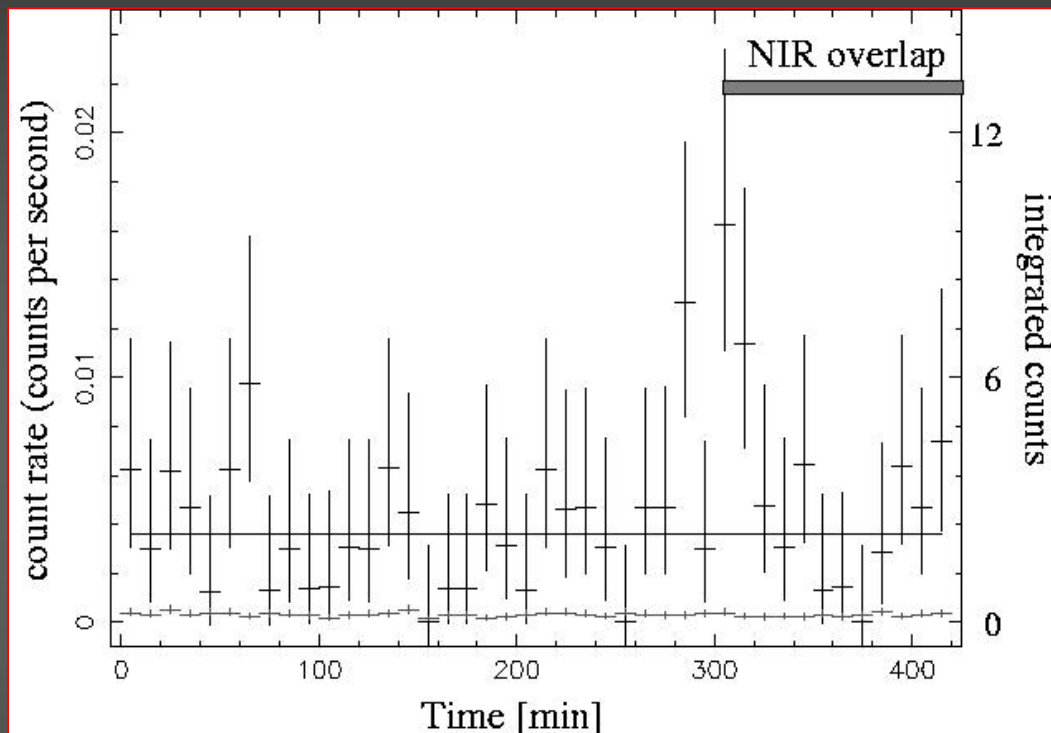


June 20 UT:01h07m–01h13m



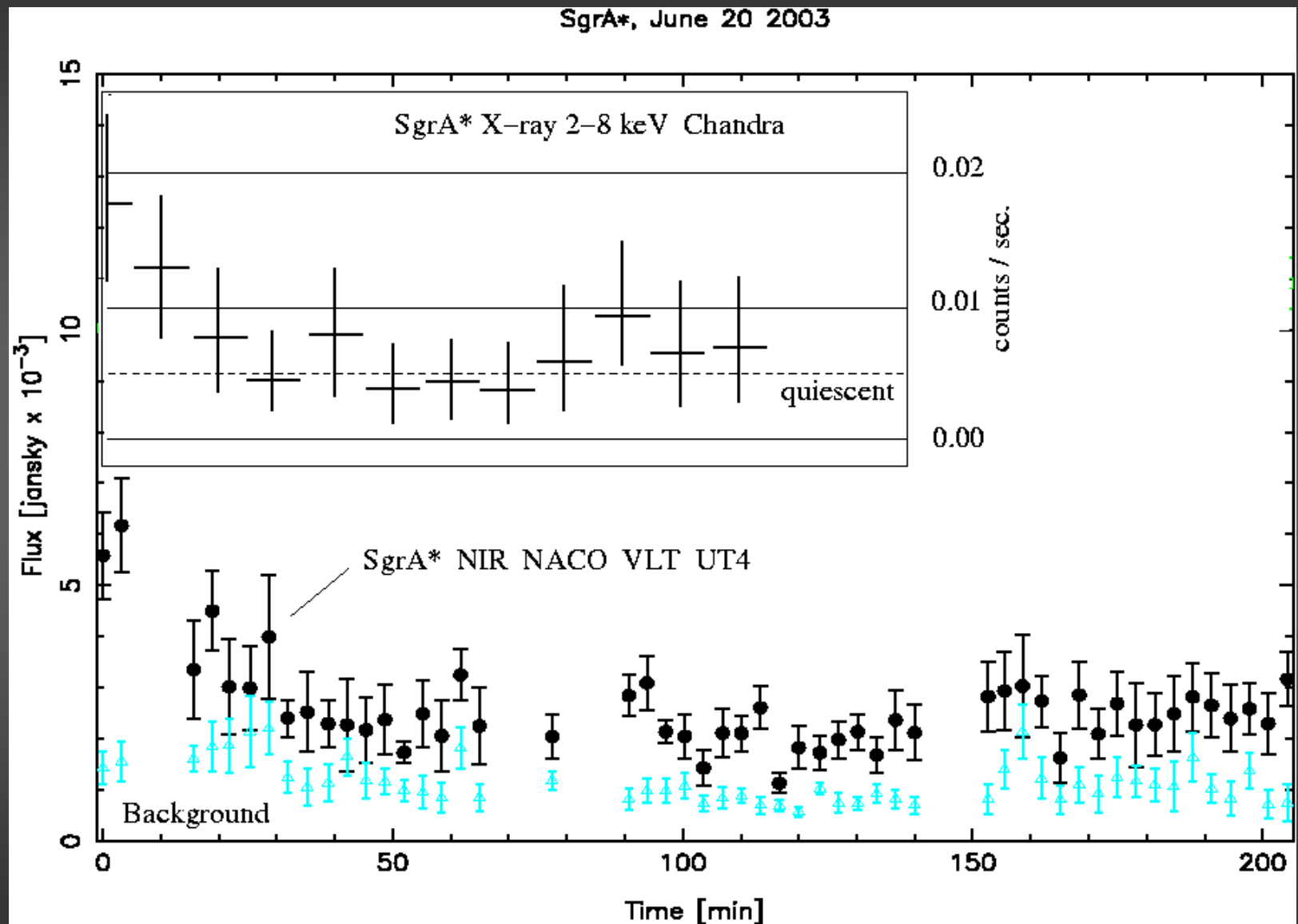
1"

Simultaneous NIR/X-ray Observations



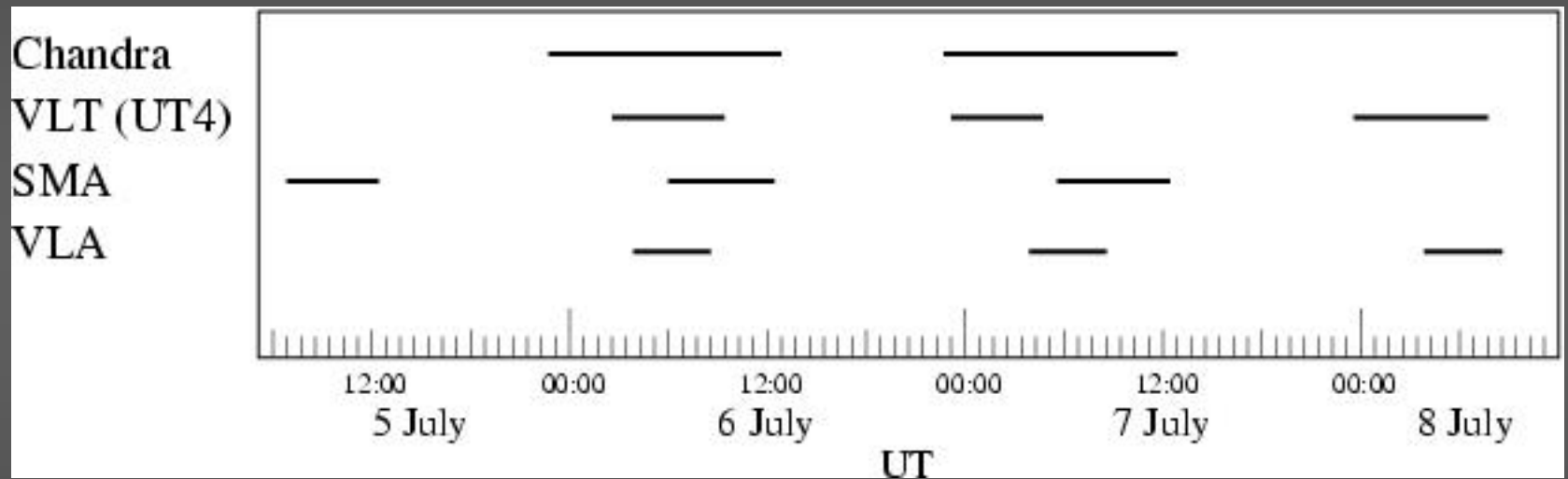
Eckart, Baganoff, Morris, Bautz,
Brandt, Garmire, Genzel, Ott, Ricker,
Straubmeier, Viehmann, Schödel,
Bower, and Goldston 2004 A&A 427, 1

SgrA*: First Simultaneous K-band/X-ray Observations

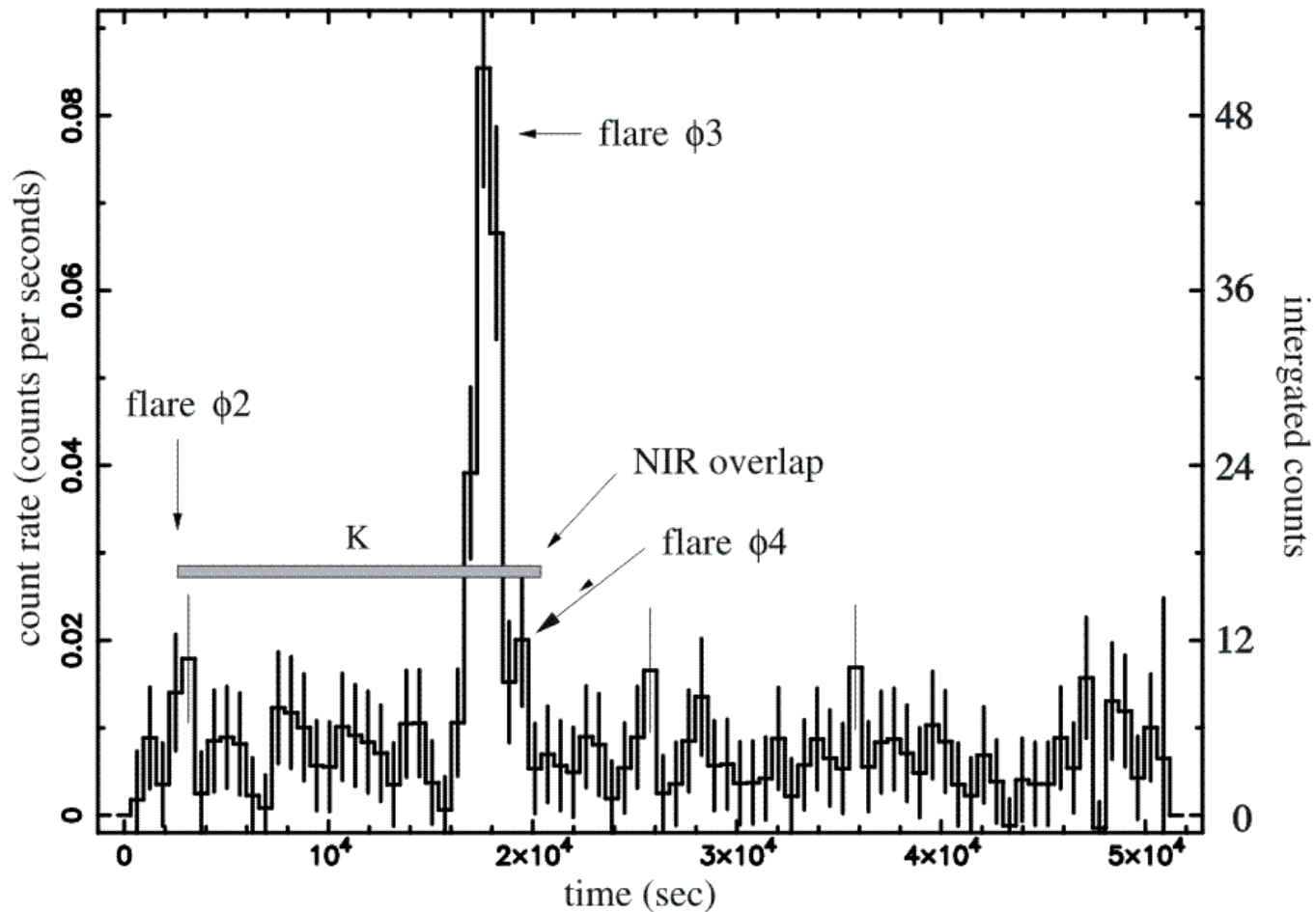


*Simultaneous NIR / X-ray
Measurements of Sgr A**
2004

mm/sub-mm Monitoring in 2004



SgrA*: Simultaneous NIR/X-ray Observations



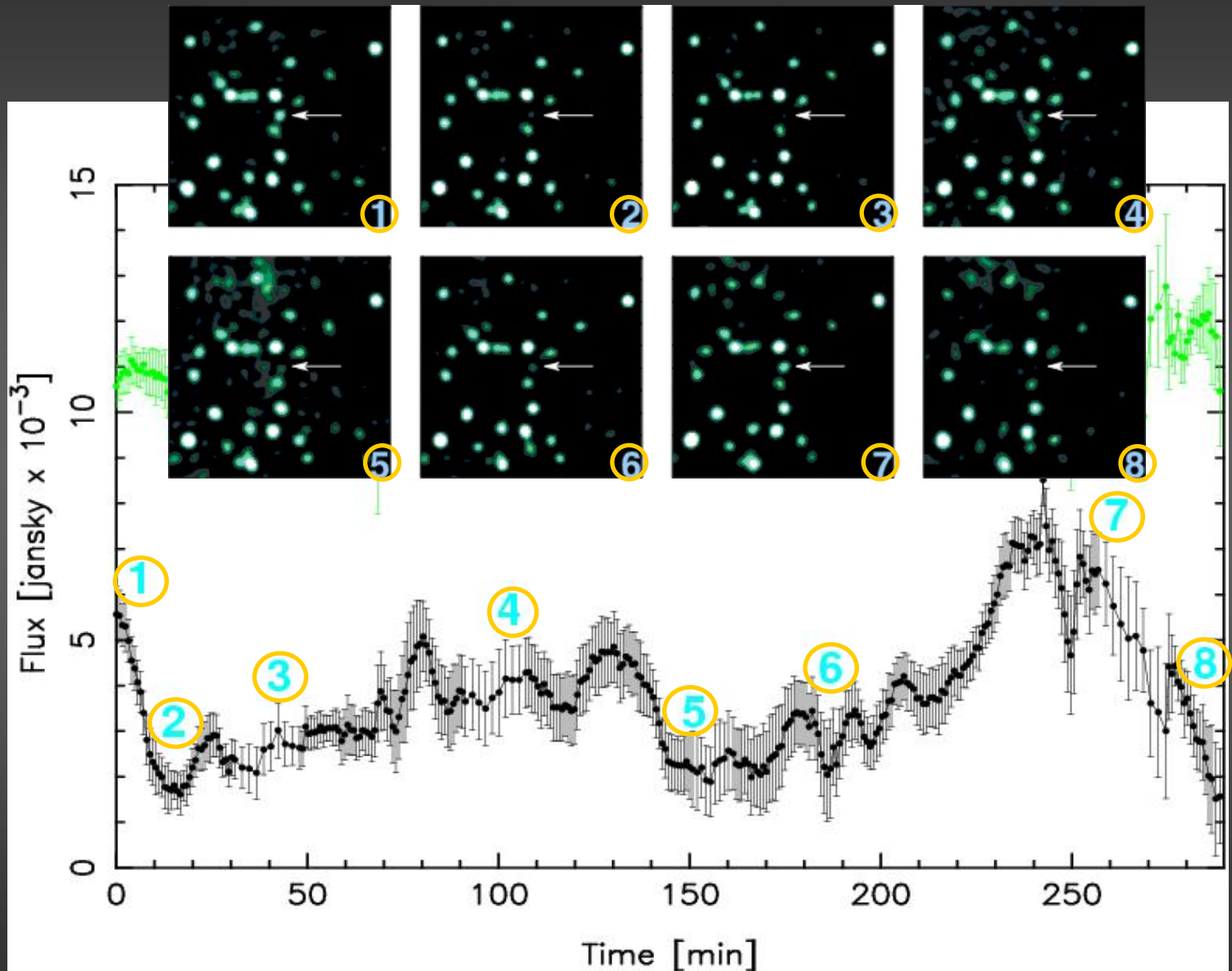
CHANDRA, 7 July 2004

Eckart et al. 2006, A&A in press

SgrA*: Simultaneous NIR/X-ray Observations

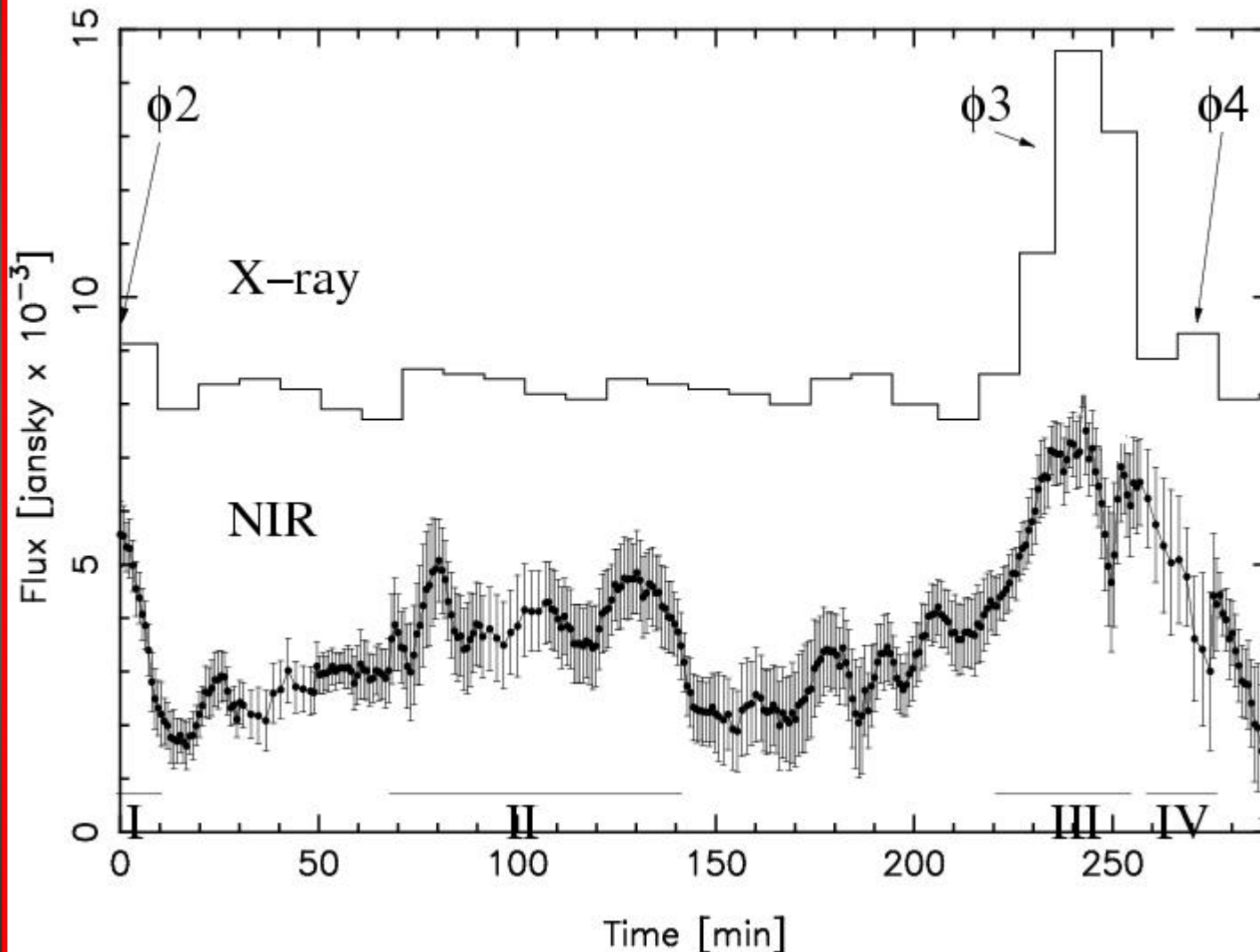
Comparison with images demonstrates the variability shown in the lightcurve.

Flare emission originates to within <10mas from the position of SgrA*



Simultaneous Flare Emission

2004-07-06T23:19:38 to 2004-07-07T04:16:37

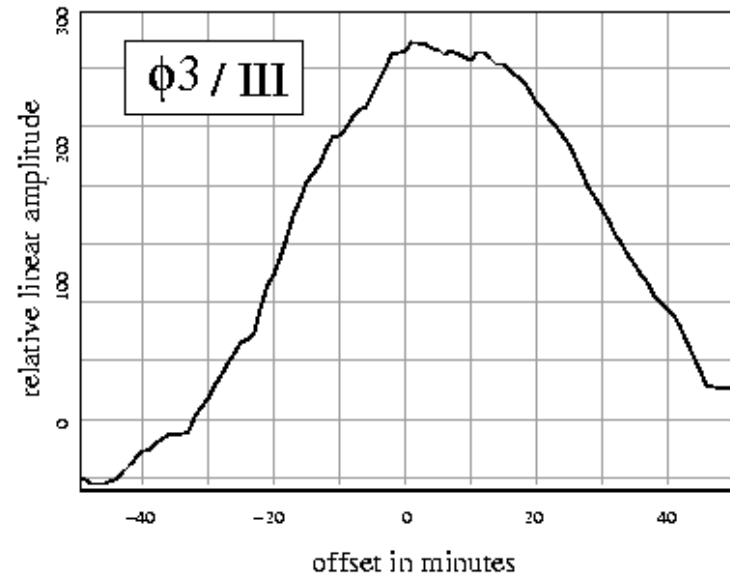


~225nJy

~6mJy

Flare emission originates to within <10mas from the position of SgrA*

Cross-Correlation of Simultaneous NIR/X-ray Flares

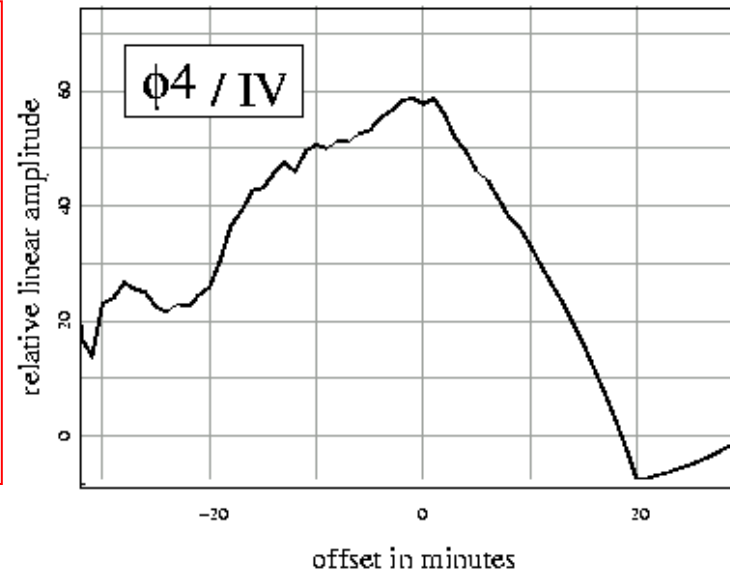


$\phi2/I$ and $\phi4/IV$ are dominated by a decaying flank; $\phi3/III$ is dominated by a rising flare flank.

Time lags are less <10-15 minutes

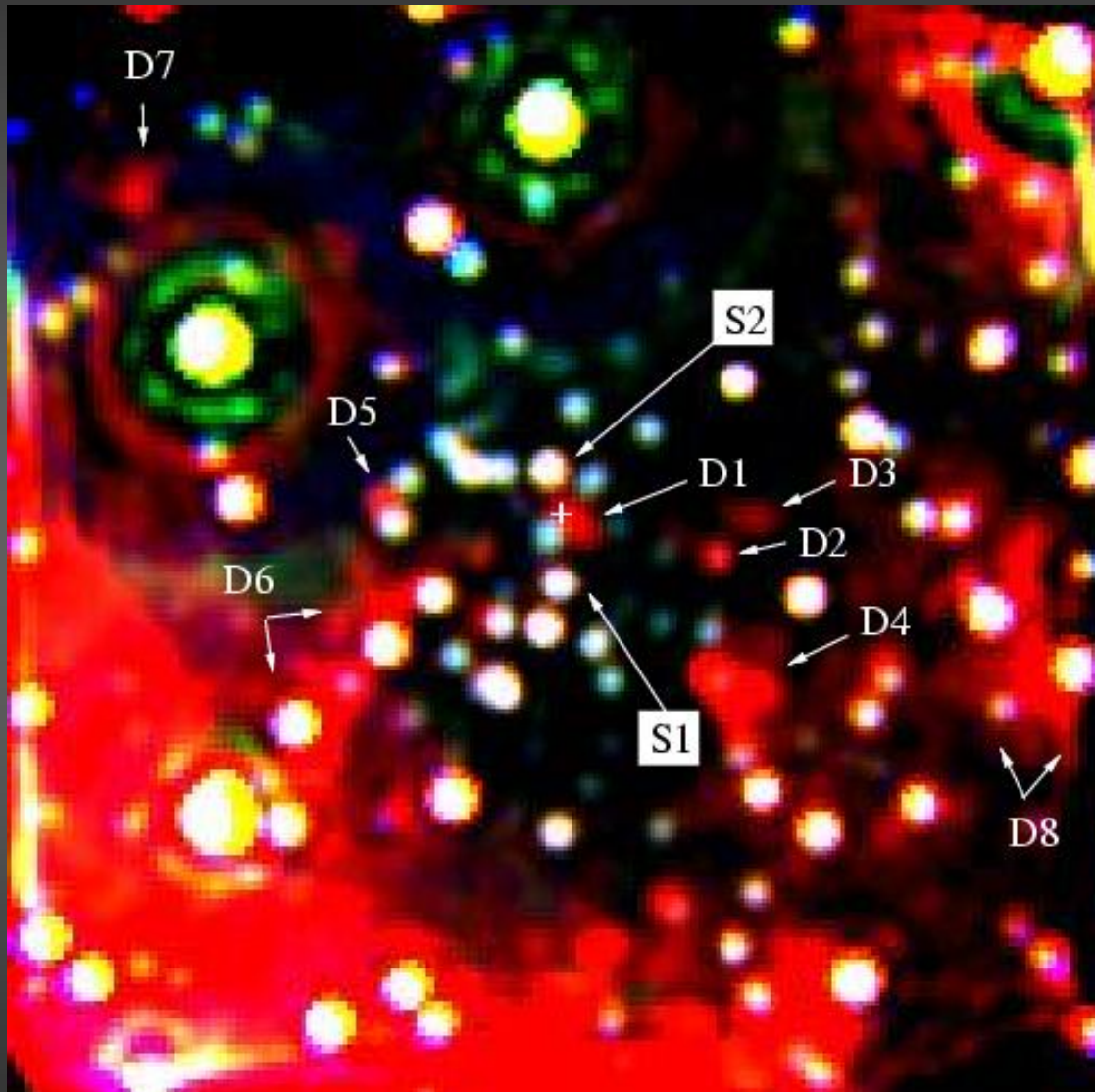
NIR and X-ray flares are well correlated.

IQ-state subtracted



*NIR/MIR spectral energy
distribution from the
central arcsecond*

Detection of a Dust Component along the Line of Sight towards SgrA*



HKL multi-color image of the central 2.6"x2.6" taken with NACO. L-band is in red.

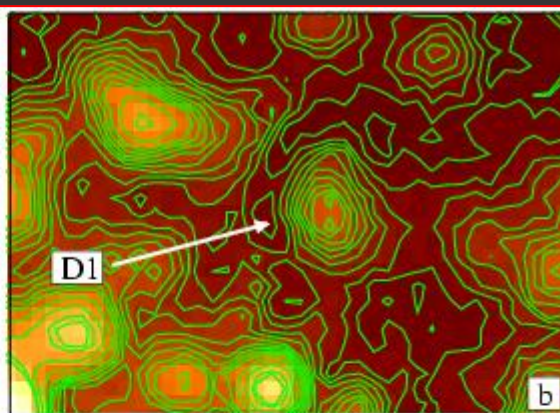
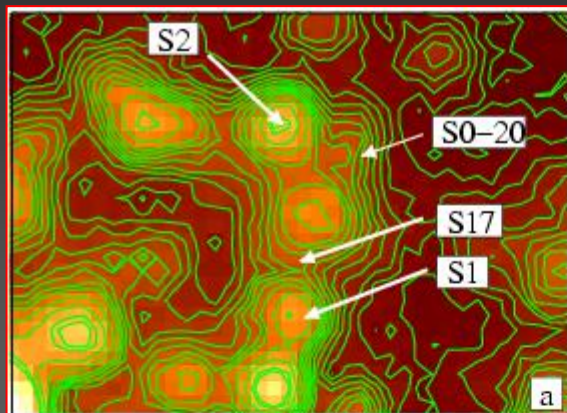
Fore-/Background dust component 26mas west of SgrA*
~1000 AU at 8 kpc
(see also Ghez et al. 2004)

High angular resolution required in the MIR!!

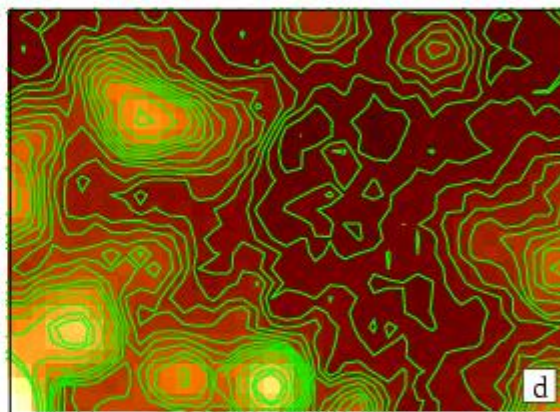
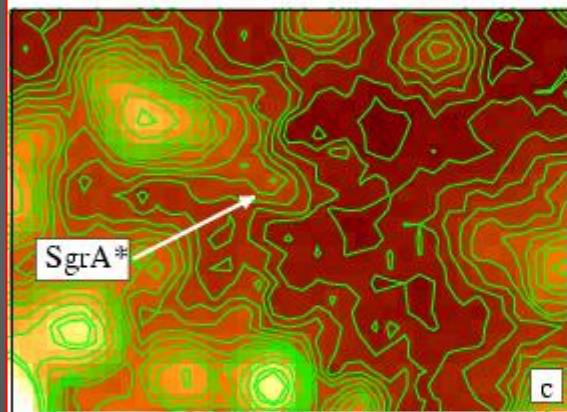
Several of those dust blobs are seen across the field

5"x5"

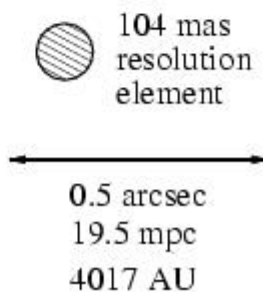
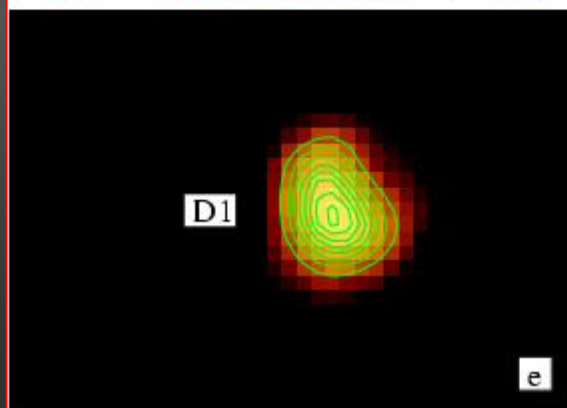
all



SgrA*



D1
only



Detection of a
Dust Component
along the
Line of Sight
towards SgrA*

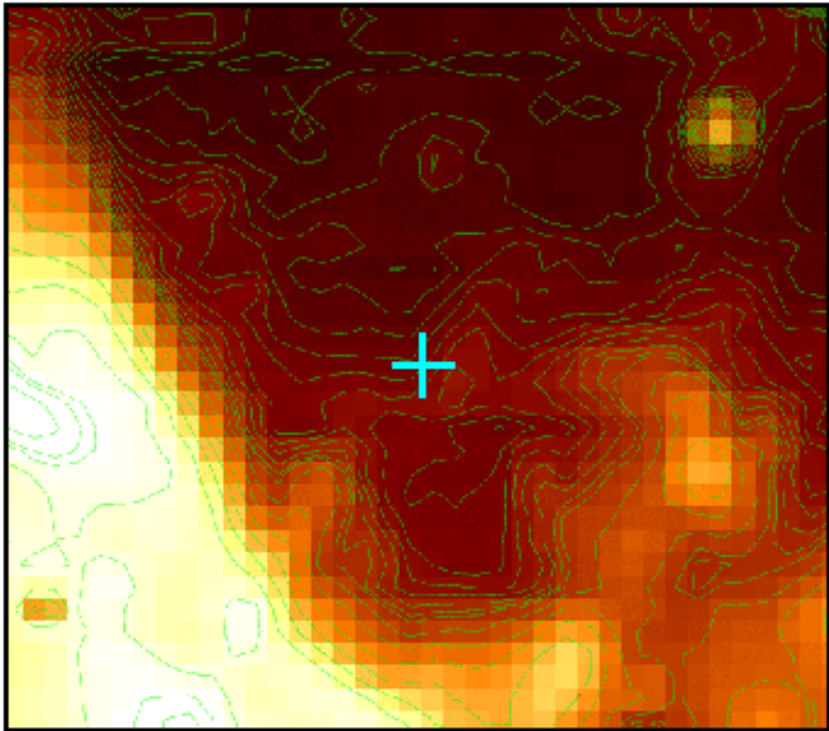
D1

S1, S2, S17, S2-20
D1 and SgrA*
subtracted

Eckart et al. 2006, A&A in press
see also Ghez et al. 2005

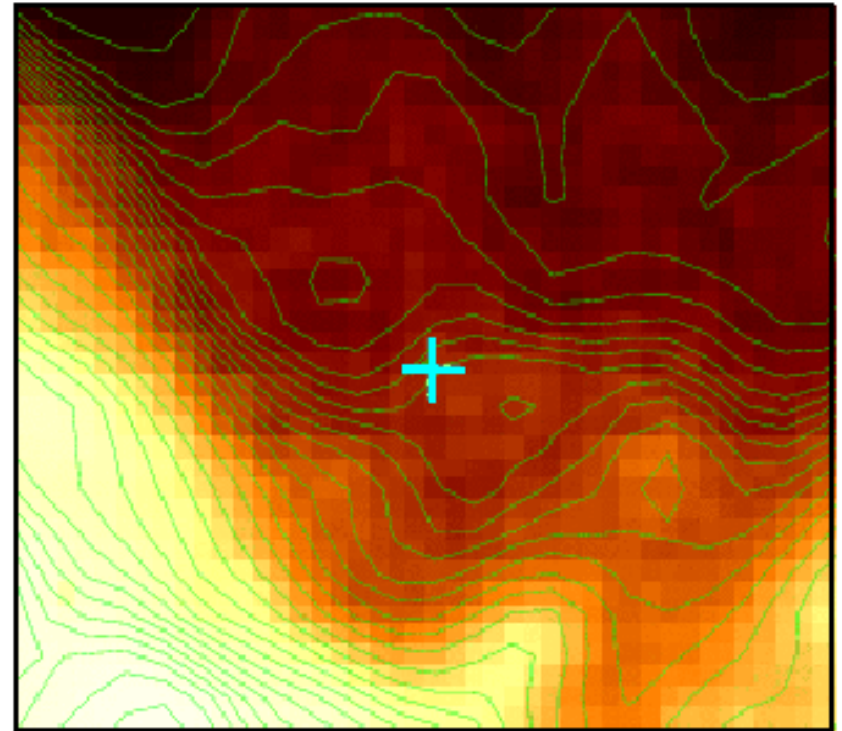
The total L-band
luminosity of the
dust component D1
is almost as large
as that of S2.

VISIR VLT Observations



8.6 μm

field of view: 5.0"x4.4"
cross marks position of SgrA*

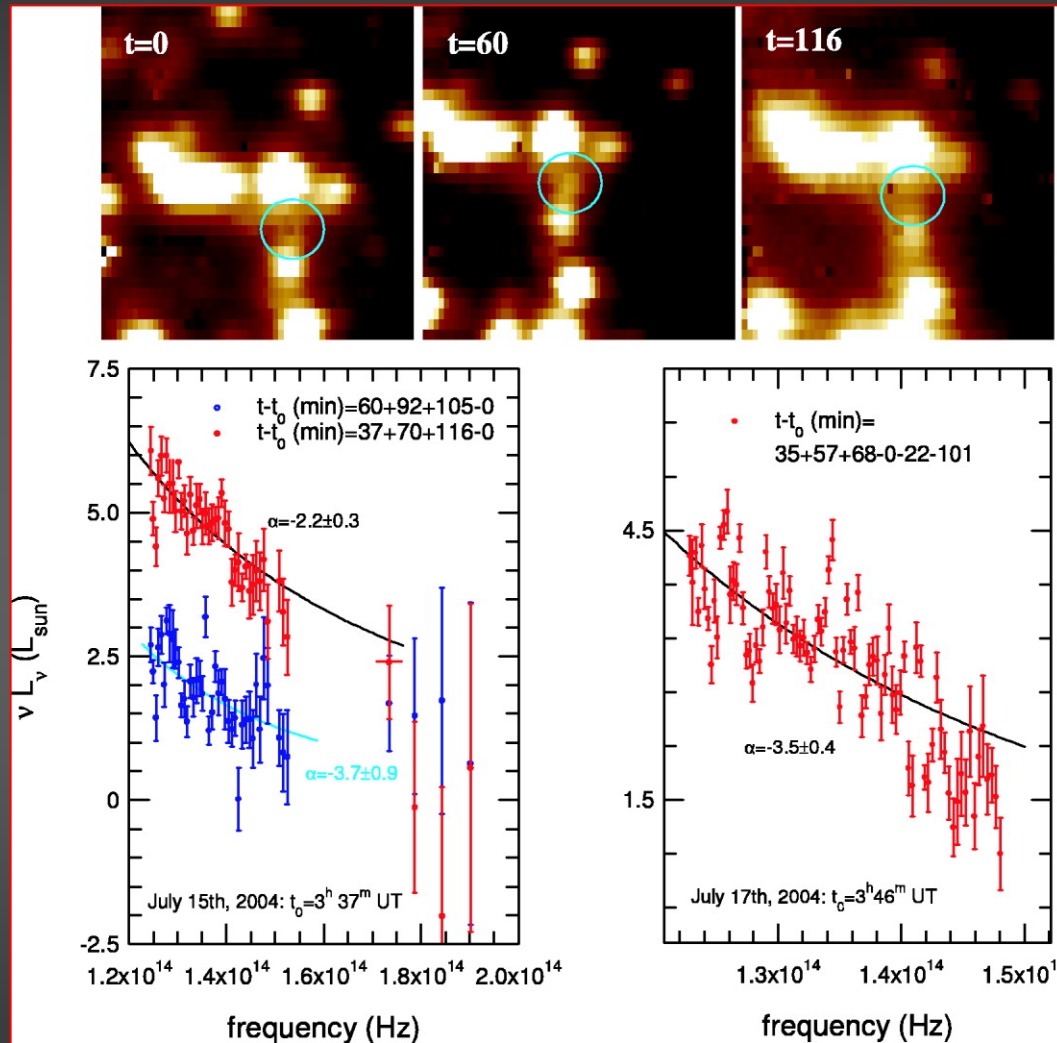


19.5 μm

positional uncertainty $\pm 0.2''$
positioning via IRS3, 7, 21, 10W and in
addition at 8.6 mm IRS 9, 6E, and 29

Eckart et al. 2006

Steep NIR Spectra of SgrA* Flares



Eisenhauer et al. 2005

see also

Gillessen et al. 2006

MIR Fluxes

3.8 μm 22 \pm 10 mJy

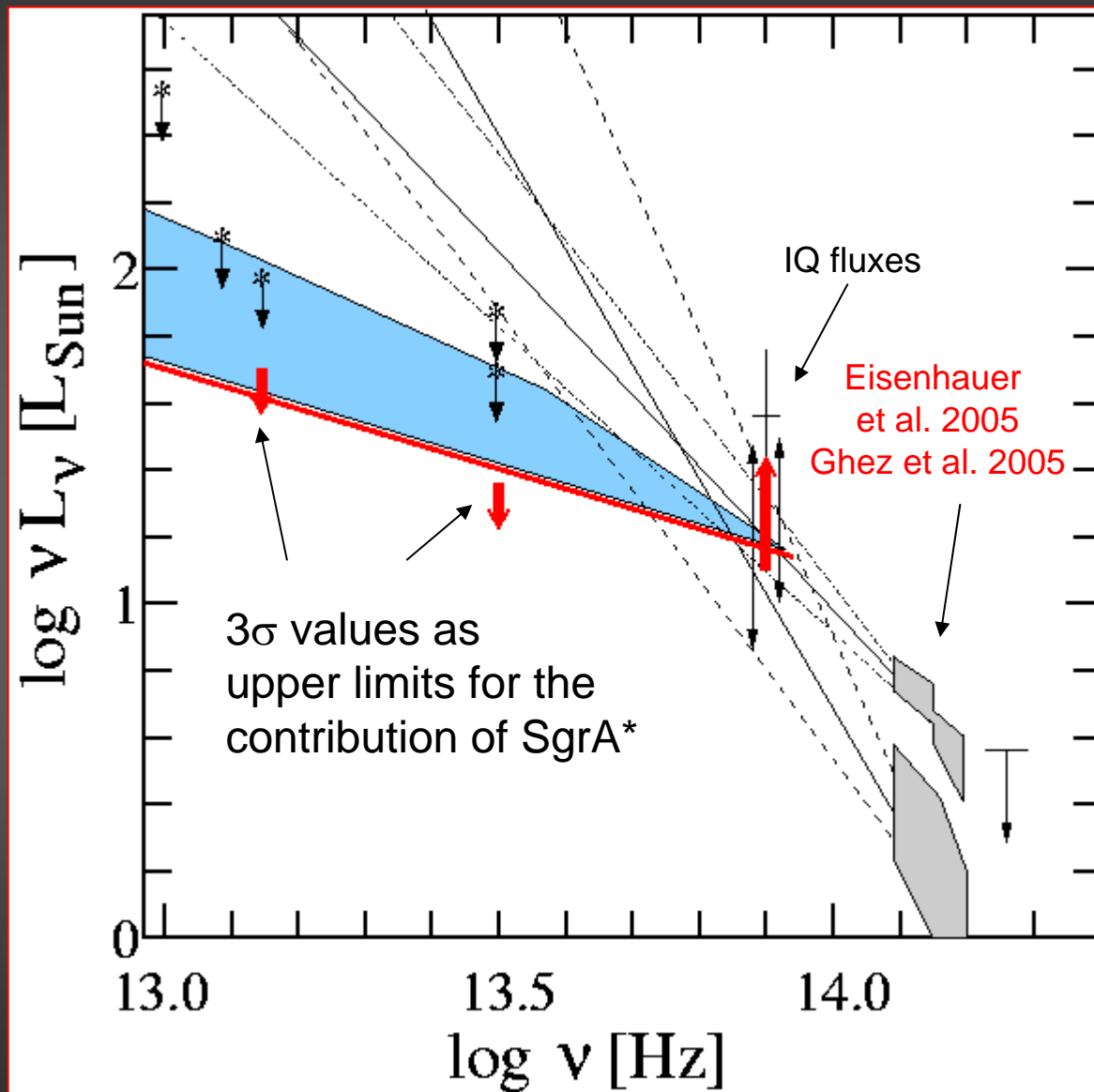
8.6 μm 50 \pm 10 mJy

19.5 μm 320 \pm 80 mJy

The emission at
8.6 μm and 19.5 μm
is dominated by dust

$$\begin{array}{ccc} & \text{spiral} & \\ & \text{ratio} & \\ S_{3.8} & \rightarrow & S_{8.6} \end{array}$$

$$S_{19.5} / S_{8.6} = \text{spiral ratio}$$



*A simple SSC Model
with a Synchrotron Spectrum
Truncated in the MIR/NIR*

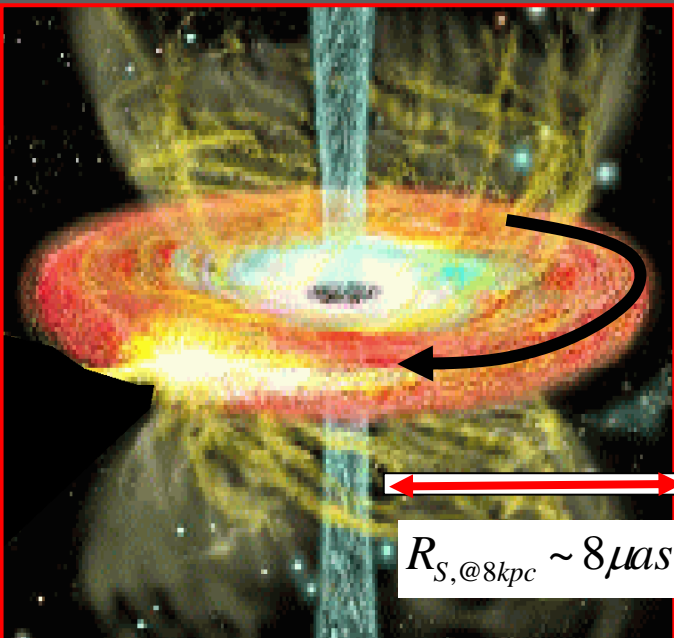
Table of Exemplary Models

model ID	S_{NIR} synchr. (mJy)	S_{NIR} SSC (mJy)	S_{N-very} (nJy)	B (G)	$\nu_{sync,pole}$ (GHz)	$S_{sync,pole}$ (Jy)	size (μas)	$\alpha_{NIR/N-very}$	c/ν_0 (μm)
IQ1	0.8	2.0	<18	17	820	3.9	7.9	1.3	-
IQ2	-	3.0	<27	5	820	7.7	8.1	1.3	-
IQ3	(25)1	0.1	<17	80	1000	16.0	17.5	1.0	15
IQ4	2.0	0.02	<15	38	1500	0.33	1.5	0.8	-
F1	(18)6	1.13	65	68	1640	11.5	8.5	1.1	5
F2	(300)6	0.1	230	100	1640	5.7	8.5	0.4	90

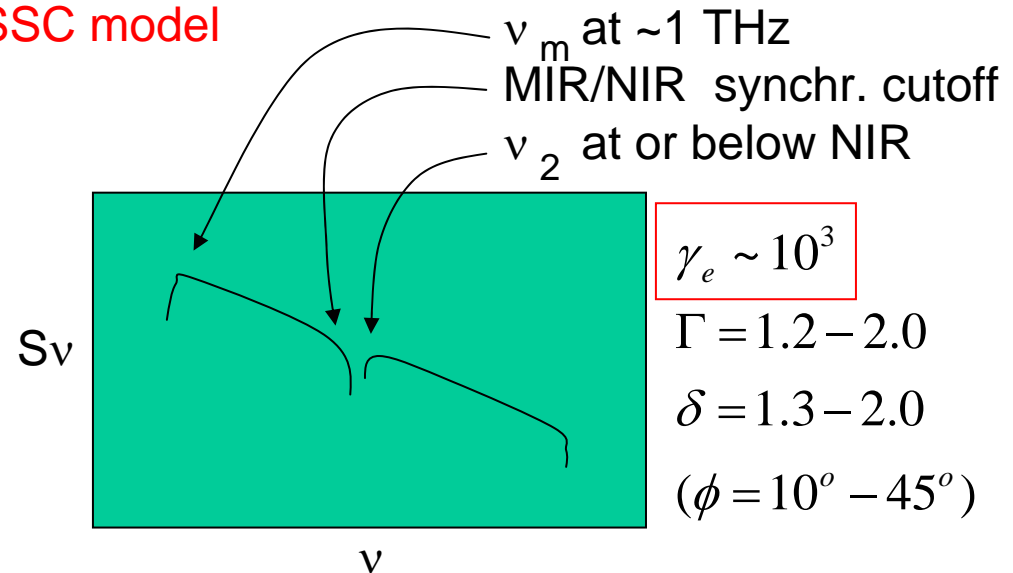
$$\gamma_e = (1 - \beta_e^2)^{-1/2}$$

$$\Gamma_{bulk} = (1 - \beta_{bulk}^2)^{-1/2}$$

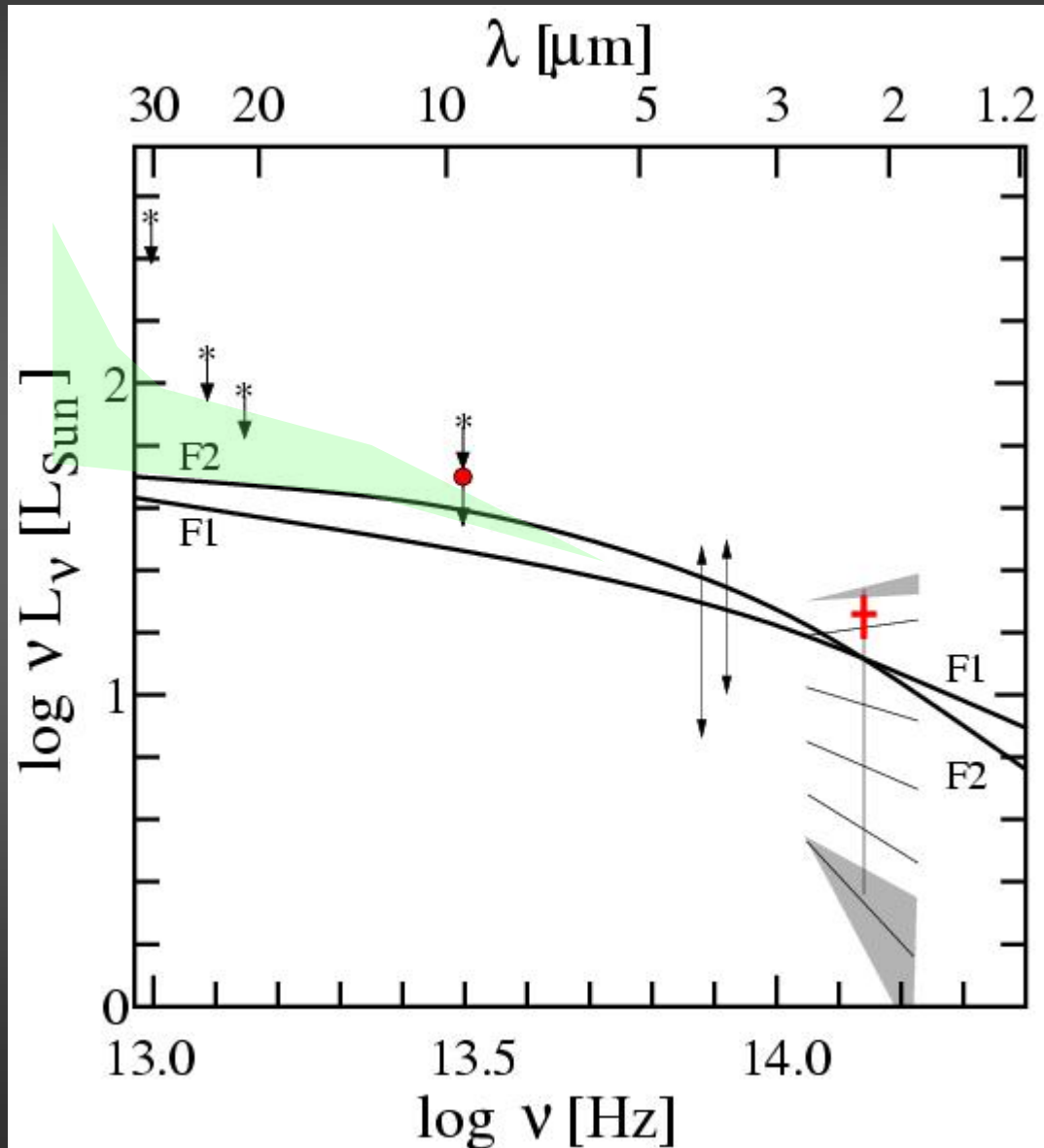
$$\delta = \Gamma^{-1} (1 - \beta_{bulk} \cos \phi)^{-1}$$



SSC model



Simultaneous weak flare models

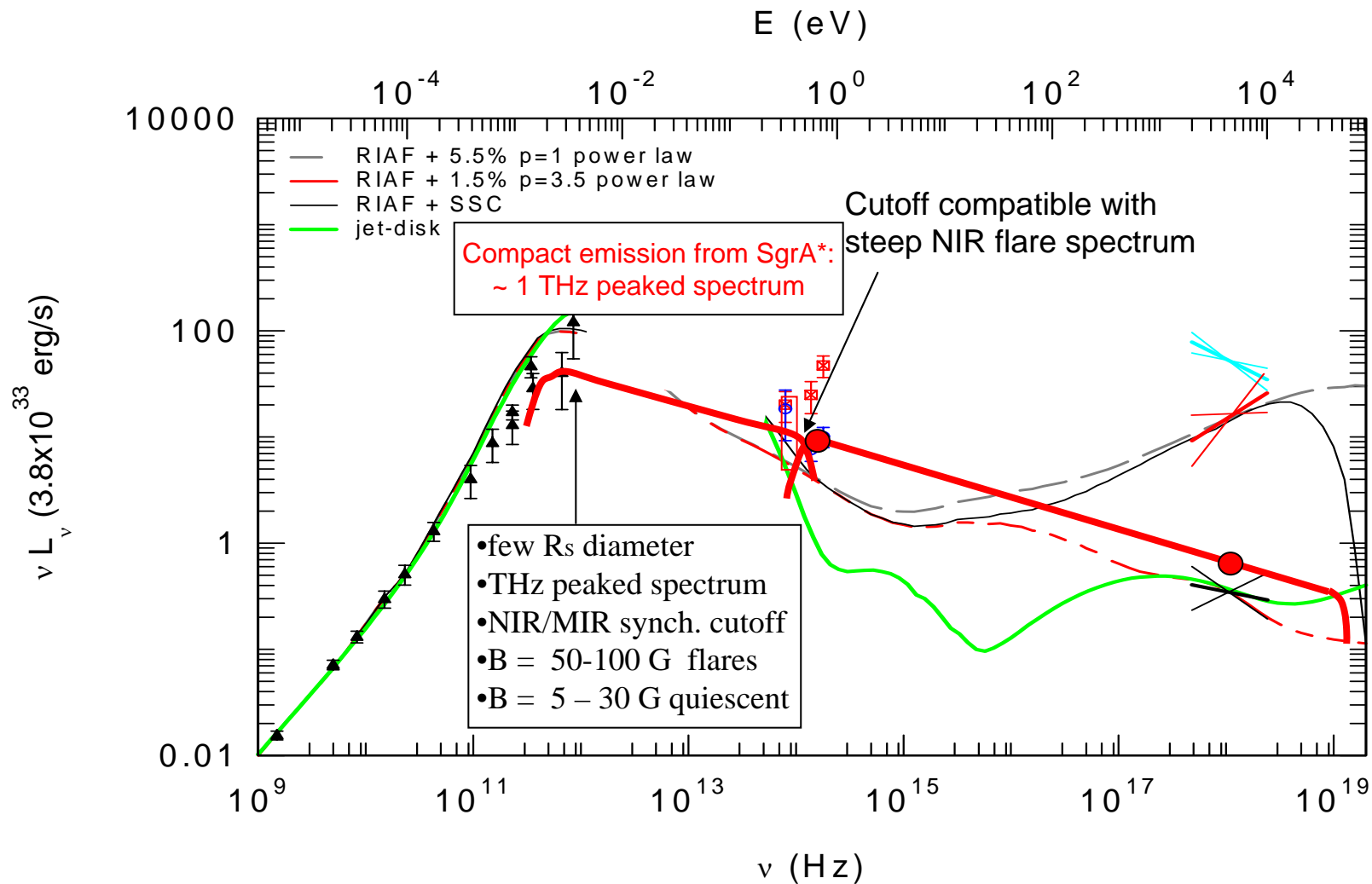


Cutoff may
shift towards
shorter wavelength:
NIR flare
spectral index may
be flatter

Model consistent
with low upper limits
in the MIR

See also
Gillessen et al. 2005
Eisenhauer et al. 2005

First simultaneous weak flare and models



Radio: Zhao, Falcke, Bower, Aitken, et al. 1999-2003

X-ray: Baganoff et al. 2001, 2003, Goldwurm et al. 2003, Porquet et al. 2003,

NIR: Genzel et al. 2003, Ghez et al. 2003

models: Markoff, Falcke, Liu, Melia, Narayan, Quataert, Yuan et al. 1999-2001

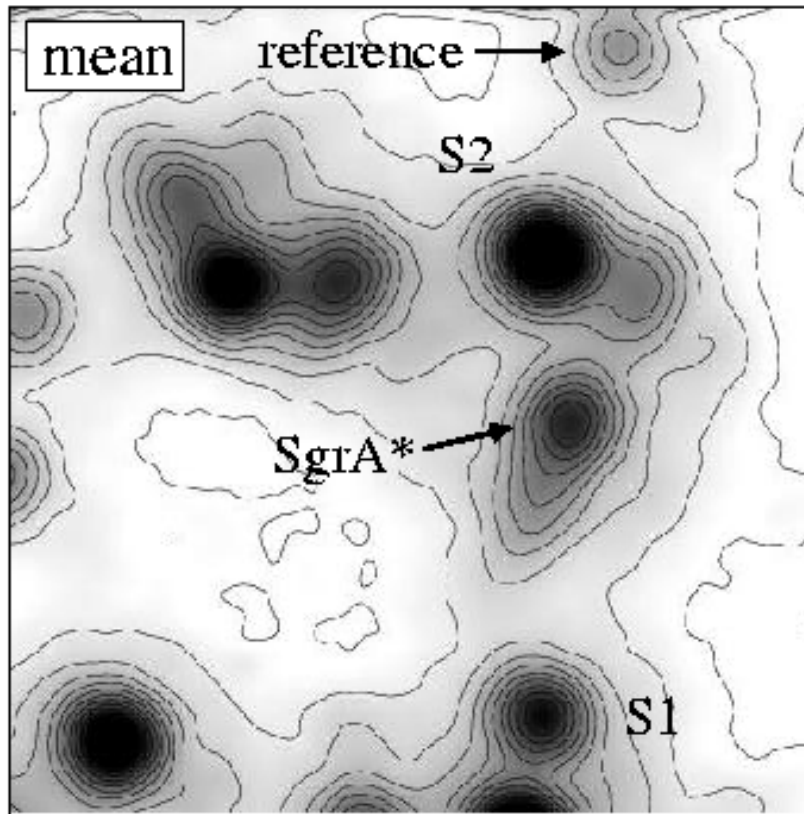
SSC model after Marscher (1983) and Gould (1979)

● — Data and model
Eckart, Baganoff, Morris et al. 2006

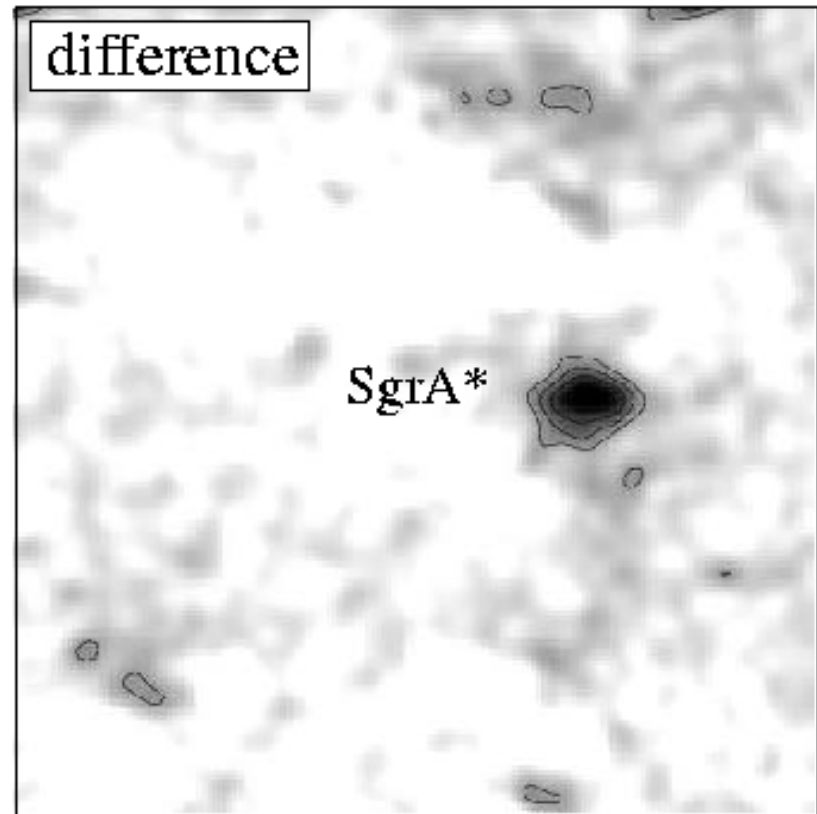
*Polarized NIR Flares
from SgrA* in
2004 and 2005*

Eckart, Schödel, Meyer, Ott, Trippe, Genzel 2006 A&A

NIR Polarized Flux Density from SgrA*



mean flux at 0 and 90 degree

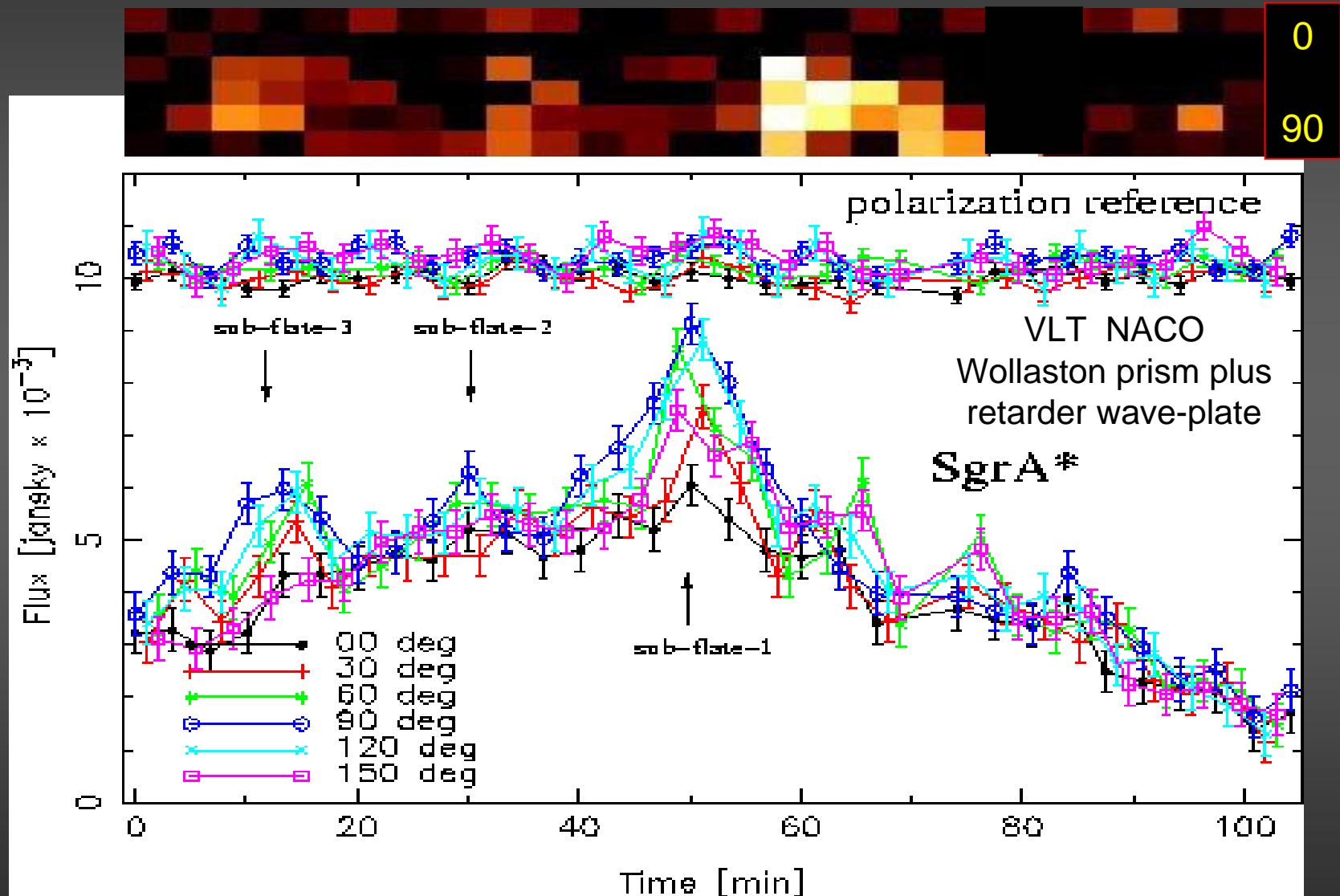


differential flux between 90 and 0 degree

July 2005: VLT NACO Wollaston prism plus retarder wave-plate

2005

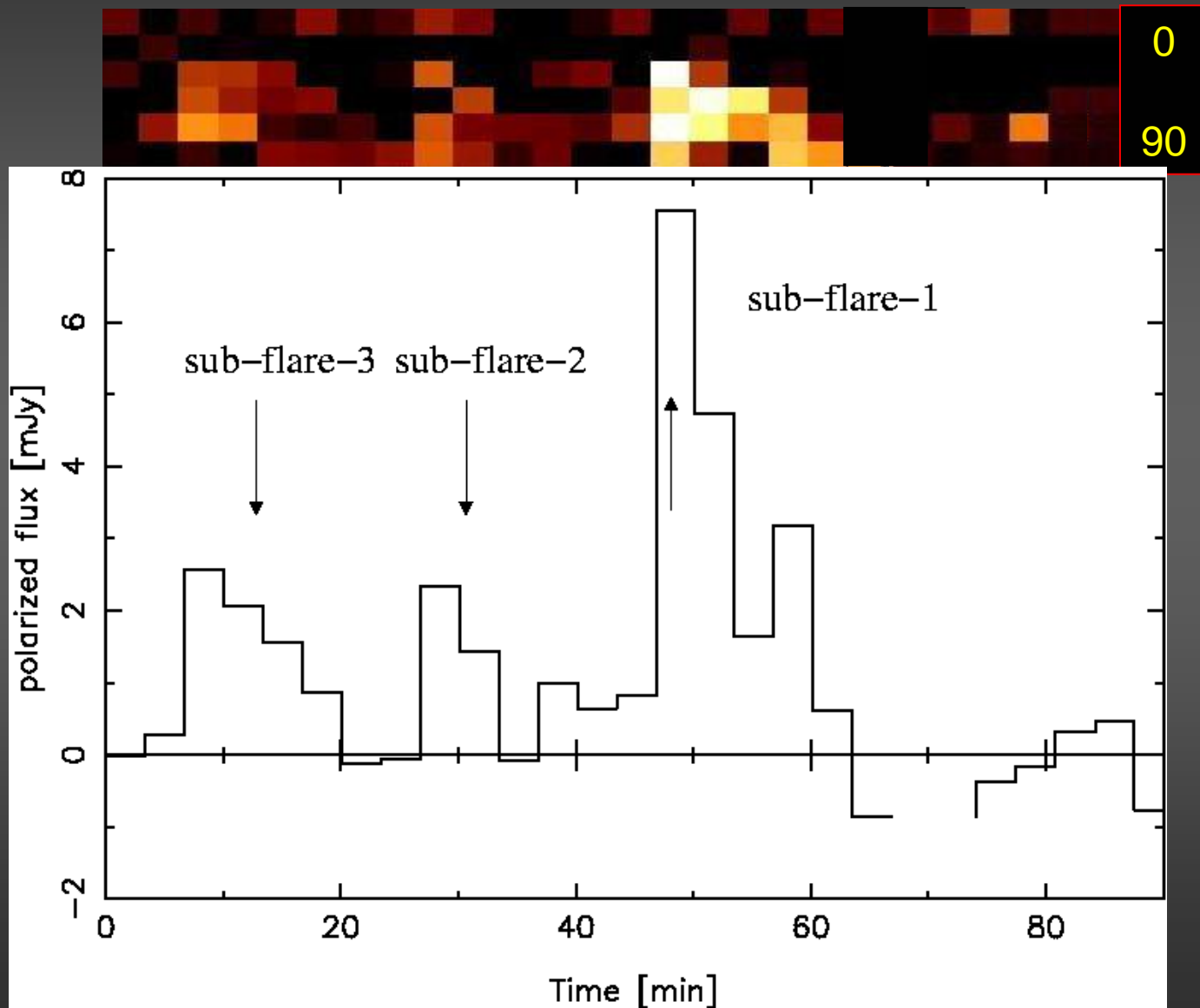
NIR Polarized Flux Density from SgrA*



Eckart, Schödel, Trippe, Ott, Genzel

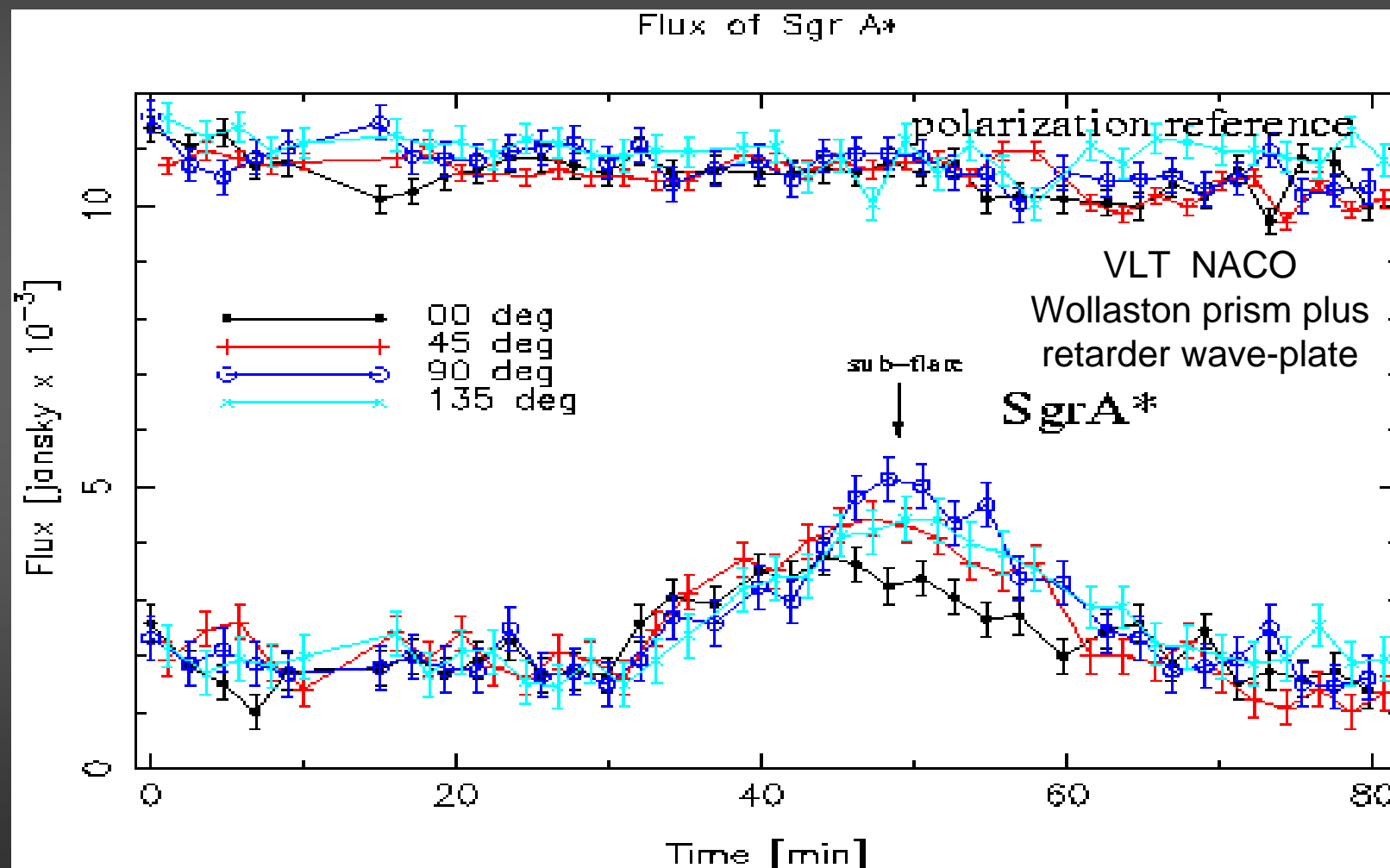
2005

Polarized Flux at 90 degrees



2004

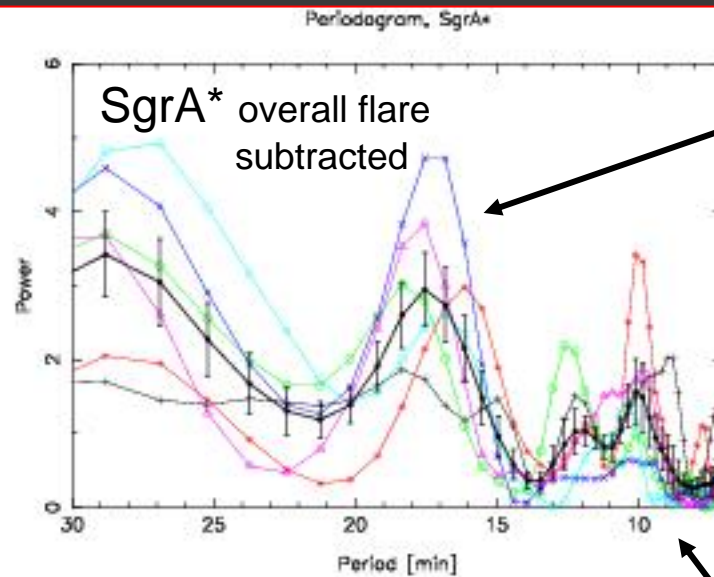
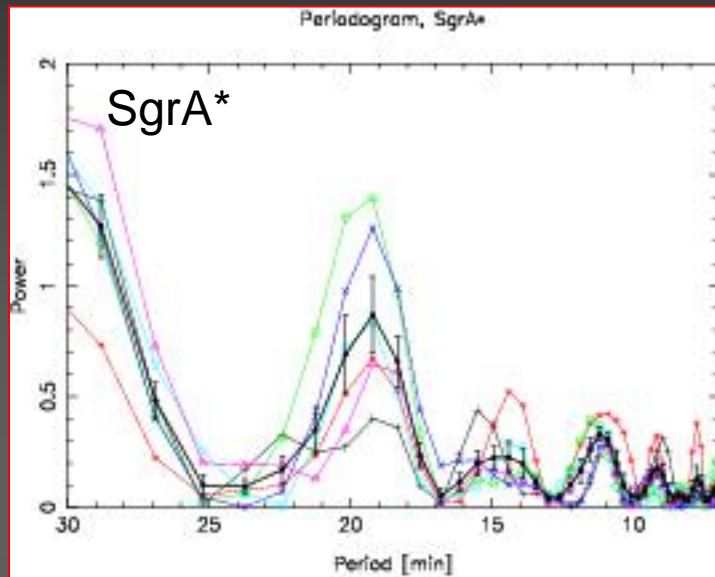
NIR Polarized Flux Density from SgrA*



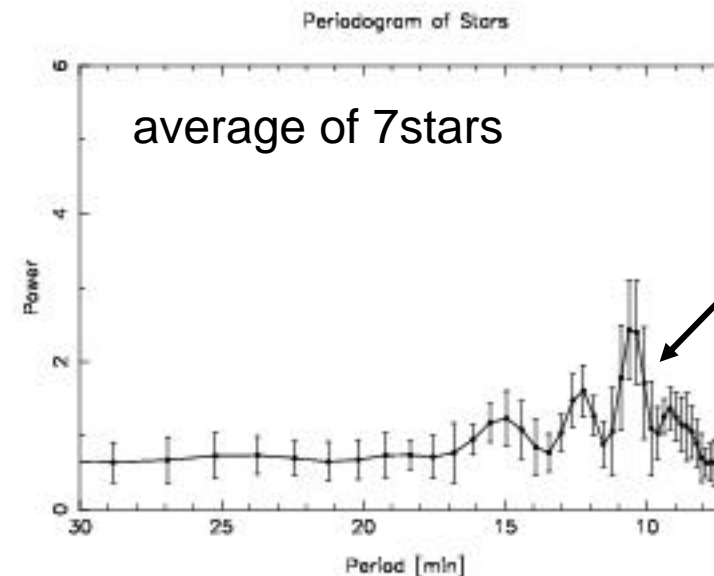
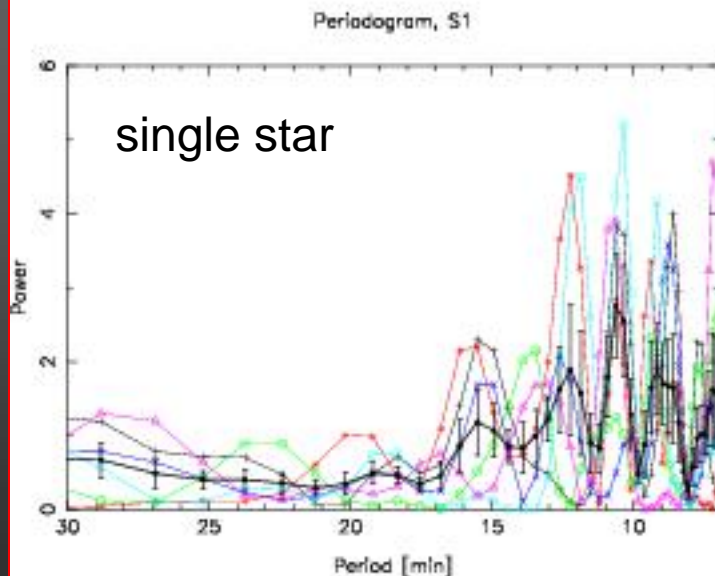
Eckart, Schödel, Trippe, Ott, Genzel

2005

NIR Polarized Flux Density from SgrA*

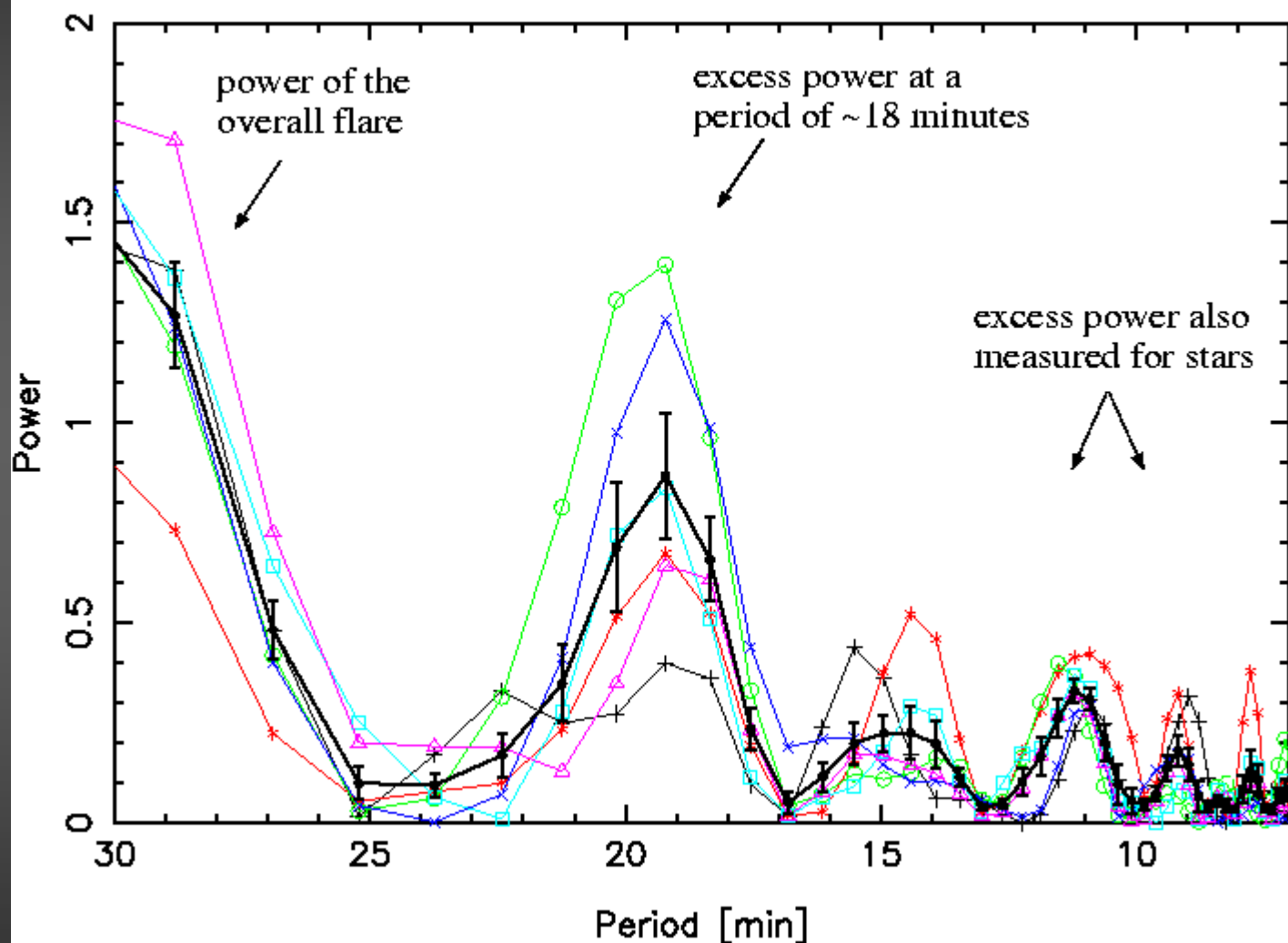


significant
excess
power in
SgrA*
at ~18min



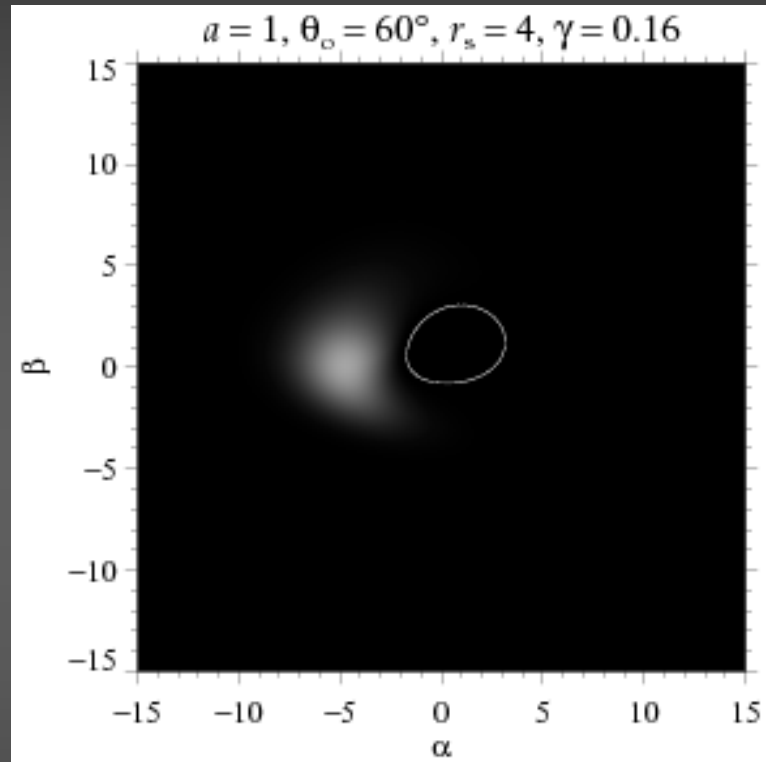
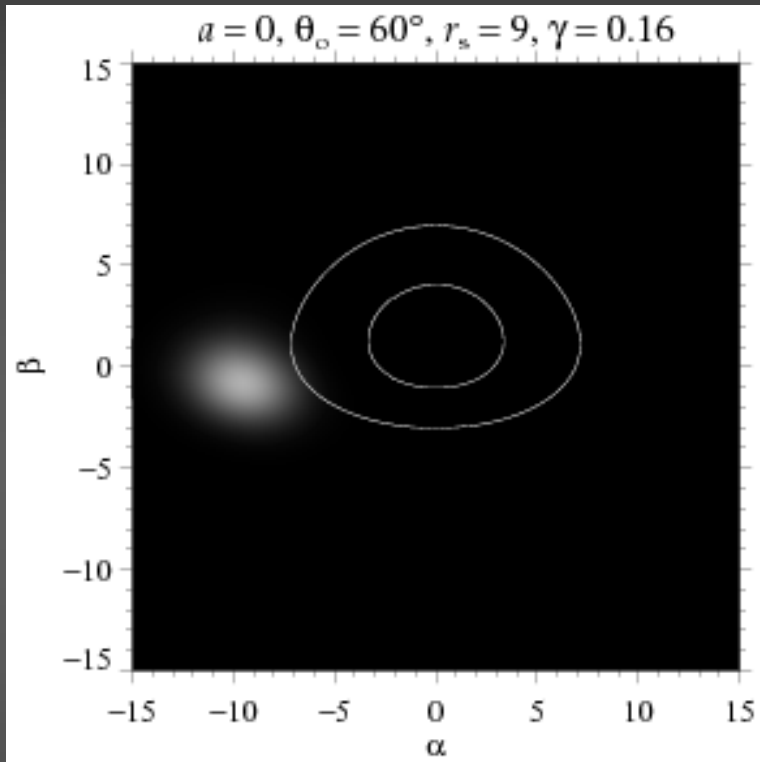
weak power in
stars and SGrA*

Periodogram, SgrA*



*Radiation from a
Temporal Accretion Disk*

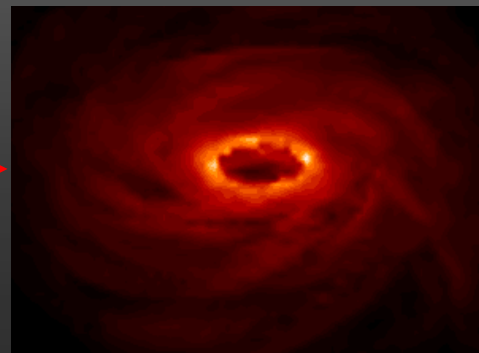
NIR Polarized Flux Density from SgrA*



Dovciak et al. 2006

Goldston, Quataert & Igumenshchev 2005, ApJ 621, 785

see also Broderick & Loeb 2005 astro-ph/0509237
Broderick & Loeb 2005 astro-ph/0506433



~4min prograde
~30min static
~60min retrograde
for $3.6 \times 10^{**6} \text{Msol}$

Cyclic Accretion Disk Modes ?

Cyclic modes associated with accretion disks are well known QPO from (Nowak & Lehr 1998):

- Kepler orbital motion
- Lense-Thirring Precession
- vertical and ...
- radial epicyclic oscillation modes

They depend on the dimensionless spin parameter $a=J/M$ and are of the order of a few 100Hz for 10 solar mass stellar BHs and about 0.6mHz for the GC MBH.



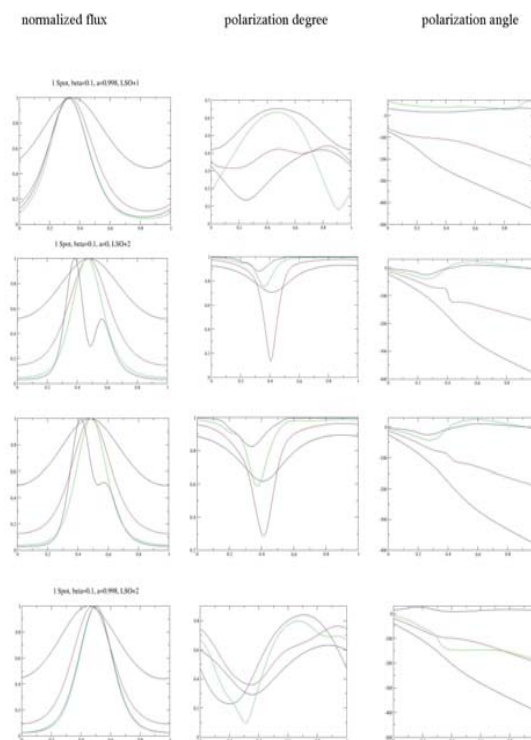
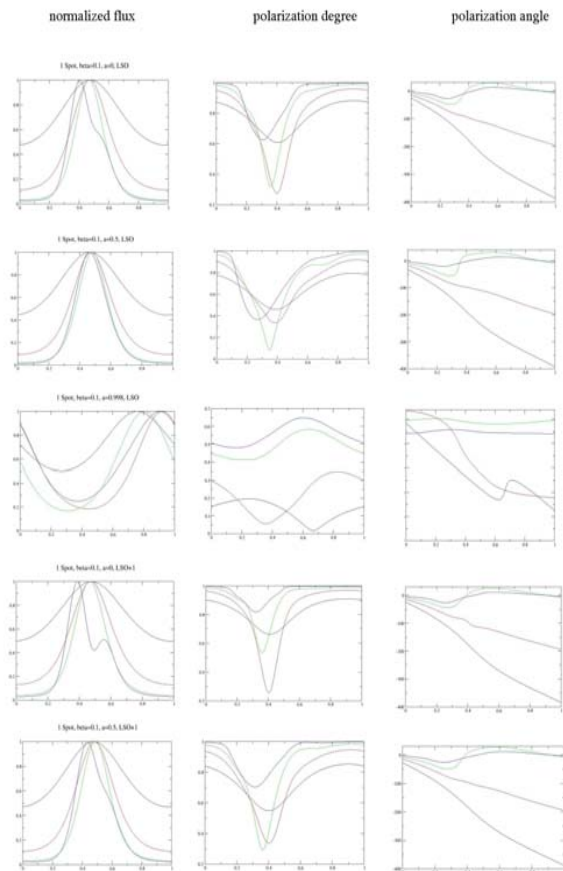
Aschenbach et al. (2004a,b) derive ~ 3.3 million solar masses and $a \sim 0.992$ as possible solutions for the Galactic Center.

If emission is not associated with LSO then 17min period may represent a lower frequency mode.

~ 4 min prograde
 ~ 30 min static
 ~ 60 min retrograde
for $3.6 \times 10^6 M_{\text{sol}}$

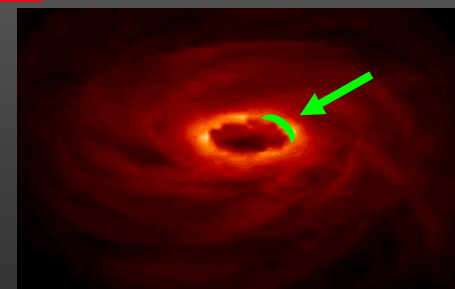
NIR Polarized Flux Density from SgrA*

total power,
degree of polarization
and position angle from
model calculations



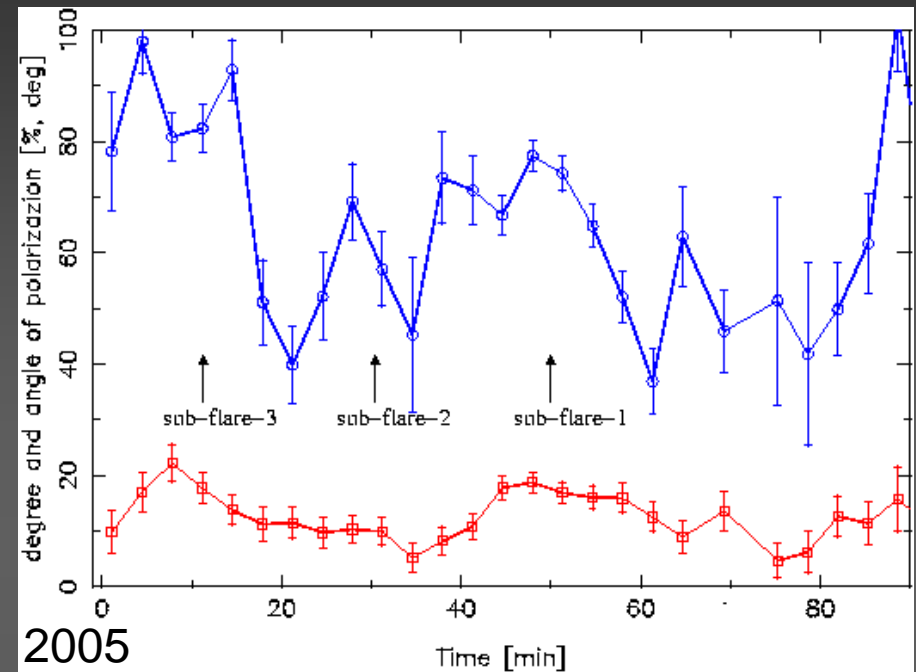
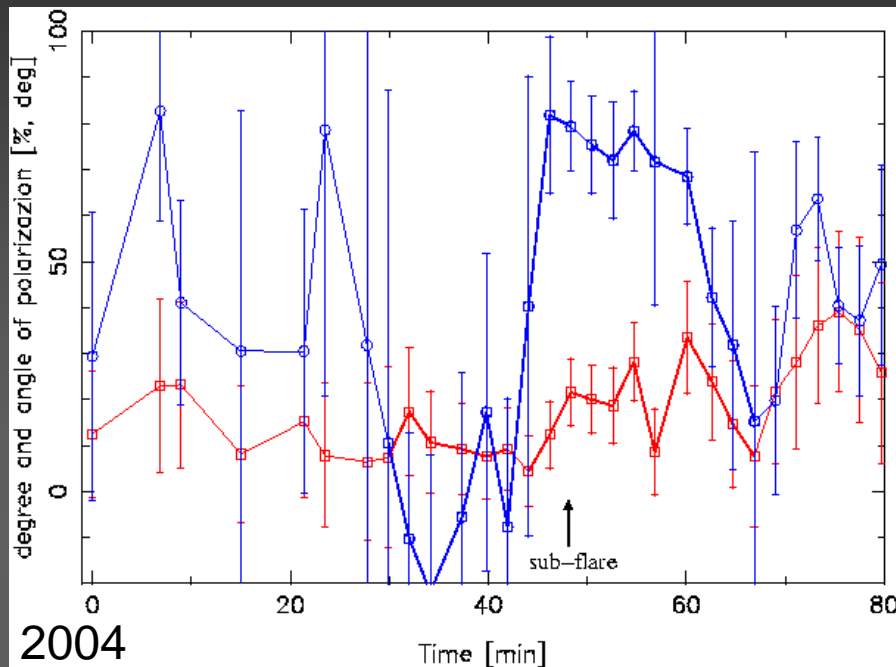
$a=0.5$ ($t \sim 20$ min),
 $i=45$,
 $r=\text{near LSO}$
Blob, $\sigma=1.1R_s$

flat spots
on disk



Code: Dovciak M., Karas, V., & Yaqoob, T., ApJS July 2004, 153, 205-221

Position angle of the polarized emission from SgrA* ?



position angle degree of polarization

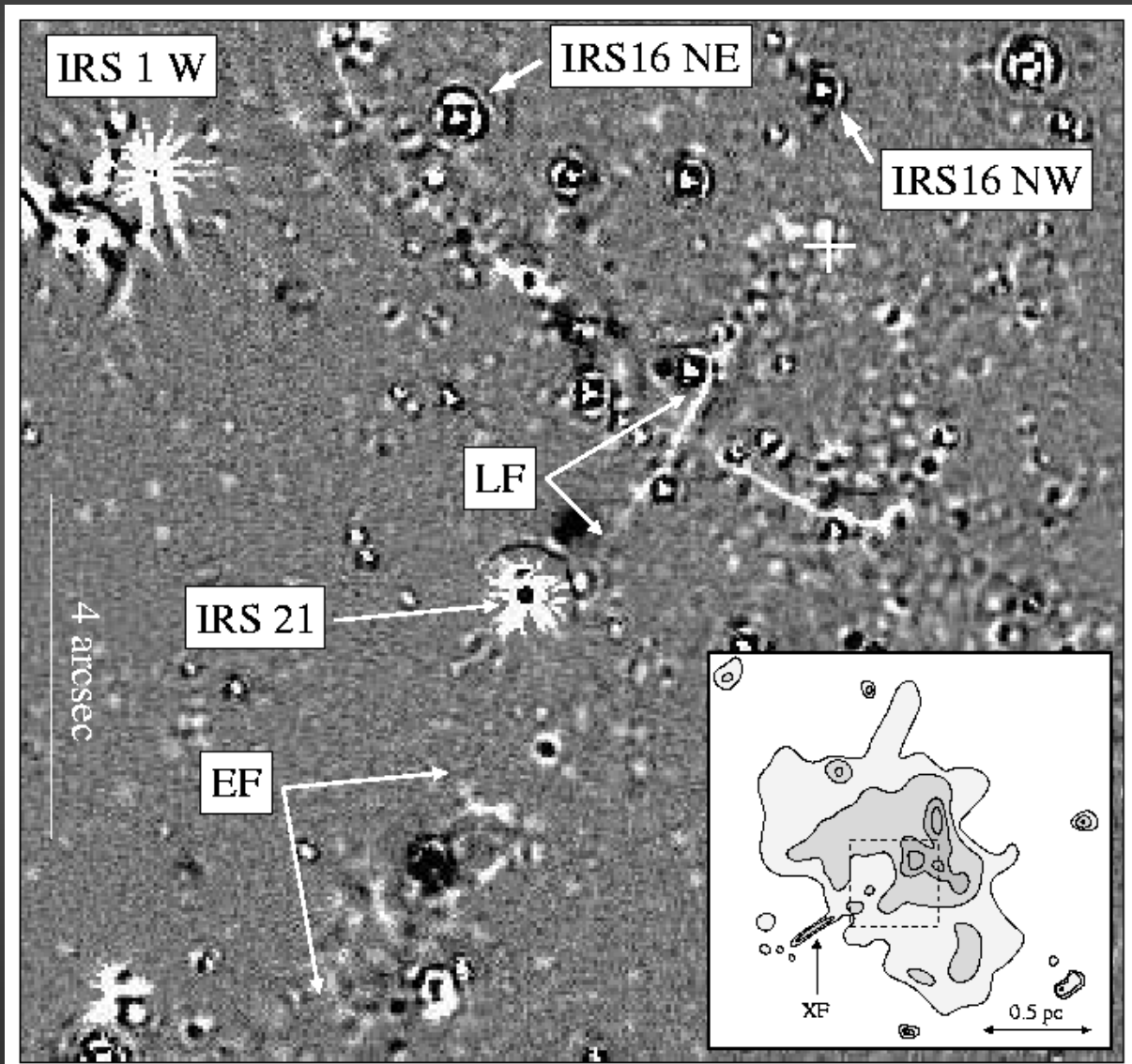
The polarization angle varies about a value of 60 ± 20 indicating that this would correspond to the PA of an accretion disk – if existent – and if the mean PA of the E-vector is perpendicular to the disk.

If the emission is due to a jet the PA of the jet is less clear:

Pollack, Taylor & Zavala 2003 find a flat distribution with a tendency of a perpendicular jet and E-vector

Rusk 1988 and Gabuzda et al. 2000 find a weak indication for parallel orientations in stronger beamed sources

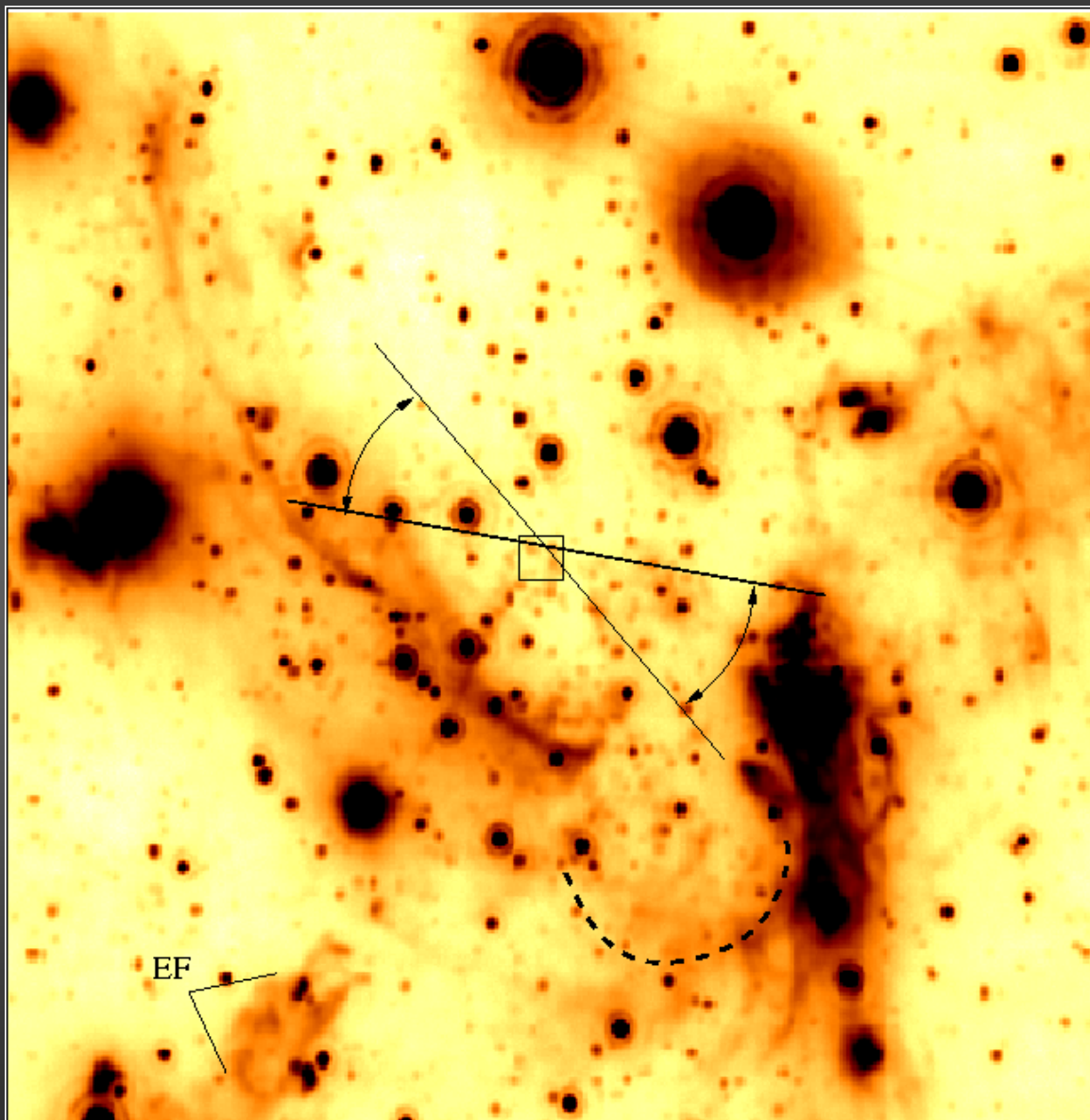
A jet or wind emerging from SgrA* ?



Two possible jet features
LF in the IR and
XF in the X-ray
(Morris et al. 2004).

Position angles:
LF ~30
XF ~60
LF is curved
LF and XF are not
colinear.

A jet or wind emerging from SgrA* ?



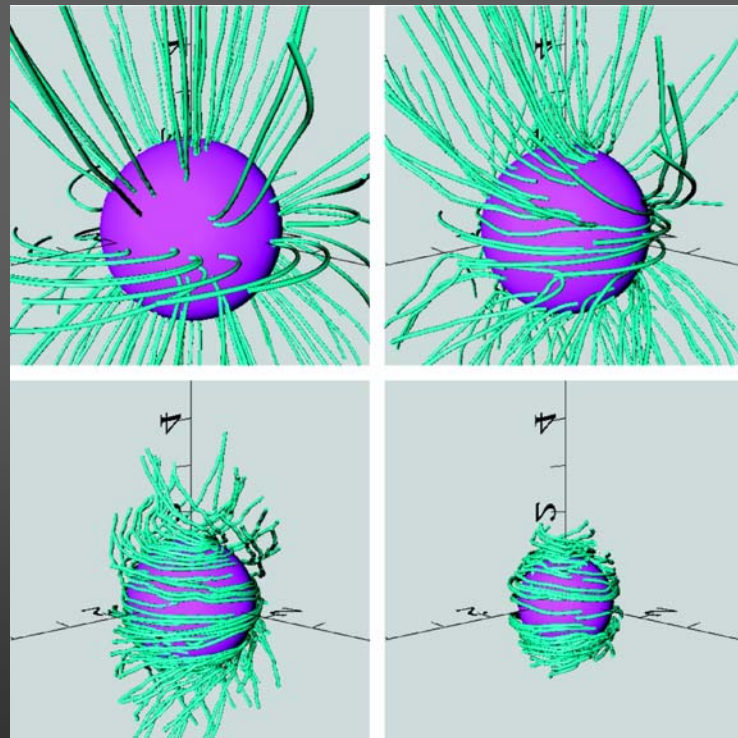
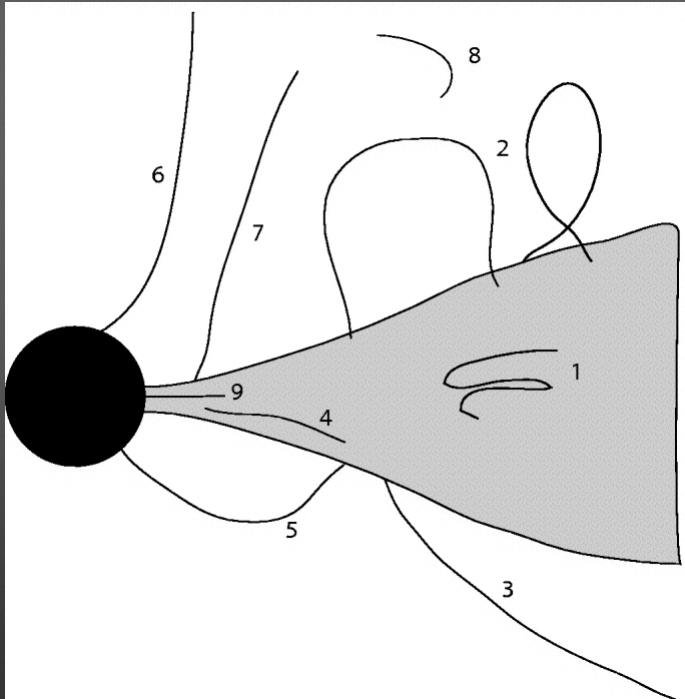
The central 0.5×0.5 square pixel at $3.8 \mu\text{m}$.

E-vector PA of 60 ± 20 with respect to prominent structures

What Magnetic Fields Can Do

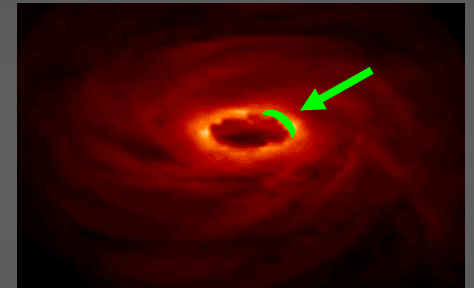
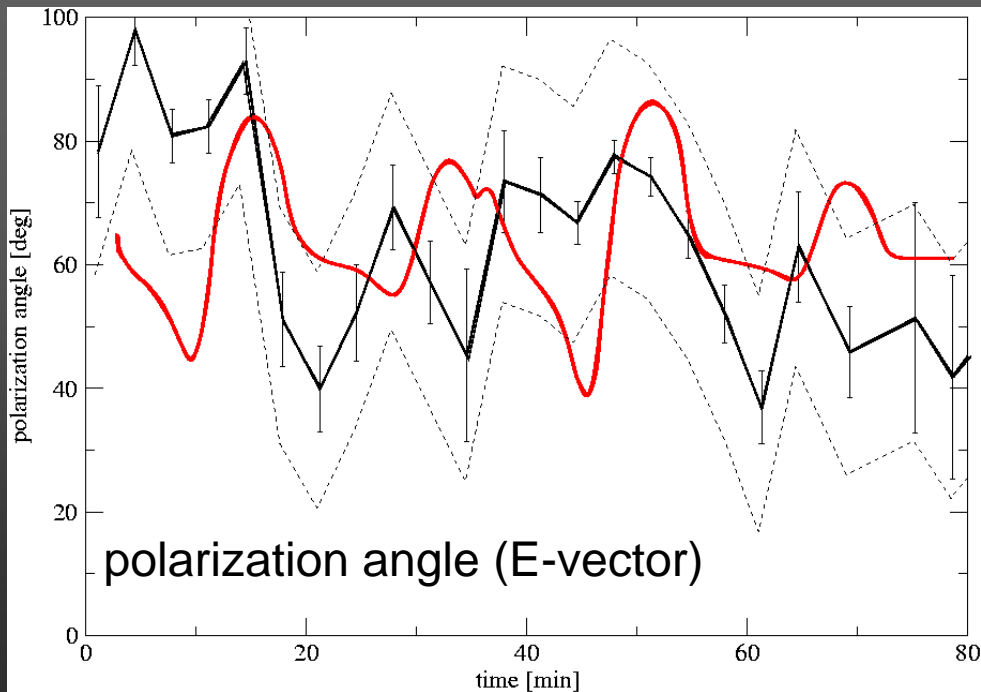
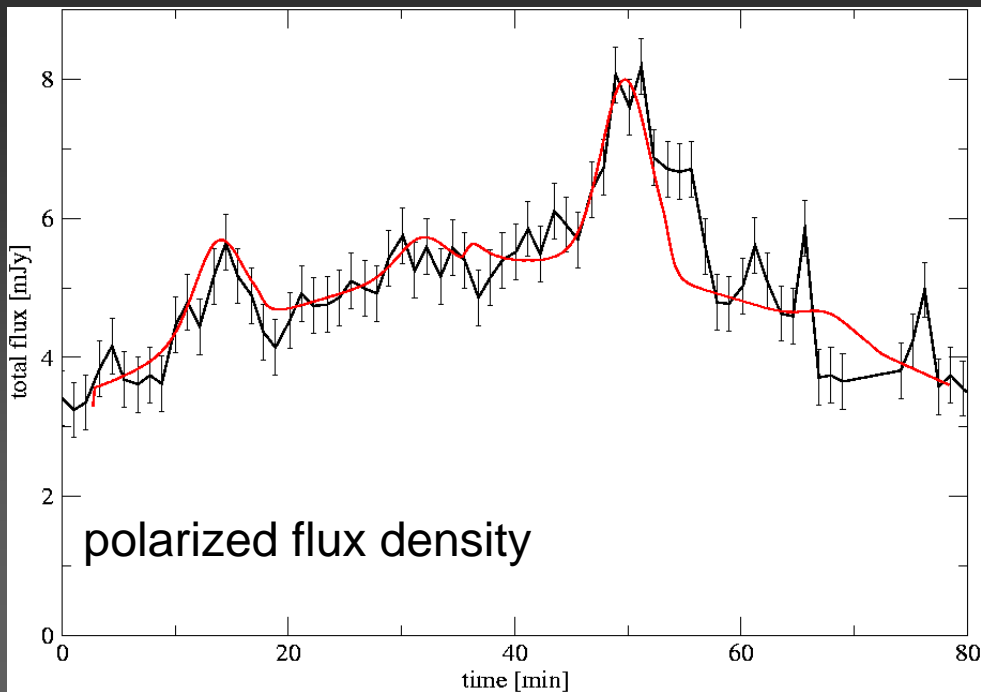
NIR Polarized Flux Density from SgrA*

Blandford, 2002 in
Lighthouses of the Universe



Hirose, Krolik, De Villiers, Hawley 2004, ApJ 606, 1083

NIR Polarized Flux Density from SgrA*



NIR Polarization Data

*Assumption:
Flare activity is due to orbital motion
~20 min quasi-periodicity is relevant*

NIR polarization data is in agreement with $a \sim 0.5$

*General Statement on
Variability of SgrA**

NIR Flare Rate

Results by Hornstein and Viehmann
scaled to 100 min.

The results of the 2005 session are in agreement with a K-band flare rate of

$$4 \pm 2 \text{ flares/day}$$

Assumption:

- characteristic flare length

$$\kappa_0 \sim 100 \pm 30 \text{ min}$$

- The NIR emission of SgrA* can be described by consecutive flares of that characteristic length

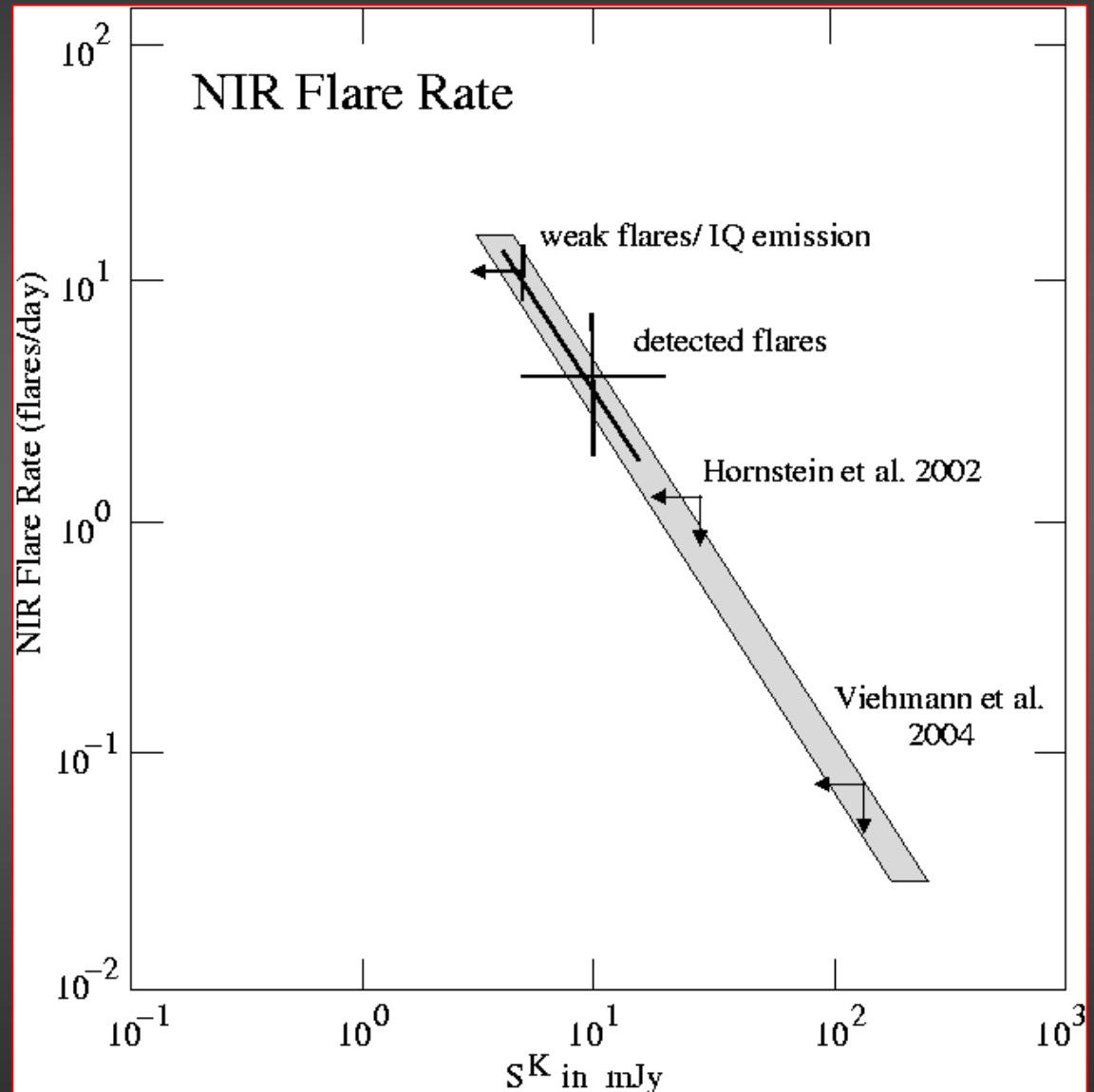
Finding:

Flare rates and limits lie on a $\zeta = -1.4 \pm 0.2$ power-law

$$N(A) = \kappa_0 A^{-\zeta} \kappa_1 \kappa_2$$

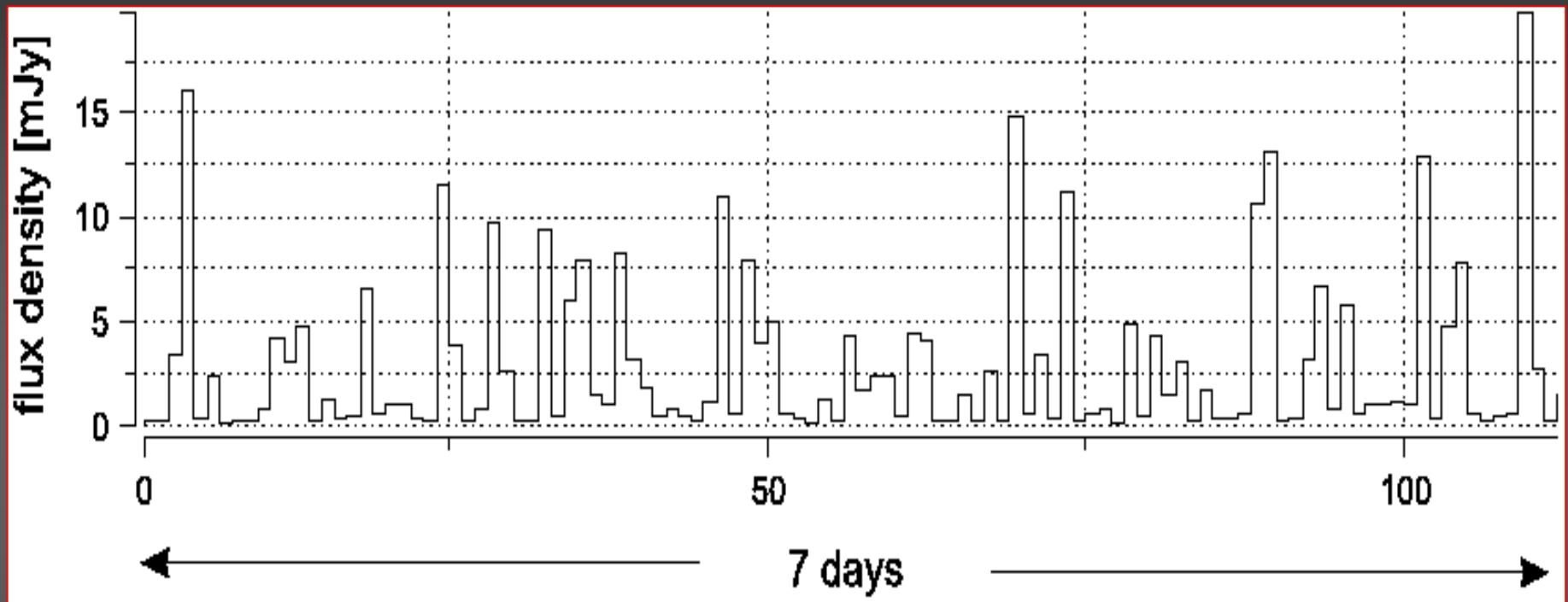
$$\kappa_1 = \exp(-A / A_{\text{high}})$$

$$\kappa_2 = \exp(-A_{\text{low}} / A)$$



value of ζ is independent on value for κ_0

Simulation of SgrA* NIR flare activity



Simulation of the NIR flare activity assuming a characteristic flare length of 100 minutes, a typical flare flux of 10-20 mJy, and a power-law dependency with a power-law index of $\zeta \sim -1.4$

Are there dominant red noise contributions?

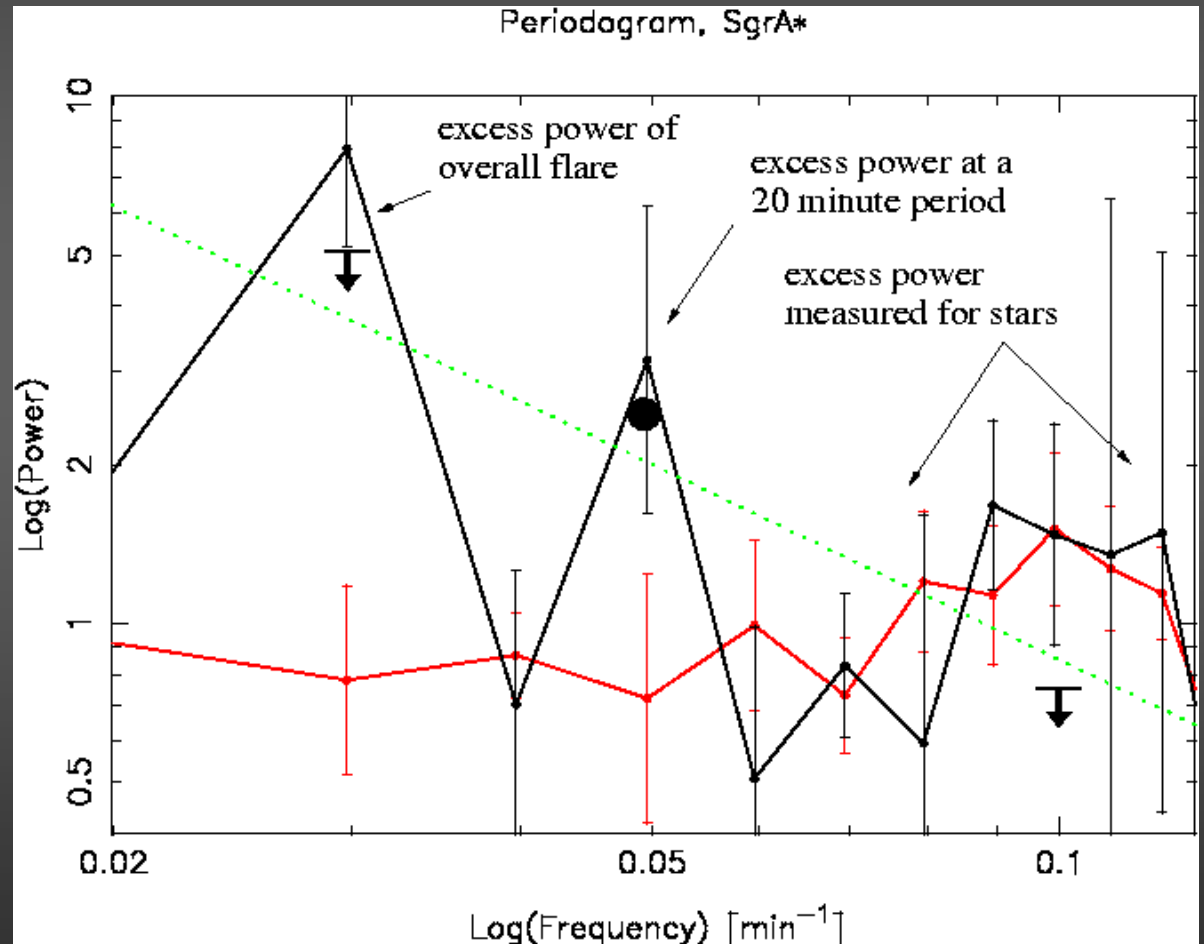
Mauerhan et al. 2005
(in the mm-range for SgrA*)
and Benlloch et al. 2001
(X-ray domain for Mrk766)
showed that for >10-20 min
variability the variability can
be describe by a red noise
power law of the form

$$P(f) \sim f^{-\beta}$$

We find

$$\beta = 1.2 \pm 0.7$$

and therefore no
significant indication for
dominant red noise
contributions in the
covered frequency range



*Are there Alternatives to
the BH Scenario?*

Neutrino Ball Scenario

supported by degeneracy pressure

Scaling relation between mass and radius
(Munyanenza, Tsiklauri, & Viollier 1999):

$$MR^3 = \frac{91.869 \hbar^6}{G^3 m_\nu^8} \left(\frac{2}{g_\nu} \right)^2$$

$$MR^3 = 3 \times 10^6 (23.18 \text{ mpc})^3 \left(\frac{17.2 \text{ keV}}{m_\nu c^2} \right)^8 g_\nu^{-2}$$

For large neutrino masses small radii can be obtained. However, to explain all nuclear dark masses ranging between 3 million (GC) and 3000 Million (M87) solar masses the

putative, as yet unidentified neutrinos

must have a mass in the range of **17keV**.

Radii for the GC are then of the order of **15mpc**



Can be excluded for the Galactic Center !

Stellar orbits near SgrA* make a universal Fermion ball scenario for extragalactic objects very unattractive

Boson Star Scenario

Torres, Capozziello & Lambiase 2000, Phys.Rev D62, 104012
supported by Heisenberg uncertainty principle

non-interaction Bosons:

Kaup 1968, Ruffini & Bonazzola 1969

$$m = 1\text{GeV}, R = 1\text{fm}, M = 10^{-19} M_{\odot}$$

self-interacting Bosons:

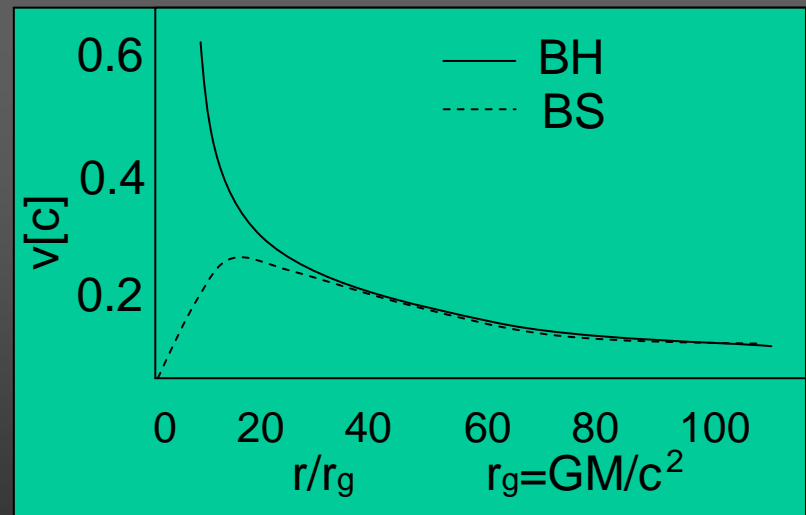
Colpi, Shapiro & Wasserman 1986, Torres, Capozziello & Lambiase 2000,
Lu & Torres 2003:

For a large range of hypothetical boson masses much larger total masses within radii of only several times their Schwarzschild radii are possible.

GC: $M[10^6] \approx M(x) / m[\text{GeV}] \times 10^{-25}$

$$x = mr, m \approx 3 \times 10^{-26} \text{GeV}$$

$$r[\text{pc}] \approx x / m[\text{GeV}] 7 \times 10^{-33}$$



Unlikely to form a stable configuration at the Galactic Center !

Boson Star Scenario

Assumption:

Flare activity is due to orbital motion close to the LOS with a quasi-periodicity of close to 20 min what is indicated by the NIR data:

For a boson star the orbital velocity at the BH LOS
Is about 3 times lower than it is for the BH case!

For a non-rotation GC BH the orbital period close to
the LOS is about 30 min

A non-rotation boson star can be excluded for the GC

Excluded for MCG-6-30-15 (Lu & Torres 2003) based on $K\alpha$ line width!

IMBHs

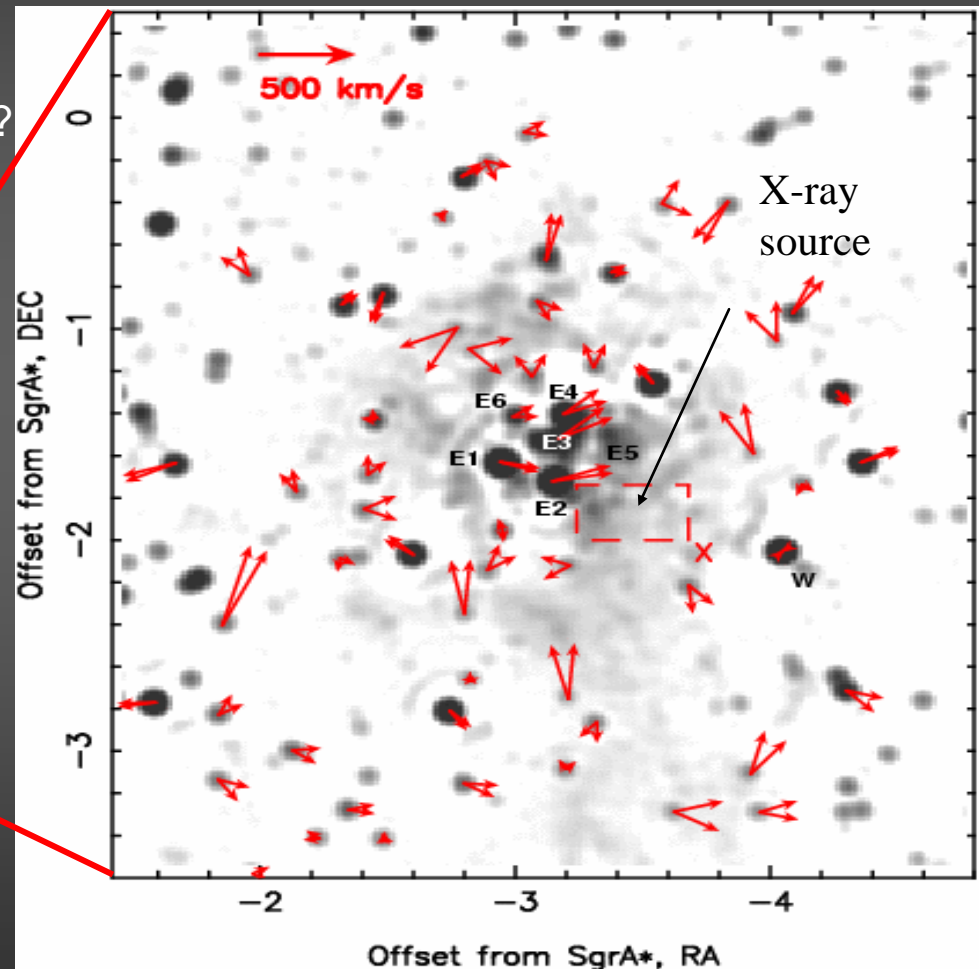
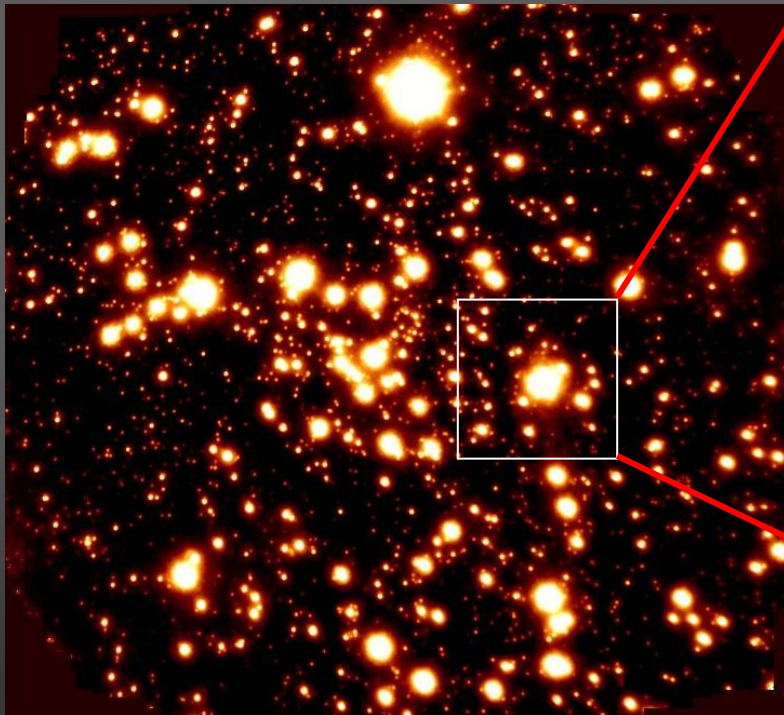
IRS13

IMBH contained in IRS13?

An IMBH at the Center of the IRS13 Concentration?

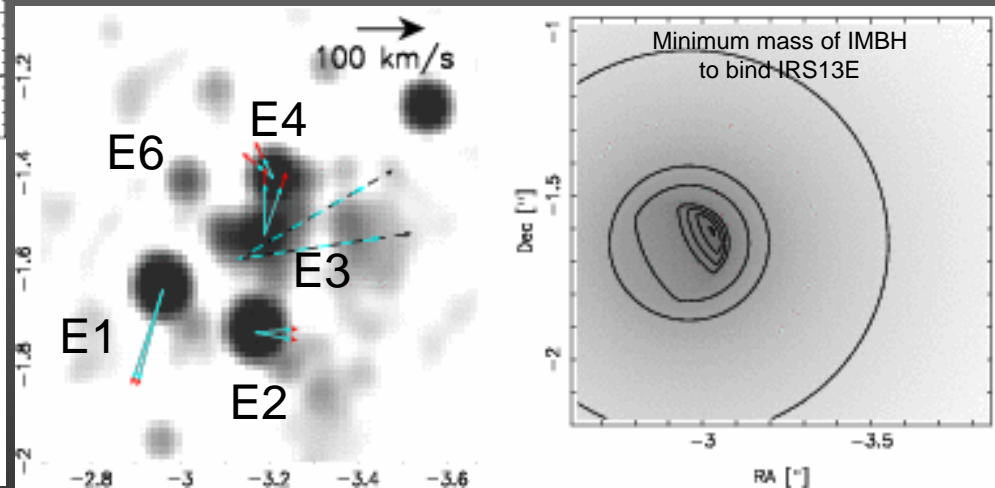
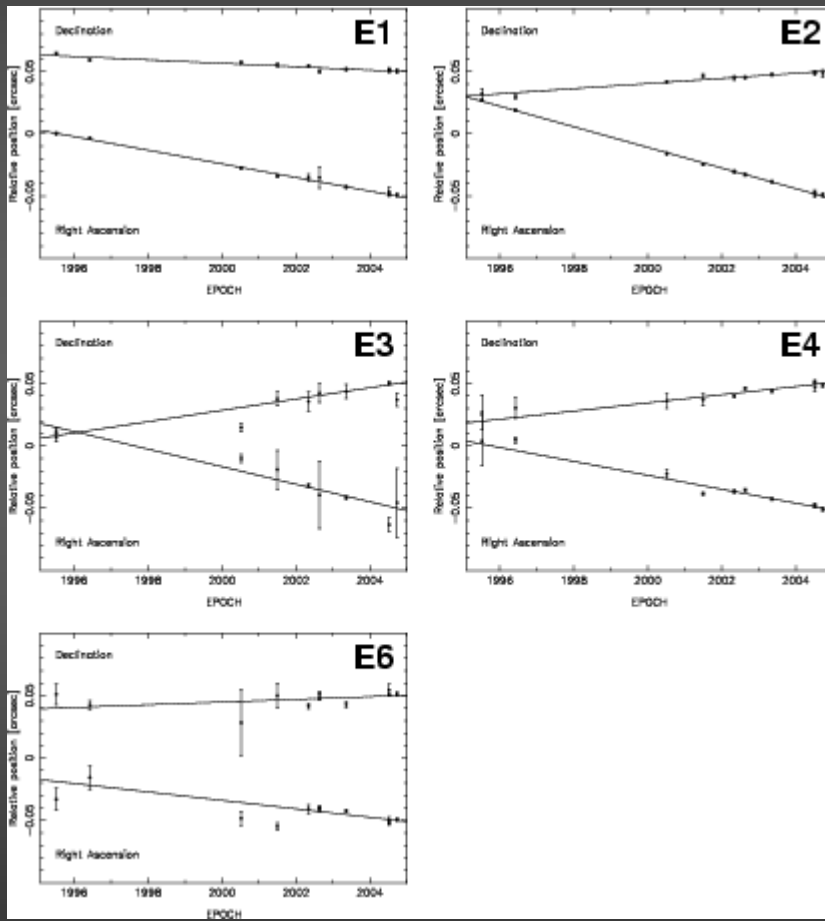
IRS13E comprises half a dozen massive stars- possibly a remnant of an infalling stellar cluster (Gerhard (2001), Genzel (2003), Kim & Morris (2003).

Is there an IMBH at the center of this complex?
Hansen & Milosavljevic (2003),
Maillard et al. (2004).



An IMBH at the Center of the IRS13 Concentration?

Proper motions of individual stars in the IRS13E complex show that the minimum mass to bind IRS13E is 10,000 M_{solar} with no compelling evidence for the actual existence of an IMBH



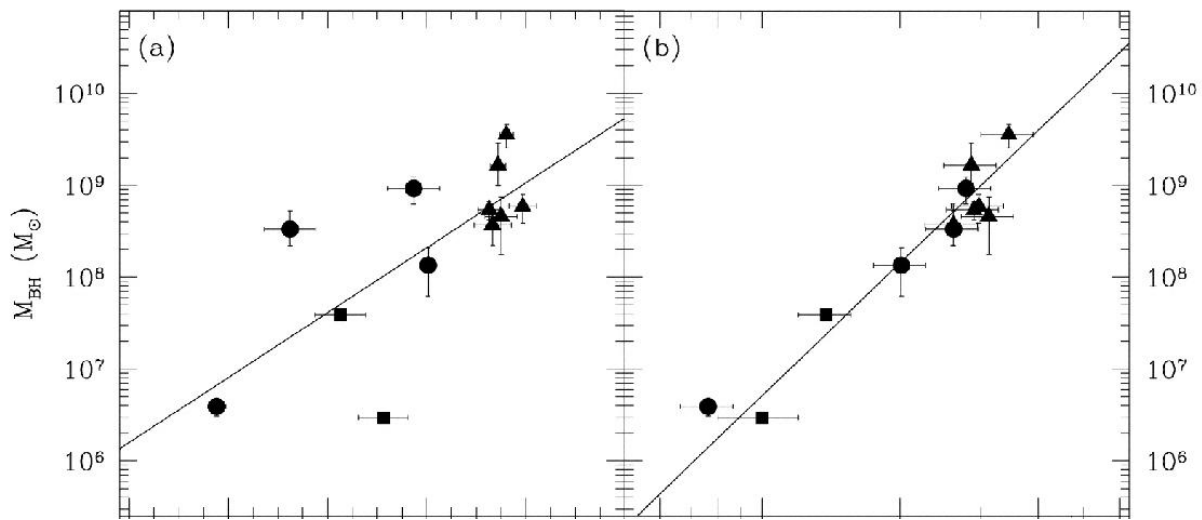
MBHs in Galactic Nuclei

Black Hole - Bulge Relationship

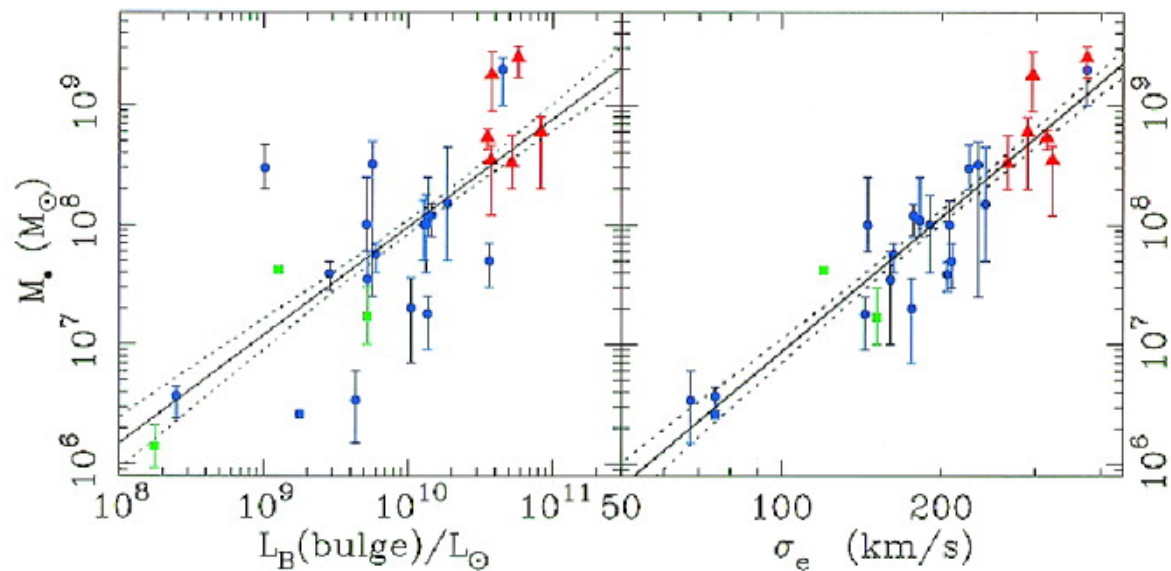
Massive Black Holes (MBH) in Nuclei of Galaxies

- Compact dark masses (probably MBHs) in Nuclei of Galaxies (Kormendy and Richstone 1995)
- MBH about 0.006 of bulge mass (Magorrian et al. 1998)
- 3D models of HST data: MBH/bulge=0.002 (Ho 1999)
- 5 to 20 times smaller MBH in Seyferts and PG QSOs via reverberation mapping (Wandel 1999, Ho 1999)?!
- With the much tighter MBH- σ relation this discrepancy seems to disappear (Ferrarese & Merritt 2000, Gebhardt et al. 2000, Shields et al. 2003)
- Nelson (2000) finds no difference between MBH- σ (OIII) masses and BH masses taken from reverberation methods and proposes to use σ (OIII)=FWHM([OIII])/2.35km/s as surrogate for σ stellar.
- LOCAL: MBH/bulge =0.0016 Kormendy & Gebhardt (2001)
How does this evolve with redshift??

M-L_{bulge} versus M- σ Relations



Farrese & Merritt 2000



Gebhardt et al. 2000

M- σ Relations

$$M_{BH} = 1.40 M_{sol} \left(\frac{\sigma_*}{200 \text{ km / s}} \right)^{4.8 \pm 0.5}$$

Merritt & Farrese 2000

$$M_{BH} = 1.20 M_{sol} \left(\frac{\sigma_*}{200 \text{ km / s}} \right)^{3.8 \pm 0.3}$$

Gebhardt et al. 2000

$$M_{BH} = 1.35 M_{sol} \left(\frac{\sigma_*}{200 \text{ km / s}} \right)^{4.02}$$

Tremaine et al. 2002

Stellar dynamics is hard. How can one extend this to higher z ??

Massive Black Holes (MBH) in Nuclei of Galaxies

- Compact dark masses (probably MBHs) in Nuclei of Galaxies (Kormendy and Richstone 1995)
- MBH about 0.006 of bulge mass (Magorrian et al. 1998)
- 3D models of HST data: MBH/bulge=0.002 (Ho 1999)
- 5 to 20 times smaller MBH in Seyferts and PG QSOs via reverberation mapping (Wandel 1999, Ho 1999)?!
- With the much tighter MBH- σ relation this discrepancy seems to disappear (Ferrarese & Merritt 2000, Gebhardt et al. 2000, Shields et al. 2003)
- Nelson (2000) finds no difference between MBH- σ (OIII) masses and BH masses taken from reverberation methods and proposes to use σ (OIII)=FWHM([OIII])/2.35km/s as surrogate for σ stellar.
- LOCAL: MBH/bulge =0.0016 Kormendy & Gebhardt (2001)

How does this evolve with redshift ??

Formation of Massive Black Holes (MBH)

Who knows how it got started??

Quasars at $z > 6$ (e.g. Becker et al. 2001);

10^{10} M \odot BHs only 10^6 yrs after Big Bang (e.g. Haiman & Loeb 2001)

- Yu & Tremaine (2002) find that half the BH mass is accreted before $z \sim 1.8$ and only 10% before $z = 3$.

- Shields et al. (2003) use FWHM([OIII]) to determine MBH at high redshifts. From $\log(\text{MBH}(\text{H}\beta) - \text{MBH}([\text{OIII}])) \sim 0$ between $0 < z < 3.5$ they conclude:

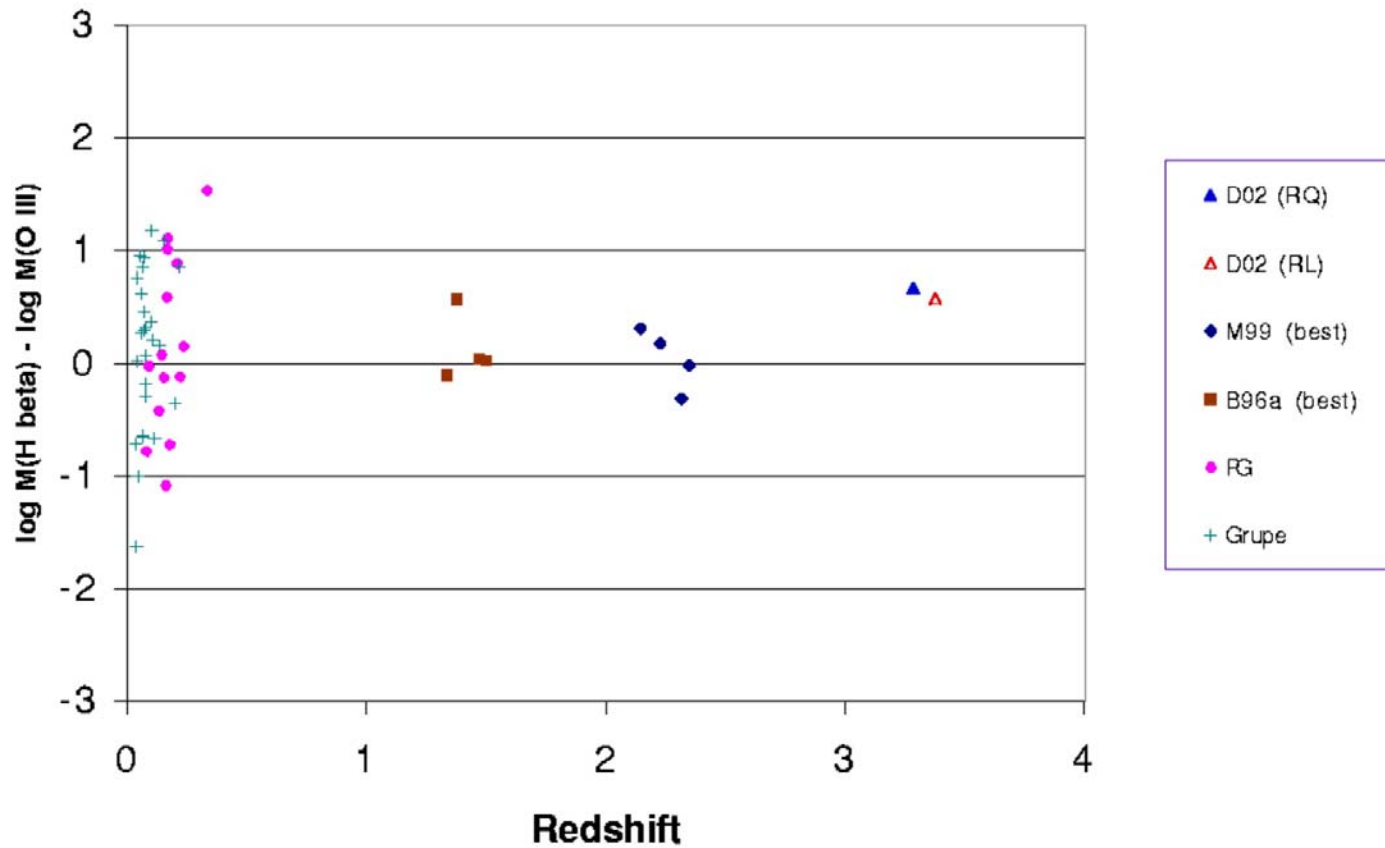
“... black holes typically grow contemporaneously with their host-galaxy bulges or else ... both are well formed by $z \sim 3$ ”.

Problem: nuclear outflows?!

- Follows: MBH-s relation is obeyed by massive QSOs even at times at which much of the accretion lies in their future.

Bromm & Loeb (2003): In dwarfs at $T > 10^4$ K virial temperatures and UV suppressed H₂ formation tend to form binary (few million M \odot) black holes.

M- σ Relation as a function of z



Shields et al. 2003

Formation of Massive Black Holes (MBH)

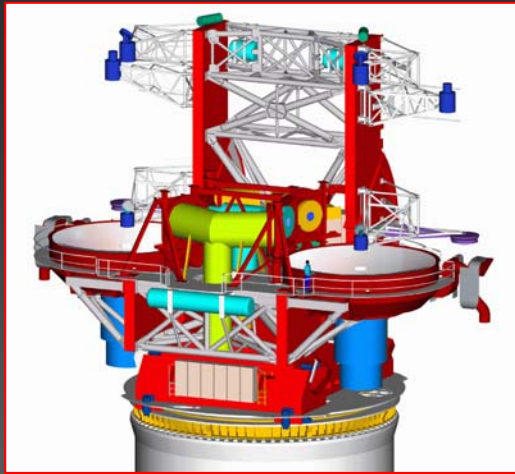
Who knows what happened at the beginning??

- Yu & Tremaine (2002) find that half the BH mass is accreted before $z \sim 1.8$ and only 10% before $z=3$.
- Shields et al. (2003) use $\text{FWHM}([\text{OIII}])$ to determine MBH at high redshifts. From $\log(\text{MBH}(\text{H}\beta) - \text{MBH}([\text{OIII}])) \sim 0$ between $0 < z < 3.5$ they conclude:
“... black holes typically grow contemporaneously with their host-galaxy bulges or else ... both are well formed by $z \sim 3$ ”.
- Follows: MBH-s relation is obeyed by massive QSOs even at times at which much of the accretion lies in their future.

How do they look like?

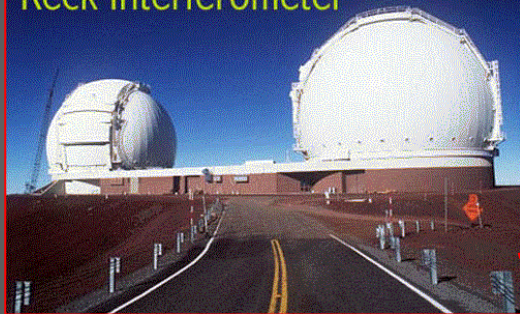
Bromm & Loeb (2003): In dwarfs at $T > 10^4$ K virial temperatures and UV suppressed H_2 formation tend to form binary (few million M_{\odot}) black holes.

Future Experiments



Angular Resolutions of Interferometers under Construction at $2\mu\text{m}$ Wavelength

Keck Interferometer



LBT

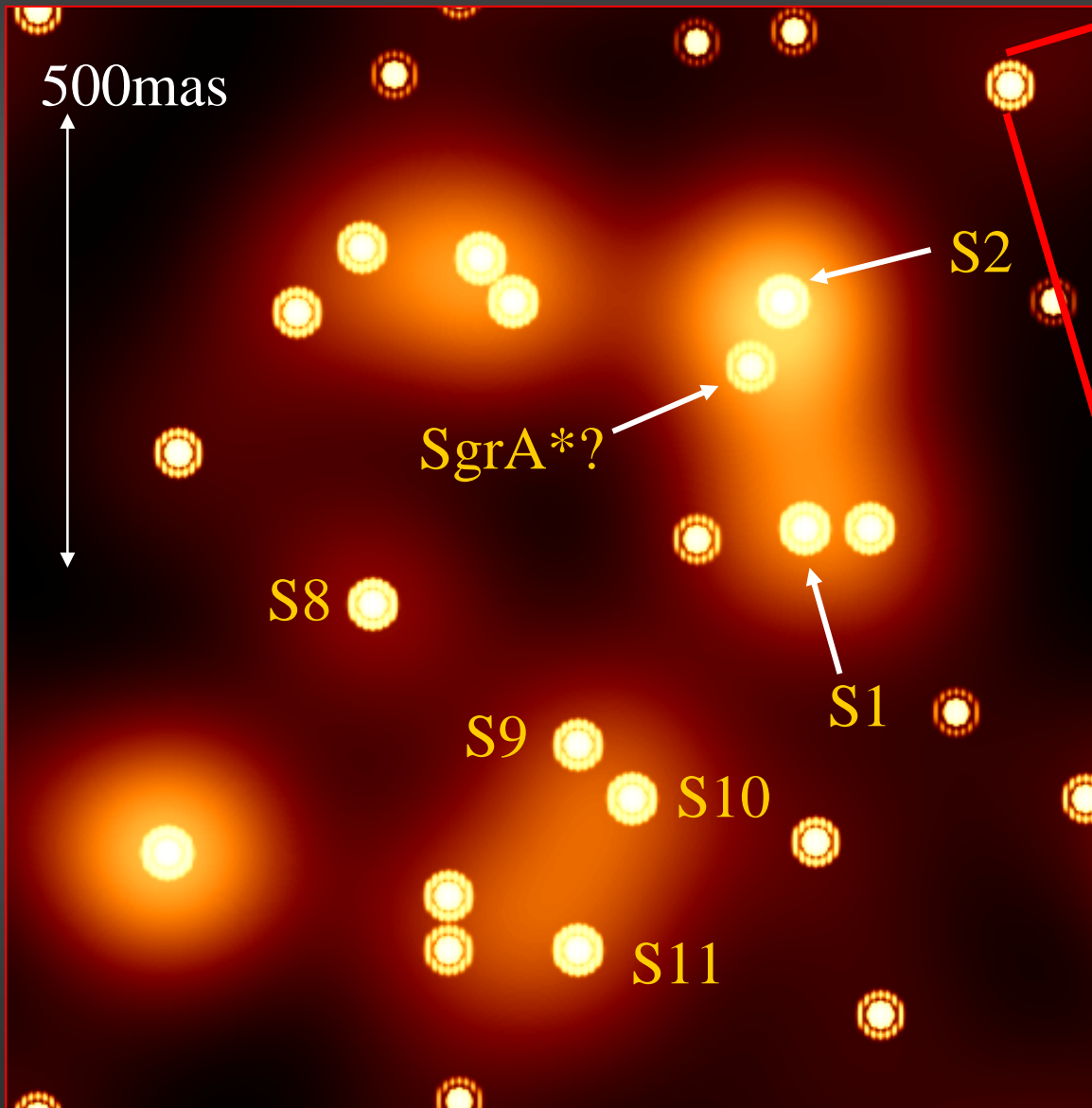
Keck

VLTI

Baseline	Res.	FOV
14.4m	30 mas	1 arcmin
85 m	6 mas	two channels
200 m	2.5 mas	1 arcsec two channels

Rubilar & Eckart 2001

The Galactic Center



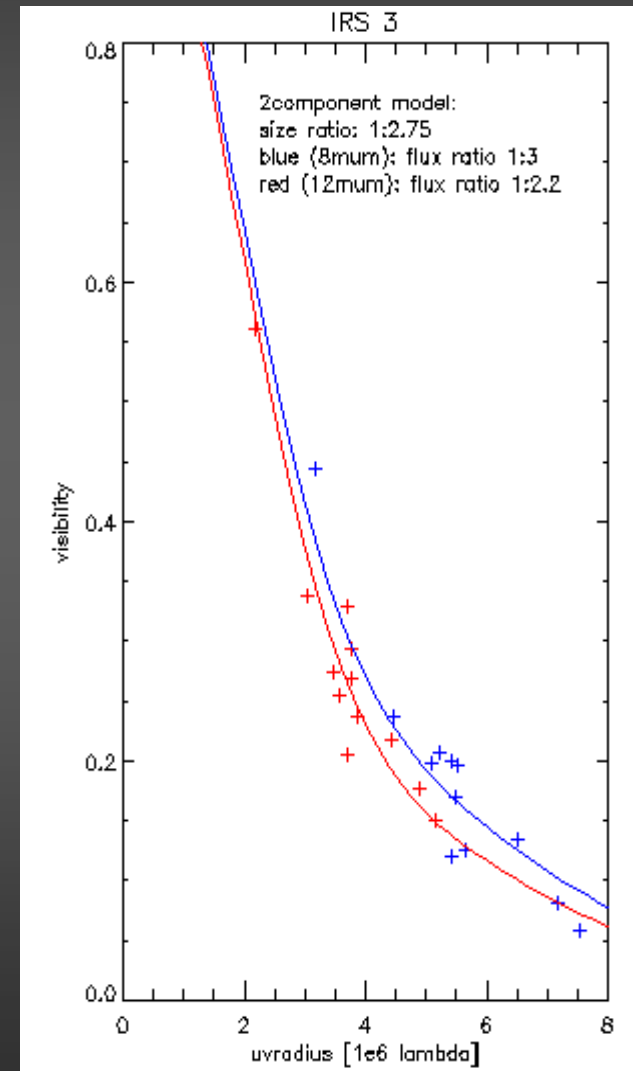
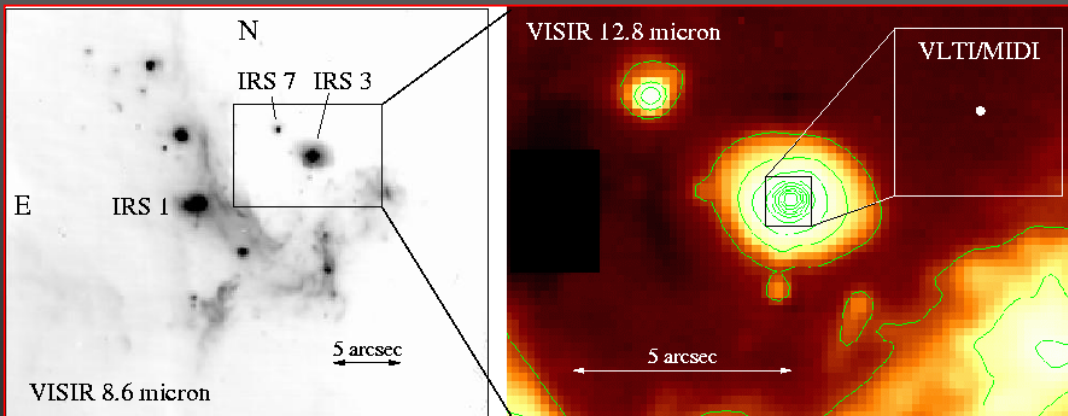
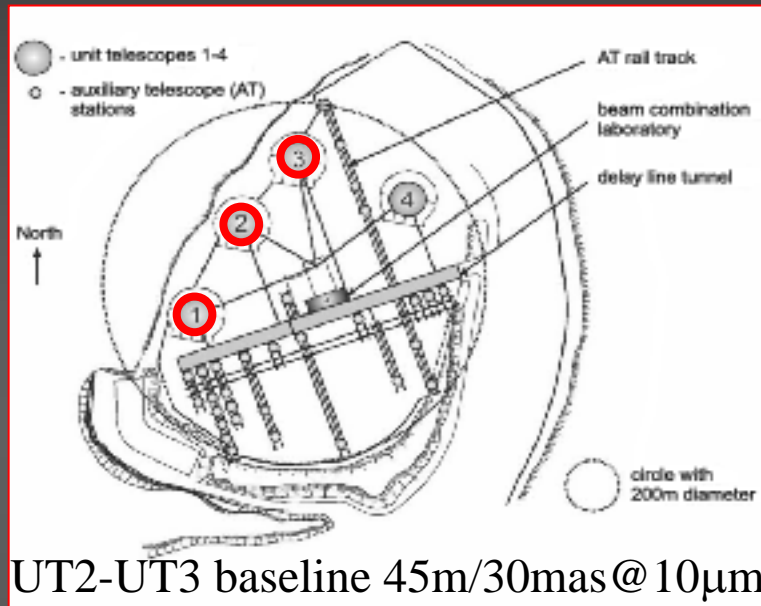
K-band LBT PSF

60mas

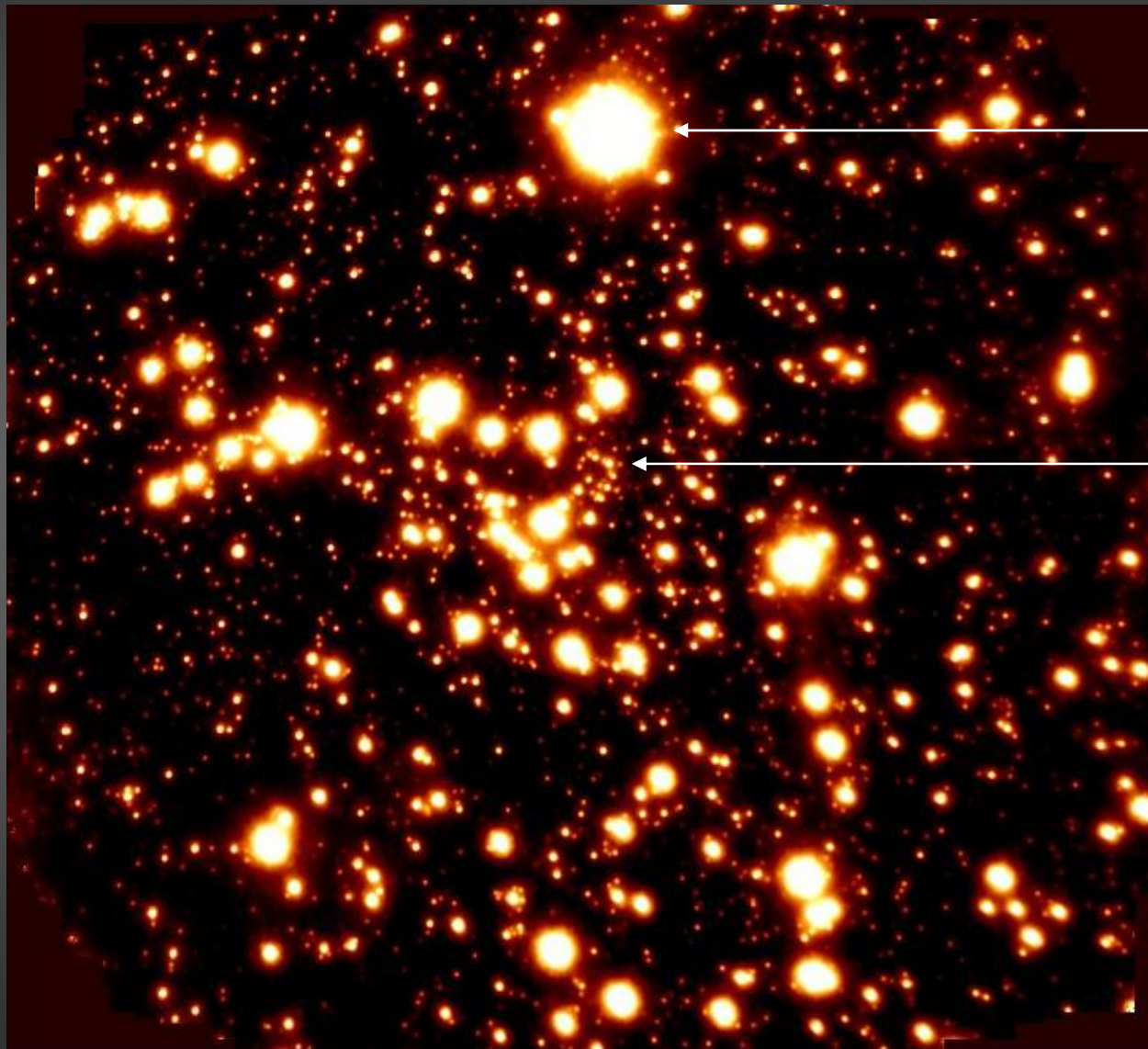
Brighter sources in the the SgrA* cluster as seen with the LBT interferometer (short exposure) at $2\mu\text{m}$ and a $\sim 50\%$ strehl ratio.

Interferometry with VLTI

Please see also spring ESO Messenger:
J.-U.Pott et al. : The brightest compact MIR source at the GC
VLT Interferometric observations of IRS3



**Pott, Eckart et al. recently detected
IRS7 with AMBER at the VLT**



IRS7

SgrA*

NACO
NIR
2 μ m

The Galactic Center

For orbits in the 30mas to 100mas range
orbital time scales are of the order of
1 to 10 years.

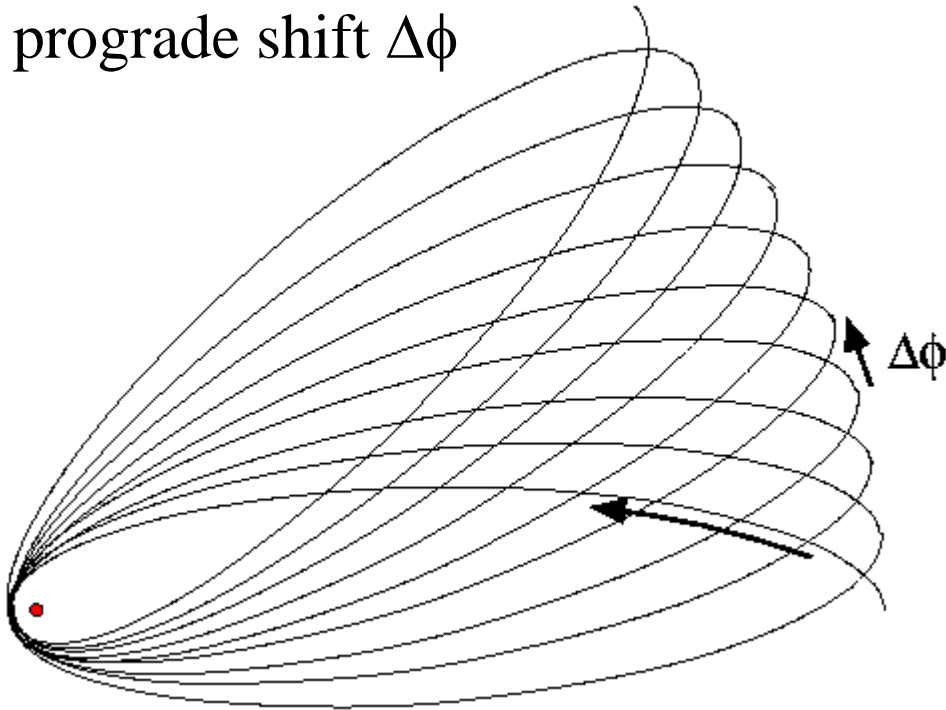
Interferometry with a large FOV provides a
large number of reference sources and exact
measurements of positions and velocities.

Sources on close orbits allow to determine
the compactness of the central mass.

Orbits

The Galactic Center

prograde shift $\Delta\phi$



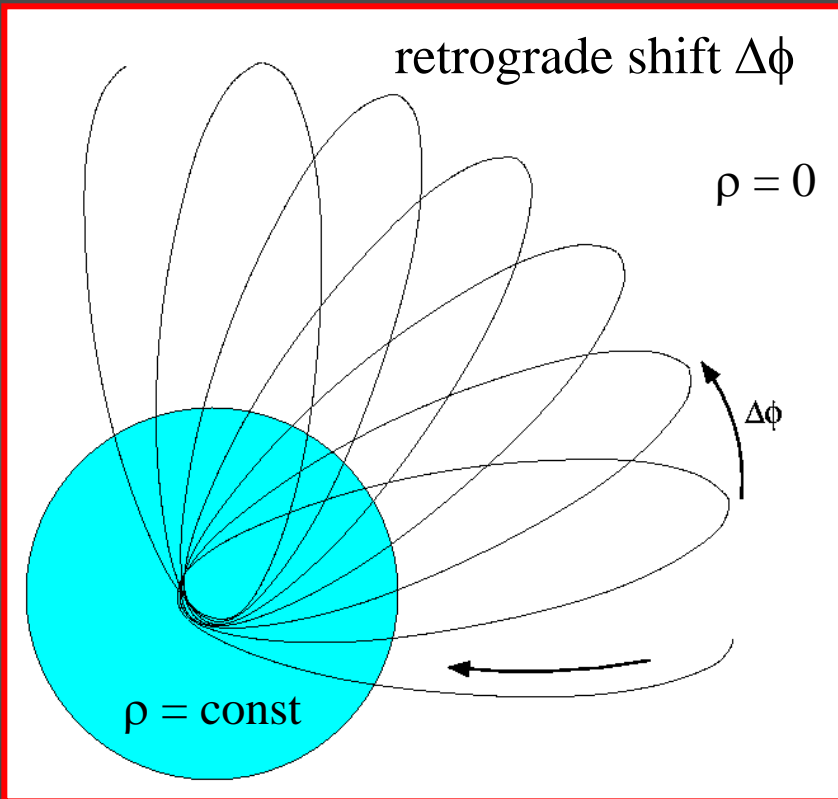
Relativistic
periastron
shift

$$\Delta\phi = \frac{3\pi R_s}{a(1-\varepsilon^2)c^2}$$

with

$$R_s = \frac{2GM}{c^2}$$

The Galactic Center



Periastron shift due to
an extended mass

$$\Delta\varphi = 2 \arccos \left\{ \frac{1}{e} \left(\frac{l^2}{GMR} - 1 \right) \right\} + \arcsin \left\{ \frac{\frac{2}{R^2} - B}{\sqrt{B^2 + 4A}} \right\} - \frac{\pi}{2}$$

with

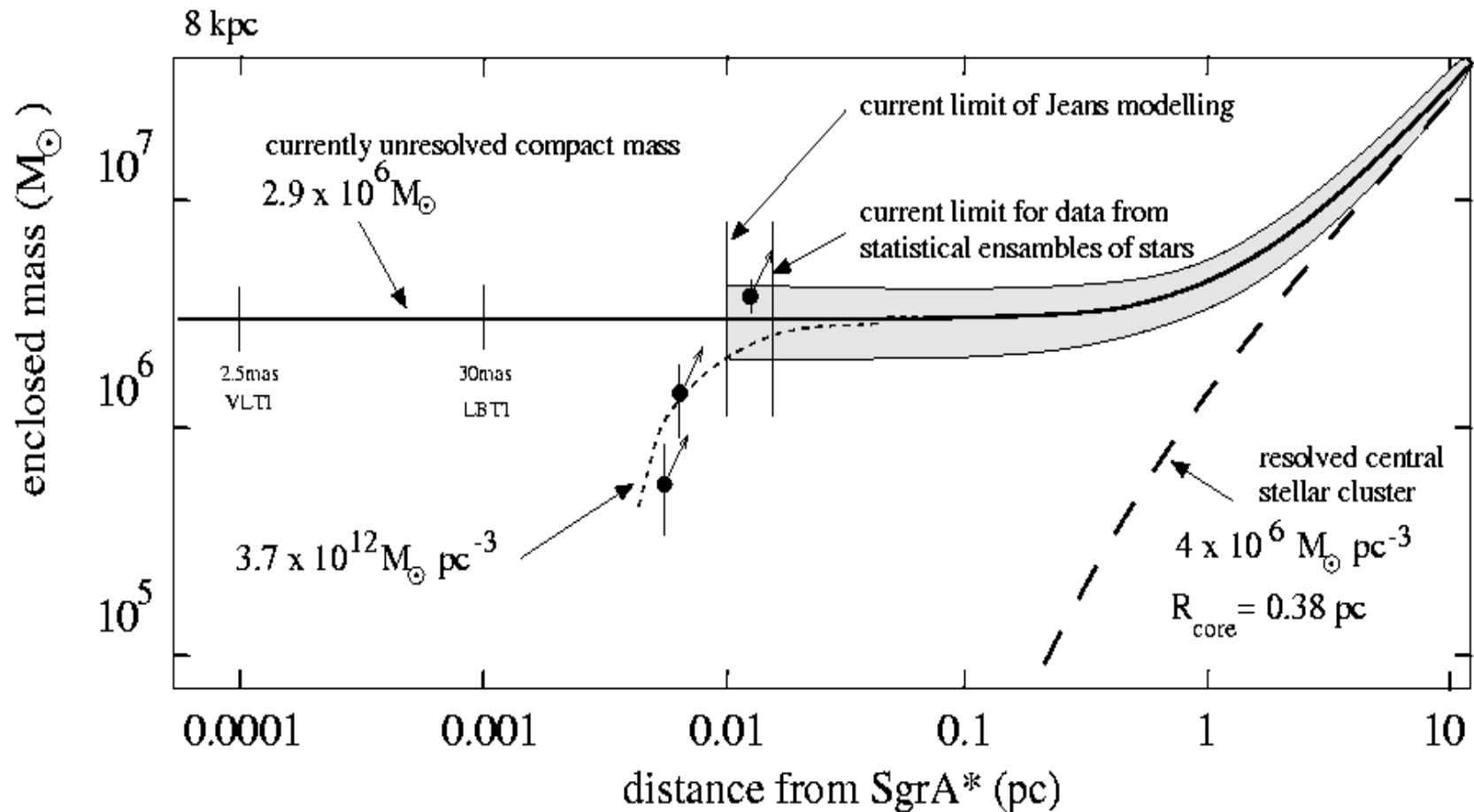
$$A = \frac{GM}{lR^3}$$

$$B = \frac{2E}{l^2} \left(1 + \frac{3GM}{2RE} \right)$$

Jiang, H.X. and Lin, J.Y., 1985, Am.J.Phys., 53, 694

$$\vec{l} = \vec{r} \times \vec{v}$$

The Galactic Center



What fraction λ of mass is in the central compact mass ?

What fraction of mass could be extended?

Lensing

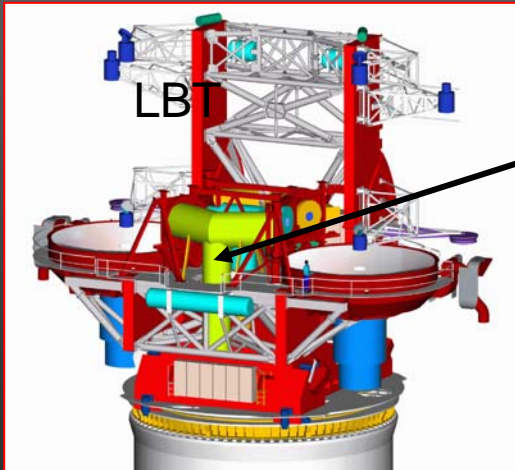
The Galactic Center

Tasks for Future Observations

- tracking stellar orbits (proper and radial m.)
- measure spectra of fast moving stars
- extending anisotropy tests to fainter magnitudes
- monitoring counter part of SgrA*
- finding and tracking sources near SgrA*
- determine periastron shifts and compactness of the central mass



GRAVITY
VLT NIR/OPT Beam Combiner:
MPE, Paris, Cologne



LINC/NIRVANA
LBT NIR/OPT Beam Combiner:
University of Cologne
MPIA, Heidelberg
Osservatorio Astrofisico di Arcetri
MPIfR Bonn

Conclusion

The Galactic Center is a Massive Black Hole

Alternative scenarii become increasingly unlikely!

It is one of the best laboratories to study

fundamental physics

in the environment of large compact nuclear masses.

Interferometric measurements in the radio and NIR/MIR combined with results from other wavelength domains

are ideally suited for future investigations





GC06
18-22 April 2006
Bad Honnef, Germany
(on the river Rhein, just
south of Köln/Bonn)



End of Part II

End